

Electronic Thesis and Dissertation Repository

7-7-2017 12:00 AM

Methylmercury Production in Two Northern Fen Peatlands

Mikhail J. Mack, *The University of Western Ontario*

Supervisor: Dr. Brian Branfireun, *The University of Western Ontario*

A thesis submitted in partial fulfillment of the requirements for the Master of Science degree in Biology

© Mikhail J. Mack 2017

Follow this and additional works at: <https://ir.lib.uwo.ca/etd>



Part of the [Biogeochemistry Commons](#), [Hydrology Commons](#), and the [Water Resource Management Commons](#)

Recommended Citation

Mack, Mikhail J., "Methylmercury Production in Two Northern Fen Peatlands" (2017). *Electronic Thesis and Dissertation Repository*. 4655.

<https://ir.lib.uwo.ca/etd/4655>

This Dissertation/Thesis is brought to you for free and open access by Scholarship@Western. It has been accepted for inclusion in Electronic Thesis and Dissertation Repository by an authorized administrator of Scholarship@Western. For more information, please contact wlsadmin@uwo.ca.

Abstract

Mercury is a naturally occurring element in the Earth's lithosphere. Although natural processes result in mercury releases into the atmosphere and subsequent cycling through ecosystems, anthropogenic activities have greatly exceeded these natural processes. Methylmercury (MeHg) is the form of mercury produced in anoxic environments, mainly by sulphate reducing bacteria, which methylate mercury as a by product to their respiration. Northern peatlands are sites of MeHg production, particularly those dominated by mosses. Experiments have shown that climate change may drive a shift from moss- to sedge-dominance and may then alter mercury biogeochemistry and downstream water quality. Measurements made in a moss-dominated poor fen and sedge-dominated intermediate fen were used to compare MeHg to assess if contrasting peatland type, nutrients status and/or hydrologic regime control MeHg production. Chapter 2 compared porewater MeHg and ancillary chemistry across two Northern Ontario fens. In the poor fen, the lower water table (mean = -21.1 cm) and pH (median = 4.90), and higher dissolved organic carbon (median = 27.46 mg L⁻¹), resulted in 3.1 times greater MeHg (median = 0.54 ng-Hg L⁻¹) compared the intermediate fen (0.17 ng-Hg L⁻¹) where the higher water table (-5.4 cm) and pH (5.63), and lower dissolved organic carbon (19.20 mg L⁻¹) limited MeHg concentrations. A seasonal water table drawdown period resulted in increased sulphate availability in both the intermediate and poor fen leading to greater MeHg in September. In Chapter 3, riparian zones in the intermediate fen were evaluated to see if groundwater nutrient supply controlled MeHg production and transport adjacent to two incised peatland streams. Rather than groundwater supply, riparian zones with a lower water table and greater fluctuations resulted in higher available sulphate (> 1.0 mg L⁻¹) and MeHg (> 0.5 ng-Hg L⁻¹) concentrations compared to those with a higher overall waters tables and smaller fluctuations. Increased sulphate availability following a seasonal water table drawdown resulted in August (1.67 ng-Hg L⁻¹) and September (3.36 ng-Hg L⁻¹) maximums in MeHg in riparian zones. The proximity (≤ 2 m) of riparian zones to stream waters then facilitated methylmercury transport to surface waters. Hydrologic variability and sulphate availability were the main drivers leading to greater MeHg in both the poor and intermediate fen.

Keywords

Biogeochemistry, Climate Change, Fen, Incised Streams, Intermediate Fen, Mercury, Methylmercury, Moss-dominated, Northern Peatlands, Poor Fen, Riparian Zones, Sulphate, Sedge-dominated, Wetlands

List of Abbreviations

18.2 MOhm	Milli-Q
^2H	Deuterium
^{18}O	Oxygen-18
ABS	Acrylonitrile butadiene styrene
AWS	Automatic weather station
BrCl	Bromine monochloride
Ca^{2+}	Calcium
Cl^-	Chloride
CS	Continuous stream
CVAF	Cold vapour atomic florescence
DGPS	Differential global positioning system
DIC	Dissolved inorganic carbon
DOC	Dissolved organic carbon
DS	Discontinuous stream
HDPE	High density polyethylene
IF	Intermediate fen
K	Hydraulic conductivity
K^+	Potassium
masl	Metres above sea level
MDL	Method detection limit
MeHg	Methylmercury
Mg^{2+}	Magnesium
MNRF	Ontario Ministry of Natural Resources and Forestry
MRL	Method reporting limit
OFRI	Ontario Forest Research Institute
OPR	Ongoing precision recovery
PETG	Polyethylene terephthalate glycol-modified
PF	Poor fen
PVC	Polyvinyl chloride
QA/QC	Quality assurance/quality control
SO_4^{2-}	Sulphate

SRB	Sulphate reducing bacteria
THg	Total mercury
TN	Total nitrogen
UNEP	United Nations Environment Programme
U.S. EPA	United States Environmental Protection Agency
VSMOW	Vienna Standard Mean Ocean Water

Co-Authorship Statement

I hereby declare that I am the sole author of this thesis, except where noted (below). I understand that my thesis may be made electronically available to the public.

Exception to sole authorship:

For all chapters, Dr. Brian Branfireun acted as an advisor, editor and offered suggestions to the treatment and presentation of data in this thesis, and will be listed as a co-author on any subsequent publications.

Acknowledgments

Thank you to my supervisor, Dr. Brian Branfireun for your guidance in forming my research questions, providing funding throughout my MSc program, as well as access to the White River research sites, and for the countless hours editing involved in preparing this thesis. Special thanks to my advisors, Dr. Hugh Henry and Dr. Katrina Moser for your guidance and support throughout my MSc program as well. Thanks to the Ministry and Natural Resources and Forestry research collaborators that assisted with field work, water analyses and coordinating field logistics. In particular, Dr. Jim McLaughlin, Dr. Maara Packalen, John Rolston, and Scott Bowman. Thank you to undergraduate field assistances Maddie Postma (University of Waterloo) and Chris Sullivan (Western University) who went above and beyond in assisting with water sampling and filtration. Thanks to my Branfireun lab mates, especially Jing Tian who assisted me nearly everyday in field. Thank you as well to Dr. Zoë Lindo and her lab for coordinating and collaborating with the Branfireun Lab. Thank you to Biotron Analytical Services laboratory staff Dr. Yong Liu and Jeff Warner for assisting with any trouble shooting during total mercury and methylmercury analysis. Thanks as well to Aaron Craig for his invaluable assistance with chemical analysis and coordination of laboratory purchases, the Branfireun Lab would not function without Aaron's hard work and analytical mind behind the scenes. I would also like to thank my parents Margaret Leibfried and Stan Mack, and brothers, Kiehlor and Stashie for your support. Lastly, I would like to thank and dedicate this thesis to the woman I love, Julia Palozzi.

Table of Contents

Abstract	i
List of Abbreviations	iii
Co-Authorship Statement.....	v
Acknowledgments.....	vi
Table of Contents	vii
List of Tables	x
List of Figures	xi
List of Appendices	xii
Chapter 1	1
1 Introduction	1
1.1 Mercury as a global pollutant	1
1.2 Methylmercury effects on aquatic ecosystems	4
1.3 Microbial methylation of mercury	5
1.4 Northern peatlands as sources of methylmercury	6
1.4.1 Northern peatlands	6
1.4.2 Methylmercury production in northern peatlands.....	8
1.5 The implications of climate change on northern peatland ecosystems and effects on net methylmercury production	11
1.6 Thesis objectives	13
1.7 References	14
Chapter 2	22
2 Porewater total mercury and methylmercury in two different northern fen peatland types	22
2.1 Introduction.....	22
2.2 Methods.....	25

2.2.1	Study site description	25
2.2.2	Hydrology and site surveys.....	29
2.2.3	Analytical methods	31
2.2.4	Statistical methods	33
2.3	Results.....	33
2.3.1	Climate and hydrology.....	33
2.3.2	Temporal porewater chemistry comparison.....	36
2.4	Discussion.....	39
2.4.1	Porewater total mercury and methylmercury.....	39
2.4.2	Conditions effecting porewater methylmercury concentrations between a sedge-dominated and moss-dominated peatland	41
2.5	Conclusions.....	42
2.6	References.....	44
Chapter 3	50
3	Production and transport of methylmercury in a sedge-dominated peatland.....	50
3.1	Introduction.....	50
3.2	Methods.....	54
3.2.1	Study site description	54
3.2.2	Field Methods	56
3.2.3	Analytical Methods.....	59
3.3	Results.....	61
3.3.1	Hydrology	61
3.3.2	Patterns of pore, stream, and groundwater chemistry.....	69
3.3.3	Stream water and riparian zone porewater interactions.....	78
3.3.4	Bivariate relationships between total mercury and methylmercury with other chemistry.....	80
3.4	Discussion.....	81

3.4.1	Hydrology and groundwater controls on sulphate delivery	81
3.4.2	Spatiotemporal patterns of stream and porewater chemistry	82
3.4.3	Transport of total mercury, methylmercury, and other solutes.....	84
3.4.4	Relationships among total mercury, methylmercury, and other solutes...	87
3.4.5	Application of riparian zone MeHg dynamics to parsimonious modeling	87
3.5	Conclusions.....	88
3.6	References.....	89
Chapter 4	94
4	Conclusions and implications	94
4.1	Results as a baseline for climate change experiments	95
4.2	Limitations	95
4.3	References.....	97
Appendix	98
Curriculum Vitae	104

List of Tables

Table 2.1: Sampling date water table level.....	35
Table 2.2: Monthly median and interquartile range of porewater chemistry from the IF and PF near White River, Ontario.	38
Table 2.3: Monthly median (interquartile range) of ancillary chemistry from an sedge-dominated intermediate fen and a moss-dominated poor fen near White Rive, Ontario.....	39
Table 3.1: Hydraulic conductivity (K) from riparian zone peat and underlying sand across the DS and CS.....	63
Table 3.2: Monthly piezometer ancillary porewater chemistry.	73

List of Figures

Figure 1.1: Total annual dry (A) and wet (b) Hg deposition maps from Dastoor & Larocque (2004).....	3
Figure 2.1: Intermediate and Poor Fen site map.	27
Figure 2.2: Intermediate Fen and Poor Fen water table levels.	35
Figure 2.3: Boxplots of PF and IF porewater chemistry.....	37
Figure 3.1: Intermediate Fen riparian zone site map.	55
Figure 3.2: Discontinuous Stream and Continuous Stream levels.....	62
Figure 3.3: Discontinuous Stream: Upstream Transect water table and hydraulic gradients.	64
Figure 3.4: Discontinuous Stream: Downstream Transect water table and hydraulic gradients.	65
Figure 3.5: Continuous Stream: Upstream Transect water table and hydraulic gradients.....	67
Figure 3.6: Continuous Stream: Downstream Transect water table and hydraulic gradients.	68
Figure 3.7: Discontinuous Stream: Upstream Transect pore and stream water chemistry.	71
Figure 3.8: Discontinuous Stream: Downstream Transect pore and stream water chemistry.	72
Figure 3.9: Continuous Stream: Upstream Transect pore and stream water chemistry.....	76
Figure 3.10: Continuous Stream: Downstream Transect pore and stream water chemistry... ..	77
Figure 3.11: Biplots of conservative tracers ^{18}O and Cl^- collected over the study period.....	79
Figure 3.12: Bivariate plots showing THg and DOC in riparian zone pore and stream waters. The DS is shown in panel A and the CS in panel B.	80

List of Appendices

Appendix A: Site Photographs..... 98

Chapter 1

1 Introduction

1.1 Mercury as a global pollutant

On Earth, mercury (Hg) is naturally present in the lithosphere. Natural processes and anthropogenic activities result in the emission of Hg into the atmosphere as gaseous elemental Hg(0) (GEM), gaseous divalent Hg (II), and particulate Hg (Pirrone et al. 2010). Historical anthropogenic Hg emissions date back thousands of years to ancient Egypt, Greece, and China (Streets et al. 2011). Beginning with the Industrial Revolution (ca. 1750), anthropogenic Hg emissions greatly accelerated, peaking between 1850 and 1915 (North American gold and silver rush) and again steadily increased post World War II due largely to coal combustion for power generation (Streets et al. 2011). In all, approximately 3.5×10^{11} metric tonnes (2008 estimate) of lithospheric Hg have been emitted and deposited because of anthropogenic activities (Streets et al. 2011). Present day estimates for all Hg emissions range from 6500–8200 metric tonnes per year (Driscoll et al. 2013). The majority (4600–5300 metric tonnes) of the annual emissions are from the re-emission of previously deposited Hg, known as secondary emissions (Driscoll et al. 2013). Primary emissions, from anthropogenic activities account for 30–35 % of global annual emissions (1900–2900 metric tonnes) (Driscoll et al. 2013). Primary natural emissions account for the smallest share of annual emissions, 80–600 metric tonnes (Driscoll et al. 2013). Natural emissions are sourced from volcanism, geothermal vents, and naturally Hg rich soil, while artisanal gold mining (amalgamation of gold using Hg and then subsequent boiling off of Hg to the atmosphere by individual miners) accounts for the largest present day anthropogenic emissions (see Pirrone et al. 2010; UNEP 2013). Other significant sources of anthropogenic Hg emission include releases from the burning of coal, processing of mining ores, production of consumer products (e.g., paint and electronics) and, industrial scale chemical manufacturing (e.g., chlor-alkali plants) (Pirrone et al. 2010; UNEP 2013). Mercury released from burning

vegetation and Hg(0) evasion from the world oceans account for the largest re-emission sources (Pirrone et al. 2010; Driscoll et al. 2013). Amos et al. (2013) estimated that ~50% the Hg in the surface oceans is sourced from anthropogenic activities. Mercury emissions released as GEM have a residence time of several months to a year in the stratosphere allowing for hemispheric circulation (Pirrone & Masson 2009). Upon re-entering the troposphere, GEM can be oxidized in reactions with aerosols and halogens to particulate bound mercury (Hg(II)) or remain as elemental Hg(0) (Pirrone & Mason 2009) whereupon it is deposited across all terrestrial and aquatic ecosystems via dry deposition or precipitation (Fitzgerald et al. 1998). Atmospheric deposition is not uniform across all landscapes, while annual total Hg deposition is not tracked globally, Dastoor & Larocque (2004) produced a comprehensive atmospheric global model to describe the atmospheric cycling of Hg for both dry and wet deposition pathways (Figure 1.1). The model results show clear north to south gradients and the effects of industrialization/population centres in eastern North America, western Europe, and China (Dastoor & Larocque 2004). Despite global efforts to curtail anthropogenic Hg emissions (e.g. Minamata Convention 2013), Hg remains a persistent pollutant threatening organisms and their ecosystems (UNEP 2013). The microbial transformation of divalent Hg(II) into mono-methylmercury (MeHg), a bioaccumulating neurotoxin, is of greatest concern to aquatic organisms and their resource beneficiaries, including humans.

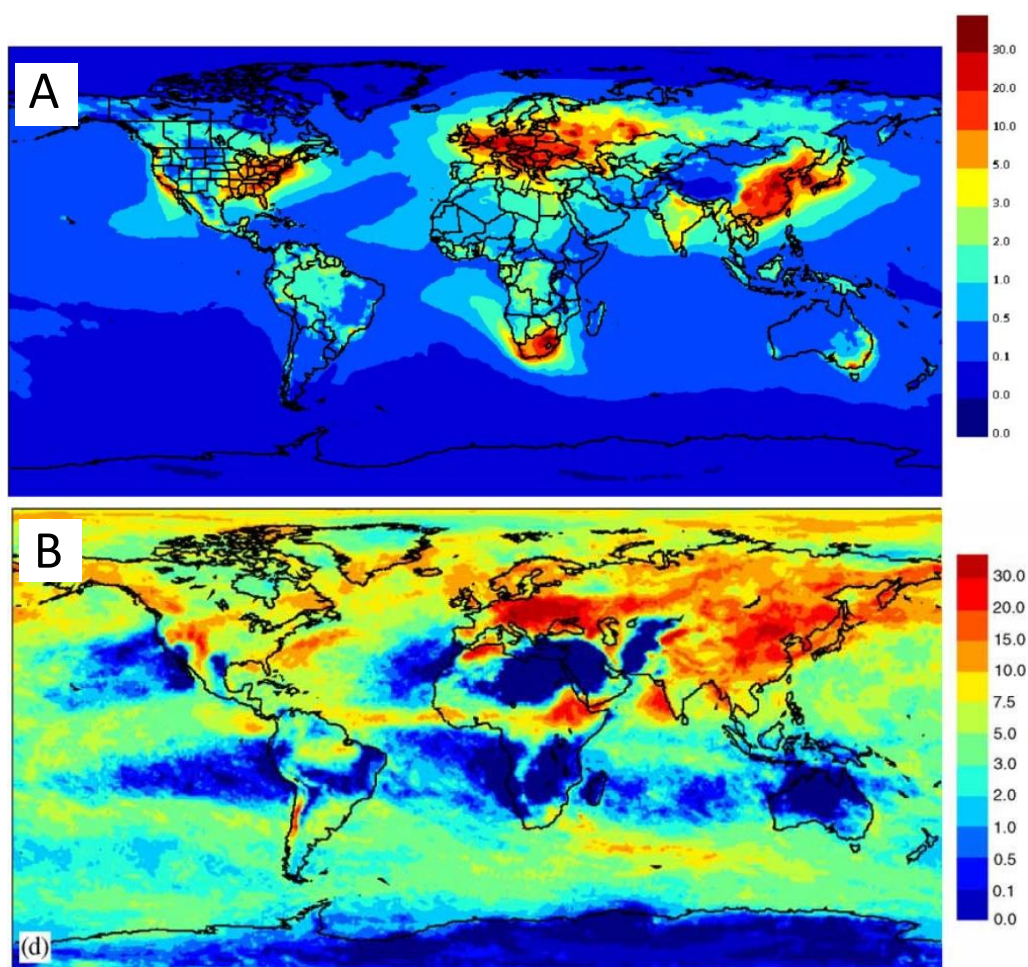


Figure 1.1: Total annual dry (A) and wet (B) Hg deposition maps from Dastoor & Larocque (2004).

Global dry and wet deposition ($\mu\text{g-Hg/m}^2$) from the GRAHM model (global/regional atmospheric heavy metals model), which integrates the physical state of the atmosphere and physio-chemical Hg speciation changes on a 30 minute time scale. Measured data for the model were from 1995 to 1997 (2.5 years). For the wet deposition map (B), data was from July 1997 and multiplied over a 12 month period.

1.2 Methylmercury effects on aquatic ecosystems

Methylmercury poses a significant threat to aquatic ecosystems because it bioaccumulates and biomagnifies in aquatic food webs (Morel et al. 1998).

Methylmercury accumulates in an organism faster than processes can break down or remove it, resulting in bioaccumulation. Concentrations of MeHg then increase in organisms with increasing trophic level and food chain length as smaller concentrations diluted across the larger biomass from lower trophic level organisms (primary producers and primary consumers) are conserved within the smaller biomass found in higher trophic level organisms (secondary, tertiary, quaternary consumers)—a process called biomagnification. Methylmercury poses the greatest threat to piscivorous organisms, the highest trophic level organisms in aquatic and some terrestrial food webs, because of bioaccumulation and biomagnification (UNEP 2013). The main pathway for human exposure to MeHg results from consumption of fish and shellfish (freshwater and marine species) (UNEP 2013).

The effects of MeHg exposure have been investigated in several human and animal studies (see U.S. National Research Council (NRC) 2000). Methylmercury is a neurotoxin with some evidence that it is also an endocrine disruptor and has been implicated as a causative factor in cardiovascular disease (U.S. NRC 2000). High concentrations ($\text{Hg} > 2$ ppm in a patient's brain) can lead to Minamata disease, a severe form of Hg poisoning, named because the effects of Hg exposure were first medically documented at the population level in Minamata, Japan, where a chlor-alkali plant released Hg and MeHg in effluent for years and local residents in turn consumed local shellfish and fish (Harada 1995). Effects of Minamata disease are largely neurological with adults experiencing ataxia, sensory loss, vision and hearing losses or impairment (Harada 1995). The developing fetus is at particular risk of neurological and developmental impairment by MeHg exposure in utero (U.S. NRC 2000). Fish and seafood containing high levels of MeHg (5–40 ppm) are geographically constrained and rare (Harada 1995), with most MeHg exposure occurring through consumption of fish with lower levels of MeHg ($\text{Hg} < 1$ ppm) (Mergler et al. 2007).

1.3 Microbial methylation of mercury

The transformation of Hg(II) to the organic form, MeHg, is principally a microbial driven process (Compeau & Bartha 1985). Seminal work by Compeau and Bartha (1985) demonstrated that sulphate reducing bacteria (SRB) in anoxic marine sediments were the primary methylators of Hg. Sulphate reducing bacteria require anoxic conditions and three reactants in order to methylate Hg: a labile carbon substrate, bioavailable forms of Hg(II) and a sulphate (SO_4^{2-}) source as an electron acceptor. Since their work, metabolic and genetic studies have further elucidated: the suggested biochemical pathways for which MeHg is formed (Choi et al. 1994), a genetic basis for microbial Hg methylation (Parks et al. 2013), and the known species of microbes capable of MeHg production (Gilmour et al. 2013).

Metabolically, MeHg production is a by product to the breakdown of labile carbon substrates (e.g., polysaccharides and amino acids) in anaerobes as they synthesize acetyl-coenzyme A (Choi et al. 1994). Acetyl-coenzyme A is a common enzyme present in many microorganisms; therefore, a genetic component has been suggested as a means of distinguishing MeHg producers from other microorganisms. Recent work by Parks et al. (2013) found that two gene clusters, HgcA and HgcB, encode for proteins corrinoid protein and ferredoxin, respectively, which act as carriers of methyl groups in known MeHg producing species (*Desulfovibrio desulfuricans* and *Geobacter sulferruducens*). A follow up study by Gilmour et al. (2013) looked for the presence of both gene clusters in all microorganism with sequenced genomes. Gilmour et al. (2013) found HgcA and HgcB gene clusters in several novel and unknown Hg methylating microorganisms, such as methanogenic, syntrophic (e.g., bacteria within fish and human digestive tracts), acetogenetic and fermentative anaerobes, from both Archaea and Bacteria domains. These genetic studies have found Hg methylation to occur in previously undocumented environments (e.g., periphyton, vertebrate digestive tracts, alkaline lakes), and expanded our knowledge of the phylogenetic diversity of associated microorganisms. Despite these discoveries of methylating microorganisms, SRB and iron-reducing bacteria (FeRB) remain the primary methylators, highlighting the need for further studies of MeHg

produced by microorganisms in anoxic soils and sediments (Gilmour et al. 2013; King et al. 2000; Fleming et al. 2006).

The measured concentrations of MeHg in anoxic soils and sediments, and connected waters, are not strictly a function of gross MeHg production; demethylation of MeHg controls the net methylmercury concentrations found in natural environments. In the environment, demethylation of MeHg occurs abiotically through photo-degradation (Sellers et al. 1996), and biotically through the *mer* operon in several microorganisms present in Hg methylating environments (Barkay et al. 2006). Hence, measures of bulk MeHg concentrations in the environment reflect net methylmercury production. The complexity of the Hg cycle (inorganic and organic forms, methylation and demethylation) in freshwater ecosystems makes predicting aquatic ecosystems at greatest risk difficult. However, catchments with greater atmospheric Hg loading and greater wetland area tend to have more MeHg in fish (St. Louis et al. 1994).

1.4 Northern peatlands as sources of methylmercury

St. Louis et al. (1994) first demonstrated that the presence of wetlands resulted in greater MeHg export from catchments to lakes and that different wetland types yielded varying amounts of MeHg (St. Louis et al. 1996). More mechanistic studies determined that MeHg was produced in the peat soils of these northern wetlands, contributing to the MeHg load of receiving waters (Krabbenhoft et al. 1995; Branfireun et al. 1996).

Northern peatlands represent a continuum of different wetland types, each with associated biogeochemical conditions governing net MeHg production.

1.4.1 Northern peatlands

Northern peatlands (north of 45° latitude) are common wetland types defined by their accumulation of peat greater than 40 cm (Canadian definition) (Gorham 1991; Rydin & Jeglum 2013). Peat is a type of organic soil composed of plant material that is slow to decompose due to waterlogged, anaerobic soil conditions and recalcitrant (difficult to break down) plant materials (Rydin & Jeglum 2013). Covering only ~3% of terrestrial

land surfaces, northern peatlands store approximately 30% of global terrestrial carbon as peat (Gorham 1991; Turunen et al. 2002). Northern peatland types are a continuum (rich, intermediate, poor fen, bog) of decreasing nutrient status and hydrologic connectivity (Bay 1969; Boelter & Verry 1977; Siegel & Glaser 1987). Regional climates where precipitation exceeds evapotranspiration on a long-term basis and where ecosystem primary productivity exceeds decomposition promote peat accumulation (Ingram 1982; Roulet 1990).

Northern peatland succession is classically characterised as a unidirectional process. Minerotrophic rich fens (high in nutrients, dominated by vascular plants, strong hydrologic connection to ground and surface waters) slowly (over millennia) transition to intermediate and poor fens which are characterised by lower nutrients, water tables and a dominant vegetative shift from sedges to mosses (Rydin & Jeglum 2013). The climax ecosystem type is the ombrotrophic bog (low nutrients, moss-dominated, weak hydrologic connection to ground and surface waters), which ultimately develop over millennia through the process of peat accumulation (Rydin & Jeglum 2013). The succession of fens (rich to intermediate to poor) into ombrotrophic bogs are associated with hydrologic, nutrient and vegetation community shifts (Rydin & Jeglum 2013). Long-term water table position alongside groundwater and surface water connectivity lower as northern peatlands accumulate greater amounts of peat and the peatland form assumes a characteristic peat dome cross section (Rydin & Jeglum 2013). Decreasing hydrologic connectivity limits available nutrients as importance of groundwater and upland runoff contributions decline over time.

Northern peatlands are typically characterised as being moss- or sedge-dominated, and such dominant vegetation types correspond to pH, moisture and nutrient gradients. Moss dominance results in acidic pH, an average water table further below the peat surface and microtopography development (hummocks and hollows), while sedge dominance corresponds to less acidic conditions, an average water table nearer to the surface and limited or no microtopography development (Rydin & Jeglum 2013). *Sphagnum* mosses

have long been considered ecosystem engineers (Jones et al. 1994), generating and maintaining anoxic, acidic and nutrient-poor conditions, driving peatland succession to a bog ecosystem state (van Breemen 1995). However, recent field (Buttler et al. 2015) and laboratory (Dieleman et al. 2015) experiments revealed that climate change conditions (warmer temperatures and increased CO₂) shift dominant plant communities from moss- to sedge-dominated which was not considered by the classic model for northern peatland succession.

1.4.2 Methylmercury production in northern peatlands

The type of northern peatland and associated nutrient status and hydrologic regime will govern net MeHg production (Tjerngren et al. 2012a, b). The presence of needed reactants required for Hg methylation (SO₄²⁻, bioavailable Hg(II), labile carbon substrates) in reduced peat soils control the potential for any northern peatland to methylate Hg. Branfireun et al. (1996) established the importance of northern peatlands, specifically moss-dominated peatlands as net MeHg producing ecosystems.

Methylmercury production and transport have been studied most in moss-dominated peatlands such as bogs and poor fens (Branfireun & Roulet 2002; Regnell & Hammar 2004; Mitchell et al. 2008a, b; Gordon et al 2016) with only limited attention given to more nutrient rich sedge-dominated peatlands (Tjerngren et al. 2012a, b). The known controls on net MeHg production in northern peatlands are important to consider when evaluating the Hg methylating potential of a given northern peatland. The microbial production of MeHg in the northern peatlands by SRB is controlled by abiotic environmental factors such as temperature, pH, bioavailable Hg(II), availability of the electron-acceptor (SO₄²⁻) and biotic factors such as species specific Hg methylation rates, microbial biomass, and competition for labile carbon substrate (i.e., electron donors).

Temperature has been shown to increase Hg methylation rates in several incubation studies (Sagemann et al. 1998; Sanz-Lazaro et al. 2011; St. Pierre et al. 2012), provided bioavailable Hg(II), labile carbon substrate, and electron-acceptors are available under anoxic conditions. Sulphate reduction rates and metabolically correlated MeHg

production rates (King et al. 2000) increase greatly between 10 and 35 °C before a rapid decline in conditions greater than 40 °C (Ingvorsen et al. 1981; Bak & Pfennig 1991; Robador et al. 2009). Peat soil temperatures affect methylation rates, but do not explain the variation in peatland net MeHg concentrations both within and across ecosystems. Instead, smaller-scale biogeochemical conditions have a greater effect on measured MeHg concentrations.

pH controls MeHg production as MeHg concentrations are typically higher under more acidic conditions and waters with greater total Hg to dissolved organic matter ratios because of greater bioavailable Hg(II) uptake by bacteria (Kelly et al. 2003). This mechanism results from an interaction between dissolved organic matter (DOM) and Hg(II) binding, with DOM becoming less negatively charged at more acidic pH levels and complexing less easily with Hg(II) (Kelly et al. 2003; Haitzer et al. 2003). In northern peatlands, pH is often a defining factor in determining peatland type, and it generally decreases as northern peatlands become moss-dominated and hydrologically decoupled (see Rydin and Jeglum 2013).

Divalent inorganic Hg is known to have a strong affinity with soil organic matter (SOM) and dissolved organic matter (DOM), resulting in most the soil Hg pool bound to carbon substrate (Åkerblom et al. 2008). Divalent Hg has an affinity to bind with thiols (R-SH) as well as other soft ligands (Riccardi et al. 2013). Binding constants for Hg(II) and DOM measured by Drexel et al. (2003) showed a preference for strong binding sites (thiols) at low Hg(II) concentrations and weaker binding sites (phenolics) at high Hg(II) concentrations. Bioavailable Hg(II) can still be bound to organic matter such as thiols or to inorganic sulfur (HgS), however, Hg(II) bound to phenols or complex high molecular weight humic molecules tends to remain unavailable for MeHg production (Gilmour et al. 1992; Barkay et al. 1997; Benoit et al. 1999; Graham et al. 2012). An important effect on partitioning between bound DOM-Hg and Hg-OM is the effect of pH, which increases bioavailable Hg(II) with decreasing pH (Haitzer et al. 2003). In pristine or non-contaminated environments, such as many northern peatlands, organic matter content and

quality (greater thiols or phenolics) along with pH greatly control the partitioning between Hg(II) unavailable and Hg(II) available along with Hg methylation rates (Kelly et al. 2003; Graham et al. 2012; Åkerblom et al. 2013).

Sulphate availability in reduced northern peatland soils regulates the metabolic activity of SRB and MeHg production (Mitchell et al. 2008b; Stickman et al. 2016). Sulphate tends to be limiting in northern peatlands because most sulphur is reduced or bound to organic matter (Novák & Wieder 1992) and direct SO_4^{2-} sources from precipitation, overland flow and groundwater are spatiotemporally constrained (Mitchell et al. 2009; Bergman et al. 2012). The sulphur pool in northern peatlands is partitioned into inorganic (e.g., SO_4^{2-} , FeS, H_2S) and organic forms (e.g., S- carbon bound, ester S) (Novák & Wieder 1992; Chapman & Davidson 2000). The sulphur pool available for Hg methylation is governed primarily by the supply of reduced and oxidized inorganic forms of sulphur (Novák & Wieder 1992; Coleman-Wasik et al. 2015). Within many northern peatland catchments, landscape units such as uplands, lakes and streams retain little sulphur and hence act as sources, whereas northern peatlands act as long-term sulphur sinks with short-term hydrologic regime changes (e.g., drought pulses) resulting in periodic sulphur releases (Devito 1995). Inputs of SO_4^{2-} transported to anoxic peat soils are derived from groundwater, overland flow (upland runoff), and precipitation (Evans et al. 1997). Deposition of sulphuric acid (acid rain) has resulted in SO_4^{2-} loading in many affected catchments in northeastern North America and industrial Europe; in the past 25 years many of these ecosystems have been steadily recovering (Devito et al. 1999; Sebestyen et al. 2011). Inputs of SO_4^{2-} tend to be assimilated quickly and reduced by SRB where then a majority of organic reduced sulphur becomes assimilated by vegetation (Bartlett et al. 2009). The rapid reduction of SO_4^{2-} by SRB can be regenerated *in situ* through oxidation of sulphides (Freeman et al. 1994; Dowrick et al. 2005). This occurs under drought conditions, where water table drawdown dewateres formally anoxic soil layers significantly increasing the amount of available SO_4^{2-} in reducing soils (Devito & Hill 1999; Dowrick et al. 2005). Northern peatland hydrology, especially water table position, controls SO_4^{2-} mobility even on small-scales (1-5 cm) through dispersion forces or fluxes

through micro- and macro-pores (Novák et al. 2005; Nunes et al. 2015). Regardless of source or delivery, SO_4^{2-} tends to be more limiting to MeHg production than labile carbon substrates (Mitchell et al. 2008b).

In northern peatlands, SRB and methanogens compete for labile carbon substrate (i.e., electron donors) in anoxic environments (Fauque 1995); typically SRB outcompete methanogens when SO_4^{2-} is available (see Muyzer & Stams 2008). The bacterial and fungal communities in northern peatlands are responsible for decomposition of carbon substrates with proportions of each community shifting depending on peatland nutrient status and hydrological regime (Winsborough & Basiliko 2010; Haynes et al. 2015; Nunes et al. 2015). In wetter and relatively more nutrient rich northern peatlands (e.g., sedge-dominated intermediate fens) methanogens may out compete SRB for labile carbon substrate if an overall higher water table maintains reduced conditions and limits SO_4^{2-} availability (Haynes et al. 2015). Despite these generalisations, spatial and temporal periods of water table drawdown in sedge-dominated intermediate fens may provide conditions suitable for greater net MeHg production suggesting a need for further investigation.

1.5 The implications of climate change on northern peatland ecosystems and effects on net methylmercury production

The abiotic and biotic controls on the production of MeHg in northern peatlands are linked to the nutrient status and hydrologic regime (water table depth and strength of groundwater connectivity) of a given peatland. Northern peatland nutrient status and hydrologic regime are sensitive to climate change (Gorham 1991; Waddington et al. 2015). Climate change effects on northern peatland decomposition biogeochemistry (Dieleman et al. 2016), dominant plant community (Dieleman et al. 2015; Buttler et al. 2015; Potvin et al. 2015) and hydrology (Waddington et al. 2015) are beginning to be elucidated, however, critical knowledge gaps still exist concerning the biogeochemistry influencing MeHg production. Known consequences of a changing climate affecting

northern peatlands are the frequency and duration of droughts (Dai 2012) alongside a shift in dominant plant community (moss to sedge) with increases in temperature and CO₂ (Dieleman et al. 2015; Buttler et al. 2015). Temperatures in the mid-latitudes of eastern North America are expected to increase by 1–5 °C by the end of the century; simultaneously, total annual precipitation is projected to increase by 0–20% with greatest change expected from October–March (Collins et al. 2013)

Although regions in mid-latitudes of North America are expected to see an increase in total annual precipitation (IPCC 2013), precipitation is likely to be more sporadic and occur at greater intensity leading to increased drought frequency and duration in the interim (Collins et al. 2013). Already, historical trends (1950–2000) have shown that drought frequency and duration have been increasing since the 1990s in North America (Sheffield & Wood 2007). A clear implication of drought in northern peatlands is water table drawdown (Waddington et al. 2015). Northern fen peatlands dominated by vascular plants (e.g., sedge-dominated fens) are particularly sensitive to evapotranspiration and drought-induced water table drawdown because of deeper rooting depths (Waddington et al. 2015). The impact of drought and subsequent water table drawdown and rebound have demonstrated the importance of *in situ* cycling of reduced to oxidized forms of sulphur to stimulate MeHg production after drought duration ends in moss-dominated northern peatlands (Coleman-Wasik et al. 2012, 2015). Similar results have yet to be observed in sedge-dominated northern fen peatlands.

Results from Dieleman et al. (2015), Buttler et al. (2015) suggest a need for researchers to better understand MeHg production in relation to northern peatlands' dominant plant community (moss or sedge) and associated nutrient status to predict future climate outcomes. To understand how moss- and sedge-dominated northern peatland MeHg production will change under a predicted vegetation shift, studying present day northern peatlands defined by moss- and sedge-dominance is a critical first step to understanding MeHg production under a changing climate. Likewise, temporal periods of *in situ* regeneration of SO₄²⁻ increases its availability following the re-oxidation of formally

anoxic peat soil and stimulates MeHg production following drought (Coleman-Wasik et al. 2015). While the influence and spatial patterning of groundwater connectivity and SO_4^{2-} gradients in fens correspond to higher porewater MeHg concentrations (Branfireun & Roulet 2002). These temporal and spatial patterns from previous studies invoke questions relating to the influence temporal variations of hydrologic regime in distinct northern peatland types (moss or sedge) and their influence on MeHg production. Seasonal and spatial observations and comparisons of two northern peatland fens, a moss-dominated poor fen and a sedge-dominated intermediate fen as representative northern peatland types can be used to decipher these knowledge gaps.

1.6 Thesis objectives

The net production of MeHg in northern peatlands is established (Branfireun et al. 1996; Mitchell et al. 2008a), however all types (e.g. sedge-dominated northern peatlands) are not well understood. Understanding the controls on net MeHg production is critical for predicting future outcomes for MeHg fate and transport in northern peatlands and their catchments. The overall object of my thesis research is to characterise the spatiotemporal patterns of, and physical and chemical controls on, MeHg concentrations in two understudied but important northern peatland types.

Specific objectives are to:

- 1) Compare THg, MeHg and other porewater chemistry in a sedge-dominated intermediate fen and a moss-dominated poor fen to determine if dominant plant community and nutrient availability influence net methylmercury production (Chapter 2).
- 2) Explore within-peatland spatial heterogeneity and temporal patterns of MeHg concentrations in a sedge-dominated intermediate fen to determine if concentrations are governed by internal surface drainages and groundwater nutrient supply (Chapter 3).

1.7 References

- Åkerblom S, Meili M, Bringmark L, Johansson K, Kleja DB, Bergkvist B (2008) Partitioning of Hg between solid and dissolved organic matter in humus layer of boreal forests. *Water, Air and Soil Pollution* 189: 239–252
- Åkerblom S, Bishop K, Björn E, Lambertsson L, Eriksson T, Nilsson MB (2013) Significant interaction effect from sulphate deposition and climate on sulfur concentrations constitute major control on methylmercury production in peatlands. *Geochimica et Cosmochimica Acta*: 1–11
- Amos, HM, Jacob DJ, Streets DG, Sunderland EM (2013) Legacy impacts of all-time anthropogenic emission on the global mercury cycle. *Global Biogeochemical Cycles* 27: 410–421
- Bak F & Pfennig (1991) Microbial sulfate reduction in littoral sediment of Lake Constance. *FEMS Microbiology Ecology* 85: 31–42
- Barkay T, Gillman M, Truner RR (1997) Effects of dissolved organic carbon and salinity on bioavailability of mercury. *Applied and Environmental Microbiology* 63: 4267–4271
- Barkay T, Miller SM, Summers AO (2006) Bacterial mercury resistance from atoms to ecosystems. *FEMS Microbiology Reviews* 37: 355–384
- Bartlett R, Bottrell SH, Coulson JP, Lee J, Forbes L (2009) 34S tracer study of pollutant sulfate behavior in a lowland peatland. *Biogeochemistry* 95: 261–275
- Bay RR (1969) Runoff from small peatland watersheds. *Hydrology* 9: 90–102
- Benoit JM, Gilmour CC, Mason RP, Heyes A (1999) Sulfide controls on mercury speciation and bioavailability to methylating bacteria in sediment pore waters. *Environmental Science & Technology* 33: 951–957
- Bergman I, Bishop K, Tu Q, Frech W, Åkerblom S, Nilsson M (2012) The influence of sulphate deposition on the seasonal variation of peat pore water methyl Hg in a boreal mire. *PLoS ONE* 7: e45547. Doi:10.1371/journal.pone.0045547
- Boelter DH & Verry ES (1977) Peatland and water in the northern lake states. USDA Forest Service Technical Report NC-31
- Branfireun BA, Heyes A, Roulet NT (1996) The hydrology and methylmercury dynamics of a Precambrian Shield headwater peatland. *Water Resource Research* 32: 1785–1794

- Branfireun BA, Roulet NT (2002) Controls on the fate and transport of methylmercury in a boreal headwater catchment, northwestern Ontario, Canada. *Hydrology and Earth Systems Sciences* 6: 785–794
- Buttler A, Robroek BJM, Laggouin-Défarge F, Jassey VE, Pochelon C, Bernard G, Delarue F, Gogo S, Mariotte P, Mitchell EAD, Bragazza L (2015) Experimental warming interacts with soil moisture to discriminate plant responses in an ombrotrophic peatland. *Journal of Vegetation Science* 26: 964–974
- Chapman & Davidson (2000) 35S-sulphate reduction and transformation in peat. *Soil Biology and Biochemistry* 33: 593–602
- Choi SC, Chase Jr T, Bartha R (1994) Metabolic pathways leading to mercury methylation in *Desulfovibrio desulfuricans*. *Applied Environmental Microbiology* 60: 4072–4077
- Coleman-Wasik JK, Mitchell CPJ, Engstrom DR Swain EB, Monson BA, Balogh SJ, Jeremiasson JD, Branfireun BA, Eggert SL, Kolka RK, Almendinger JE (2012) Methylmercury declines in a boreal peatland when experimental sulfate deposition decreases. *Environmental Science & Technology* 46: 6663–6671
- Coleman-Wasik JK, Engstrom DR, Mitchell CPJ, Swain EB, Monson BA, Balogh SJ, Jeremiasson JD, Branfireun BA, Kolka RK, Almendinger JE (2015) The effects of hydrologic fluctuation and sulfate regeneration on mercury cycling in an experimental peatland. *Journal of Geophysical Research: Biogeosciences* 120: 1697–1715
- Collins M, Knutti R, Arblaster J, Dufresne JL, Fichetef P, Friedlingstein P, Gao X, Gutowski WJ, Johns T, Krinner M, Shongwe M, Tebaldi C, Weaver AJ, Wehner M. (2013) Long-term climate change: Projections, commitments and irreversibility. In: *Climate change 2013: The physical science basis. Contributions of Working Group I to the fifth assessment report of the Intergovernmental Panel on Climate Change* (Stocker TF, Qin D, Plattner GK, Tignor M, Allen SK, Boschung J, Nauel A, Xia Y, Bex V, Midgley PM [eds]). Cambridge University Press, Cambridge, United Kingdom and New York, NY, USA.
- Compeau GC, Bartha R (1985) Sulphate-Reducing Bacteria: Principal methylators of mercury in anoxic estuarine sediment. *Applied Environment Microbiology* 50: 498–402
- Dai A (2012) Increasing drought under global warming in observations and models. *Nature Climate Change* 3: 52–58

- Dastoor AP, Larocque Y (2004) Global circulation of atmospheric mercury: a modelling study. *Atmospheric Environment* 38: 147-161
- Devito KJ & Hill AR (1999) Sulphate mobilization and porewater chemistry in relation to groundwater hydrology and summer drought in two conifer swamps on the Canadian shield. *Water, Air, and Soil Pollution* 113: 97-114
- Devito KJ (1995) Sulphate mass balance of Precambrian Shield wetlands: the influence of catchment hydrogeology. *Canadian Journal of Fisheries and Aquatic Sciences* 52: 1750-1760
- Devito KJ, Hill AR, Dillon PJ (1999) Episodic sulphate export from wetlands in acidified headwater catchments: predicting at the landscape scale. *Biogeochemistry* 44: 187-203
- Dieleman CM, Branfireun BA, McLaughlin JW, Lindo Z (2015) Climate change drives a shift in peatland ecosystem plant community: Implications for ecosystem function and stability. *Global Change Biology: gcb12643*
- Dieleman CM, Lindo Z, McLaughlin JW, Craig AE, Branfireun BA (2016) Climate change effect on peatland decomposition and porewater dissolved organic carbon biogeochemistry. *Biogeochemistry* 128: 385-396
- Dowrick DJ, Freeman C, Lock MA, Reynolds B (2005) Sulphate reduction and the suppression of peatland methane emission following summer drought. *Geoderma* 132: 384-390
- Drexel RT, Haitzer M, Ryan JN, Aiken GR, Nagy KL (2003) Mercury(II) sorption to two Florida everglades peats: Evidence for strong and weak binding and competition by dissolved organic matter released from the peat. *Environmental Science & Technology* 36: 4058-4064
- Driscoll CT, Mason RP, Chan HM, Jacob DJ, Pirrone N (2013) Mercury as a global pollutant: sources, pathways, and effects. *Environmental Science & Technology* 47: 4967-4983
- Evans HE, Dillon PJ, Molot LA (1997) The use of mass balance investigations in the study of the biogeochemical cycle of sulfur. *Hydrological Processes* 11: 765-782
- Fauque, GD (1995) Ch. 8: Ecology of sulphate reducing bacteria. *Sulphate Reducing Bacteria* (Ed. Barton L). Plenum Press, New York, New York. 217-241.

- Fitzgerald WF, Engstrom DR, Mason RP, Nater EA (1998) The case for atmospheric mercury contamination in remote areas. *Environmental Science & Technology* 32: 1–7
- Fleming EJ, Mack EE, Green PG, Nelson DC (2006) Mercury methylation from unexpected sources: molybdate-inhibited freshwater sediments and an iron-reducing bacterium. *Applied and Environmental Microbiology* 72: 457–464
- Freeman C, Hudson J, Lock MA, Reynolds B, Swanson C (1994) A possible role of sulphate in the suppression of wetland methane fluxes following drought. *Soil Biology and Biochemistry*. 10: 1439–1442
- Gilmour CC, Henry EA, Mitchell R (1992) Sulfate stimulation of mercury methylation in freshwater sediments. *Environmental Science & Technology*. 26: 2281–2294
- Gilmour CC, Podar M, Bullock, Graham AM, Brown SD, Somenahally AC, Johns, A, Hurt RA, Bailey KL, Elias DA (2013) Mercury methylation by novel microorganisms from new environmental. *Environmental Science & Technology* 47: 11810–11820
- Gordon J, Quinton W, Branfireun BA, Olefeldt D (2016) Mercury and methylmercury biogeochemistry in a thawing permafrost wetland complex, Northwest Territories, Canada. *Hydrological Processes* 30: 3627–3638
- Gorham E (1991) Northern Peatland: Role in the carbon cycle and probable responses to climate warming. *Ecological Application* 1: 182–195
- Graham AM, Aiken GR, Gilmour CC (2012) Dissolved organic matter enhances microbial mercury methylation under sulfidic conditions. *Environmental Science & Technology* 46: 2715–2723
- Haitzer M, Aiken GR, Ryan JN (2003) Binding mercury(II) to aquatic humic substances: Influence of pH and source of humic substances. *Environmental Science & Technology* 37: 2436–2441
- Harada M (1995) Minamata Disease: Methylmercury poisoning in Japan caused by environmental pollution. *Critical Reviews in Toxicology* 25: 1–24
- Haynes KM, Preston MD, McLaughlin JW, Webster K, Basiliko N (2015) Dissimilar bacterial and fungal decomposer communities across rich to poor fen peatlands exhibit functional redundancy. *Canadian Journal of Soil Science* 95: 219–230
- Ingram HAP (1982) Size and shape in raised mire ecosystems: a geophysical model. *Nature* 297: 300–303

- Ingvorsen K, Zeikus JG, Brock TD (1981) Dynamic of bacterial sulfate reduction in a eutrophic lake. *Applied and Environmental Microbiology* 42: 1029–1036
- IPCC, 2013 Annex I: Atlas of global and regional climate projections [van Oldenborgh GM, Collins M, Arblaster JH, Christensen J, Marotzke J, Power SB, Rummukainen, Zhou T (eds.)] In: *Climate Change 2013: The physical science basis. Contributions of the Working Group I to the fifth assessment report of the Intergovernmental Panel on Climate Change* (Stocker TF, Qin D, Plattner M, Tignor SK, Allen J, Boschung A, Nauels, Y, Xia V, Bex V, Midgley PM [eds.]) Cambridge University Press, Cambridge, United Kingdom and New York, NY, USA.
- Jones CG, Lawton JH, Shachak M (1994) Organisms as ecosystems engineers. *Oikos* 69: 373–386
- Johnson MG, Granath G, Tahvanainen T, Pouliot R, Stenøien HK, Rochfort L, Rydin H, Shaw AJ (2014) Evolution of niche preference in *Sphagnum* peat moss. *Evolution* 69: 90–103
- Kelly CA, Rudd JWM, Holoka MH (2003) Effect of pH on mercury uptake by an aquatic bacterium: implications for Hg cycling. *Environmental Science & Technology* 37: 2941–2946
- King JK, Kostka JE, Frischer ME, Saunders FM (2000) Sulphate-reducing bacteria methylate mercury at variable rates in pure culture and in marine sediments. *Applied and Environmental Microbiology* 66: 2420–2437
- Krabbenhoft DP, Benoit JM, Barbiarz CL, Hurley JP, Andren AW (1995) Mercury cycling in the Allequash Creek watershed, northern Wisconsin. *Water, Air and Soil Pollution* 80:425–433
- Mergler D, Anderson HA, Chan LHM, Mahaffey KR, Murry M, Sakamoto M, Stern AH (2007) Methylmercury exposure and health effects in humans: A worldwide concern. *Journal of the human Environment* 36: 3–11
- Mitchell CPJ, Branfireun BA, Kolka RK (2008a) Spatial characteristics of net methylmercury production hot spots in peatlands. *Environmental Science & Technology* 44: 1010–1016
- Mitchell CPJ, Branfireun BA, Kolka RK (2008b) Assessing sulphate and carbon controls on net methylmercury production in peatland: An *in situ* mesocosm approach. *Applied Geochemistry* 23: 503–518

- Mitchell CPJ, Branfireun BA, Kolka RK. (2009) Methylmercury dynamics at the upland-peatland interface: Topographic and hydrogeochemical controls. *Water Resources Research* 45: W02406
- Morel FMM, Kraepiel AML, Amyot M (1998) The chemical cycle and bioaccumulation of mercury. *Annual Review of Ecology, Evolution and Systematics* 29: 534–566
- Muyzer G, Stams AJM (2008) The ecology and biotechnology of sulphate-reducing bacteria. *Nature Reviews: Microbiology* 1892–1906
- Novák M, Wieder RK (1992) Inorganic and organic sulfur profiles in nine *Sphagnum* peat bogs in the United States and Czechoslovakia. *Water, Air and Soil Pollution* 65: 353–369
- Novák M, Adamová M, Wieder RK, Bottrell SH (2005) Sulfur mobility in peat. *Applied Geochemistry* 20: 673–681
- Nunes FLD, Aquilina L, Ridder JD, Francez AJ, Quaiser A, Caudal JP, Vandenkoornhuyse, Dufresne A (2015) Time-scales of hydrological forcing on the geochemistry and bacterial community structure of temperate peat soils. *Nature Scientific Reports* 5:14612–14622
- Parks JM, Johs A, Podar M, Bridou R, Hurt RA, Smith SD, Tomanicek SJ, Qian Y, Brown SD, Brandt CC, Palumbo AV, Smith JC, Wall JD, Elias DA, Liang L (2013) The genetic basis for bacterial mercury methylation. *Science* 339: 1332–1335
- Pirrone N, Mason R (Eds.) (2009) Mercury fate and transport in the global atmosphere: Emissions, measurements and models. Springer-Verlag New York, USA. PP: 1–47
- Pirrone N, Cinnirella S, Fend X, Finkelman RB, Friedli HR, Leaner J, Mason R, Mukherjee AB, Stracher GB, Streets DG, Telmer K (2010) Global mercury emissions to the atmosphere from anthropogenic and natural sources. *Atmosphere Chemistry and Physics* 10: 5951–5964
- Potvin LR, Kane ES, Chimner RA, Kolka RK, Lilleskov, EA (2015) Effects of water table position and plant functional group on plant community, aboveground production, and peat properties in peatland mesocosm experiment (PEATcosm). *Plan Soil* 387: 277–713
- Raccardi D, Guo HB, Parks JM, Gu B, Summers AO, Miller SM, Liang L, Smith JC (2013) Why mercury prefers soft ligands. *The Journal of Geophysical Letters* 4: 2317 –2322

- Regnell O, Hammar T (2004) Coupling of methyl and total mercury in a minerotrophic peat bog in southeastern Sweden. *Canadian Journal of Fisheries and Aquatic Sciences* 61: 2014–2023
- Robador A, Bruchert V, Jorgensen BB (2009) The impact of temperature on the activity and community composition of sulphate-reducing bacteria in arctic versus temperate marine sediments. *Environmental Microbiology*. 11: 1692–1703
- Roulet N (1990) The hydrological role of peat-covered wetlands. *The Canadian Geographer* 34: 82–83
- Rydin H, Jeglum JK (2013) *The Biology of Peatlands*, 2nd Edition. Oxford University Press, Oxford, United Kingdom. PP: 127–147
- Sagemann J, Jorgensen BB, Greeff O (1998) Temperature dependence and rates of sulphate reduction in cold sediments of Svalbard, Arctic Ocean. *Geomicrobiology* 15: 85–100
- Sanz-Lazaro C, Valdemarsen T, Marin A, Holmer M (2011) Effect of temperature on biogeochemistry of marine organic-enriched systems: implications in a global warming scenario. *Ecological Applications* 21: 2664–2677
- Sebestyen, SD, Dorrance, C, Olson, DM, Verry, ES, Kolka, RK, Elling, AE Kyllander, R. (2011) Ch. 2: Long-term monitoring sites and trends at the Marcell Experimental Forest. *Peatland Biogeochemistry and Watershed Hydrology at the Marcell Experimental Forest*: 15–71. CRC Press, LLC Boca Raton, Florida, USA.
- Sellers P, Kelly CA, Rudd JWM, MacHutchon AR (1996) Photodegradation of methylmercury in lakes. *Nature* 380: 6576–6580
- Sheffield J, Wood EF (2007) Global trends and variability in soil moisture and drought characteristics, 1950-2000, from observation-driven simulation of terrestrial hydrologic cycle. *Journal of Climate* 21: 432–458
- Siegel DI, Glaser PF (1987) Groundwater flow in a bog-fen complex, Lost River Peatland, northern Minnesota. *Journal of Ecology* 75: 743–754
- St. Louis VL, Rudd JWM, Kelly CA, Beaty KG, Bloom NS, Flett RJ (1994) Importance of wetlands as sources of methylmercury to boreal forest ecosystems. *Canadian Journal of Fisheries and Aquatic Sciences* 51: 1065–1076
- St. Louis VL, Rudd JWM, Kelly CA, Beaty KG, Flett RJ, Roulet NT (1996) Production and loss of methylmercury and loss of total mercury from boreal forest

- catchments containing different types of wetlands. *Environmental Science & Technology* 30: 2719–2729
- St. Pierre KA, Chételat J, Yumvihoze E, Poulin AJ (2014) Temperature and sulfur cycle control monomethylmercury cycling in high Arctic coastal marine sediments from Allen Bay, Nunavut, Canada. *Environmental Science & Technology* 48: 2680–2687
- Stickman RJS, Fulthorpe RR, Coleman-Wasik JK, Engstrom DR, Mitchell CPJ (2016) Experimental sulfate amendment alters peatland bacterial community structure. *Science of the Total Environment* 566-567: 1289–1296
- Streets DG, Devane MK, Lu Z, Bond TC, Sunderland EM, Jacob DJ (2011) All-time releases of mercury to the atmosphere from human activities. *Environmental Science & Technology* 45: 10485–10491
- Tjerngren I, Karlsson T, Björn E, Skjällberg U (2012a) Potential Hg methylation and MeHg demethylation rates related to the nutrient status of different boreal wetlands. *Biogeochemistry* 108: 335–350
- Tjerngren I, Meili M, Björn E, Skjällberg U (2012b) Eight boreal wetland as sources and sinks for methylmercury in relation to soil acidity, C/N ratio, and small-scale flooding. *Environmental Science & Technology* 46: 8052–8060
- Turunen J, Tomppo E, Tolonen K, Reinikainen A (2002) Estimating carbon accumulation rate of undrained mires in Finland-application to boreal and subarctic regions. *The Holocene* 12: 69–80
- U.S. National Research Council (2000) *Toxicological Effects of Methylmercury*. National Academy Press. Washington D.C.
- UNEP (2013) *Global Mercury Assessment 2013: Sources, emissions, releases and environmental transport*. UNEP Chemicals Branch, Geneva, Switzerland. PP: 19-37
- van Bremen N (1995) How *Sphagnum* bogs down other plants. *Trends in Ecology and Evolution* 10: 270–275
- Waddington JM, Morris PJ, Kettridge N, Granath G, Thompson DK, Moore PA (2015) Hydrologic feedbacks in northern peatlands. *Ecohydrology* 8: 113–127
- Winsborough C, Basiliko N (2010) Fungal and bacterial activity in northern peatlands. *Geomicrobiology Journal* 27: 315–320

Chapter 2

2 Porewater total mercury and methylmercury in two different northern fen peatland types

2.1 Introduction

Methylmercury presents a risk to aquatic ecosystems and fish consumers through bioaccumulation and biomagnification in aquatic food webs resulting in concentrations that can affect the nervous and endocrine systems of higher trophic level organisms such as piscivorous fish, birds, and humans (UNEP 2013). Northern peatlands are known sources of MeHg to the aquatic environment (Driscoll et al. 1994; Rudd 1995; St. Louis et al. 1996; Branfireun et al. 1996). Sulphate reducing bacteria are the principle microorganisms responsible for MeHg production which occurs when bioavailable divalent Hg(II) binds with a methyl group ($-\text{CH}_3$) as by product during SRB respiration (Compeau & Bartha 1985; Choi et al. 1994). Limiting reactants to MeHg production are SO_4^{2-} as an electron acceptor, labile carbon sources as electron donors (Mitchell et al. 2008b), and bioavailable Hg (II) (Haitzer et al. 2002). Methylmercury produced in northern peatlands can be transported to connected streams and lakes at varying efficiencies depending on peatland hydrological connectivity to surface waters and temporal hydrologic conditions (Branfireun & Roulet 2002; St. Louis et al. 2004). Once present in freshwater aquatic ecosystems such as lakes and streams, MeHg is the principle form (often assumed to be ~95%) of Hg found in fish (Bloom 1992). It has been known for over two decades that lakes receiving greater inputs from wetlands have higher observed MeHg concentrations (St. Louis et al. 1994).

Northern peatlands (north of 45°) are peat accumulating wetlands (> 40 cm) found throughout the boreal regions of Canada, Russia, Scandinavia and in the northern states of Alaska, Minnesota and Michigan in the United States (Gorham 1991; Rydin & Jeglum 2013). Northern peatland types exist on a continuum of decreasing nutrient status and hydrologic connectivity which transition over time (Zoltai & Vitt 1995). The classical successional stages for northern peatlands are rich fen $>$ intermediate fen $>$ poor fen $>$

bog (Rydin & Jeglum 2013). Rich fens and intermediate fens have greater hydrologic connectivity than poor fens and bogs along with greater concentrations of nutrients (Vitt & Chee 1990; Zoltai & Vitt 1995). Succession of northern peatlands is not unidirectional however, disturbances such as flood, wildfires, and climate change can revert peatlands to previous nutrient and hydrologic statuses (Rydin & Jeglum 2013; Waddington et al. 2015).

The effects of climate change include warmer atmospheric temperatures (+1–5 °C above ambient by 2100 in more mid to northern latitudes) in concert with more variable precipitation inputs leading to increased drought frequency and duration in the mid- and high latitudes of eastern North America (Collins et al. 2013; IPCC 2013), where northern peatlands are most abundant (Gorham 1991; Zoltai & Vitt 1995). Experimental results from a mesocosm study applying +4 and +8 °C above ambient temperatures showed that intact moss-dominated poor fen peat monoliths shifted to sedge-dominated at elevated temperatures (Dieleman et al. 2015). Additionally, a mesocosm field experiment in a moss-dominated peatland in the Jura Mountains of France by Buttler et al. (2015) where peat soils were warmed 1–5 °C above ambient suggested increased vascular plants benefited most as well. The implications of Dieleman et al. (2015) and Buttler et al. (2015) suggested a reversal of northern peatland succession, from moss to sedge. The effects of drought and corresponding hydrologic feedbacks (e.g., increased aerobic decomposition, decreasing hydrologic connectivity, increased shrub growth) relating to water table drawdown affect decomposition, water movement and plant community structure in northern peatlands as well (see Waddington et al. 2015). A factorial mesocosm water table manipulation experiment (high and low treatments × 3 plant functional groups) using transported intact peat monoliths in the upper peninsula of Michigan, USA showed that a lower water table benefitted vascular plants most. Water table drawdown is known to affect biogeochemical processes in peat soils (e.g., methanogenesis, decomposition) through exposing previously saturated peat to aerobic conditions, including methylmercury production through the regeneration of SO_4^{2-} the

electron acceptor of SRB (Coleman-Wasik et al. 2015), a limiting reactant in MeHg production (Branfireun et al. 1999; Jeremiason et al. 2006).

While many studies concerning MeHg production and fate in northern peatlands have focused on moss-dominated poor fens and bogs (Branfireun et al. 1996; Heyes et al. 2000; Branfireun & Roulet 2002; Regnell & Hammar 2004; Mitchell et al. 2008a,b; Gordon et al. 2016), few studies have examined a gradient of peatland types which included higher nutrient status sedge-dominated fens (notable exceptions being Tjerngren et al. 2012a, b), highlighting the need for further comparisons between higher and lower nutrient peatlands. Tjerngren et al. (2012a, b) showed that a northern peatland fen with an intermediate nutrient status, pH ~5, and sedge-dominated vegetation had the highest net MeHg production, greater than production in low nutrient moss-dominated bogs and poor fens and higher nutrient rich fens using field and laboratory methods.

Placing the results of Tjerngren et al. (2012a, b) within the context of a climate change driven shift in dominant plant community (Dieleman et al. 2015; Buttler et al. 2015) and hydrologic feedbacks (Potvin et al. 2015; Waddington et al. 2015) raises research questions relating to the overall MeHg production in moss- and sedge-dominated fen peatlands. Specifically, in relation to chemical variables such as dissolved organic carbon, major ions, pH, peatland hydrology regime (long-term patterns) and temporal hydrologic fluctuations (short-term patterns), which are all associated with dominant plant community (Boelter & Verry 1977; Vitt & Chee 1990).

In this study, the temporal patterns of porewater MeHg concentrations and other chemical variables across a sedge-dominated (*Carex* spp. L.) intermediate fen are compared to that of a moss-dominated (*Sphagnum* spp. L.) poor fen over one growing season (June–September) and after fall plant senescence (October) in two northern peatlands found in the southern boreal region of Northern Ontario, Canada. A previous study by Webster & McLaughlin (2010) found significant differences between major ions, dissolved carbon, and pH between the sedge- and moss-dominated peatlands in this study; showing greater amounts of dissolved inorganic carbon and major ions along with more alkaline pH in the

sedge-dominated intermediate fen compared to the moss-dominated poor fen. The objective of this study was to compare THg, MeHg and other porewater chemistry (major ions, dissolved carbon, pH) in a sedge-dominated intermediate fen and a moss-dominated poor fen to determine if northern fen peatland type, nutrient availability, and/or temporal hydrologic variation control net methylmercury production. From these objectives two hypotheses were formed:

Hypothesis 1: Temporal periods (weeks to months) of water table drawdown will increase porewater sulphate concentrations and explain patterns of MeHg concentrations observed in porewaters from a sedge-dominated intermediate fen and moss-dominated poor fen.

Hypothesis 2: Consistently higher concentrations of dissolved organic carbon and lower pH conditions at the moss-dominated poor fen will lead to greater THg and MeHg concentrations compared to the sedge-dominated intermediate fen.

2.2 Methods

2.2.1 Study site description

This study was conducted in Northern Ontario, in an intermediate and poor fen (48.35 °N, -85.34 °W) (Figure 2.1). The sites are located 40 km south-southwest of White River, Ontario, Canada and are situated 1.0 km apart in an 817 ha sub-watershed of the Lake Superior Drainages Basin. Both sites are long-term research ecosystems for the Ministry of Natural Resources and Forestry (MNR) based in Sault St. Marie, ON. Elevations in the watershed range from 400 to 600 masl (McLaughlin & Webster 2010). Upland forest soils are bouldery, coarse, loamy sand, mixed, frigid Typic Podzol underlain by shallow dense basal till and Precambrian bedrock (McLaughlin & Webster 2010). The surrounding upland boreal-mixed wood forest consists primarily of white birch (*Betula papyrifera* Marsh.), balsam fir (*Abies balsamea* [L.] Mill), black spruce (*Picea mariana* [Mill.] B.S.P.), with small stands of jack pine (*Pinus banksiana* Lamb.), trembling aspen (*Populus tremuloides* Michx.) and white spruce (*Picea glauca* [Moench.] Voss.). Climate

normals (1981–2010) from nearby Wawa Airport (47.96° N, -84.78° W) report mean monthly temperatures ranging from -14° C in January to 15.3°C in August with mean annual precipitation 970 mm, 320 mm of which as snowfall (Environment Canada), The average growing season ranges from 70 and 100 days per year (McLaughlin 2009).

The 4.5 ha poor fen is characterised by acidic porewaters (pH 4–5) and water inputs primarily from precipitation and to a lesser extent, shallow groundwater (Figure 2.1D). Vegetation is dominated by mosses (*Sphagnum* spp. L.), ericaceous shrubs such as bog Labrador tea (*Rhododendron groenlandicum* Oeder.) and leatherleaf (*Chamaedaphne calyculata* [L.] Moench.), with stunted black spruce (*Picea mariana* [Mill.] B.S.P.) and

tamarack (*Larix laricina* [Du Roi.] K. Koch.) forming a sparse canopy (see Appendix A: Figure A1 and Figure A2 for site photos). Peat is 1.5–3.5 m thick (Myers et al. 2012).

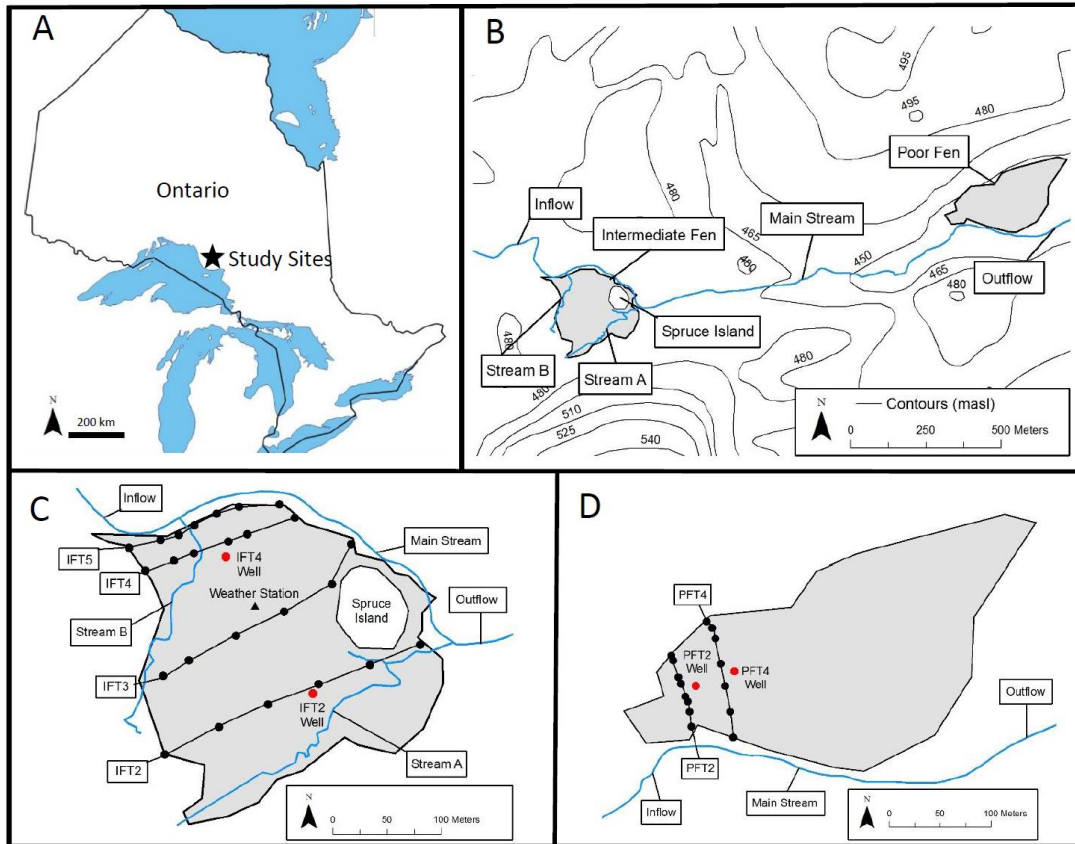


Figure 2.1: Intermediate and Poor Fen site map.

Locations of study sites (48.35 °N, -85.34 °W) in Northern Ontario (A). Proximity of sedge-dominated intermediate fen (gray shading) to moss-dominated poor fen (gray shading) and surrounding upland topography (B). Intermediate fen shown (C) with major infrastructure (transects, reference wells and weather station). Poor fen shown (D) with major infrastructure (transects and reference wells).

The water table is typically below the peat soil surface. Two previously established MNRF transects, PFT2 and PFT4 were sampled for porewater chemistry and were 50 and

88 m in length, respectively. Each transect ran the width of fen from upland to the bordering stream. Porewater samples were from 50 cm piezometers, 5 cm I.D. Schedule 40 PVC (polyvinyl chloride) slotted 20 cm and wrapped in Nitex® mesh (200µm mesh size). The MNRF previously installed the 50 cm piezometers were to a depth of 50 cm and integrated porewaters from 30 to 50 cm below the peat surface. Two MNRF reference wells adjacent to PFT2 and PFT4 have pressure transducers (Solinst® Levelogger II®), which measure total pressure (atmospheric + hydraulic head) in cm-H₂O (accuracy 0.1 %) and temperature (accuracy 0.1 °C) ever 15 minutes throughout the frost-free season. To calculate water table level (cm-H₂O above pressure transducer), I used barometric pressure measured from a pressure transducer recording at soil surface level was subtracted from each wells' pressure transducer.

The intermediate fen is a 5.3 ha northern peatland with sedge (*Carex* spp. L.) and ericaceous shrubs sweet gale (*Myrica gale* L.) as dominant vegetation types (Figure 2.1C). Porewaters are acidic to circumneutral pH (5.5–7) and porewaters reflect groundwater connectivity; with higher base cation concentrations of calcium (Ca²⁺) (≥ 10 mg/L) and magnesium (Mg²⁺) (≥ 1.9 mg/L) and dissolved inorganic carbon (DIC) (≥ 30 mg/L) than the poor fen (McLaughlin & Webster 2010; Webster & McLaughlin 2010), which characterise the fen an intermediate fen (moderately rich fen) peatland (Vitt & Chee 1990). Though mostly a treeless low gradient peatland, limited micro-topography development can be observed in hummocks consisting of moss (*Sphagnum* spp. L.) and sweet gale (*Myrica gale* L.) with sparse tamarack (*Larix laricina* [Du Roi.] K. Koch.) (see Appendix A: Figure A3 for a site photo). Peat soil is 0.5–3 m thick (Myers et al. 2012). Underlying peat soils are coarse sandy deposits and compacted fine sandy sediment (McLaughlin and Webster 2010). Incised primary rivulets (Stream A and Stream B) segment the low gradient intermediate fen surface and include several secondary rivulets. The primary rivulets are perennial and drain into a main stream, which flows along the east-southeast peatland boundary. The water table is typically near the surface of the peat with diurnal and seasonal fluctuations depending on evapotranspiration and precipitation. Four MNRF transects 135, 52, 89, and 100 m in

length divide the west-east length of the intermediate fen and are separated by 25 m. Transects are henceforth referred to as IFT2, IFT3, IFT4, IFT5 and except for IFT5 with 7 piezometer locations, have 6 piezometers locations each. Porewater samples were from 50 cm piezometers. Similar to the poor fen, two reference wells and, a barometric pressure recorder were instrumented with Solinst® LeveloggersII® and measured total pressure (cm-H₂O) every 15 minutes.

2.2.2 Hydrology and site surveys

Myself and MNRF collaborators made water table measures and purged sampling piezometers using a peristaltic pump 18–24 hours prior to collecting porewaters samples. We used a 5 m measuring tape to make manual measures of water tables levels. We determined the water table level by visual contact of tape measure end with water surface. Levels were recorded from top of piezometer with 0.5 cm precision. I conducted infrastructure and site surveys of both the intermediate fen and poor fen using differential global positioning system (DGPS) equipment (Topcon HiPer Ga) (Topcon Positioning Systems Canada, Inc.). I made a total of 284 and 68 survey points (North [m], East [m], Elevation [m]) from the intermediate fen and poor fen, respectively.

2.2.2.1 Water chemistry

We collected porewater samples once monthly in concert with MNRF collaborators' monthly sample regime. Porewater sampling occurred on June 27, July 19, August 16, September 20, and October 12 in the PF. While in the IF, porewater sampling occurring on June 28, July 20, August 17, September 21, and October 12. For Hg sampling, I collected a field duplicate sample every ten samples at each site. For all porewater sampling we purged entire piezometer sampling volume 18–24 hours prior to porewater sampling. I pre-cleaned all Hg sampling equipment prior to sampling using ultraclean techniques. Peristaltic pump tubing and 2 L high density polyethylene (HDPE) 18.2 MOhm H₂O (Milli-Q H₂O) field bottles were all acid washed in 10% hydrochloric acid bath, rinsed 3 times using 18.2 MOhm H₂O, dried completely, and double ziplock bagged before use. We collected porewater samples for Hg from 50 cm deep piezometers using a

peristaltic pump (Geotech Environmental Equipment, Inc.) fitted with Masterflex® C-FlexUltra tubing (Cole-Palmer Instrument Co.). We used double-bagged sterile or ultracleaned 250 mL PETG (polyethylene terephthalate glycol-modified) (Thermo Scientific™ Nalgene™) bottles for Hg samples. Prior to pumping any porewater in the sample bottle, we cleared an equivalent tube volume (~50–100 mL) of porewater through the sampling tubing. We stored samples in a cooler until arriving back at the field laboratory facility, where they were refrigerated at ~4 °C. Between samples, we pumped 18.2 MOhm H₂O through the sampling line by ‘clean hands’, as ‘dirty hands’ operated the peristaltic pump. At the end of sampling, 18.2 MOhm H₂O was pumped through the sample line and served as a quality assurance/quality control (QA/QC) pump blank.

Field porewater pH and conductivity ($\mu\text{S m}^{-1}$) were measured the day of sampling in the field by MNRF collaborators using an Oakton 10 Series pH/conductivity/temperature meter in 50 piezometers along transects PFT2, PFT4, IFT2, IFT3, IFT4 and IFT5. Ministry collaborators recorded pH and conductivity to 0.01 and 0.1 precision, respectively.

Ministry collaborators collected porewater samples for dissolved inorganic and organic carbon, and major ions the same day as I collected porewater Hg samples using a their own peristaltic pump (Geotech Environmental Equipment, Inc.) and MasterFlex® tubing. They collected samples in 500 mL opaque high-density polyethylene (HDPE) bottles and stored at ~4 °C until arriving at the Ontario Forestry Research Institute (OFRI) in Sault Ste. Marie, Ontario where samples were then filtered in preparation for analysis by the MNRF.

After collection, I brought back porewater Hg samples to nearby field laboratory (40 km drive) and where we then filtered each sample using 0.5 μm glass fibre filters (Macherey-Nagel™). We used clean techniques to change filters, rinse filtration equipment with 18.2 MOhm and handle samples. After filtration, I immediately preserved each sample using 0.5% by volume OmniTrace® hydrochloric acid (0.1 ppb Hg max). After the end of each filtering session, we ran 18.2 MOhm H₂O through the filtration equipment into a sample

bottle to create a filter blank. We filtered and preserved all Hg samples within 12 hours of collection and stored samples in field laboratory refrigerators at 4° C. All filtering equipment, which through the operation of filtering porewater samples came in contact, were made from fluoropolymers. I acid washed (10% hydrochloric acid) all filtering equipment and rinsed the equipment three times with 18.2 MOhm H₂O before and after each filtration session.

2.2.3 Analytical methods

Porewater Hg samples were brought to the Biotron Analytical Service Laboratory (Western University, London, ON) and stored at 4°C until I analysed each for THg and MeHg. Porewater samples were analysed for major ions and dissolve inorganic and organic carbon at Ontario Forestry Research Institute (OFRI) in Sault Ste. Marie, ON by MNRF staff.

2.2.3.1 Total mercury in water

I conducted THg analysis following the methods described by the United States Environment Protection Agency (U.S. EPA) Method 1631. To measure THg in water, I poured out 25.0 mL aliquots from each sample and oxidized each using bromine monochloride (BrCl) solution in 40 mL sterile borosilicate clear glass vials fitted with Teflon™ lined septum and polyethylene caps. Once I added BrCl, I shook the aliquots with caps on and then caps were removed. I then left the caps off the glass bottles for 10 minutes to allow BrCl to react prior to recapping glass vials. I then allowed BrCl oxidation to occur for a minimum of 12 hours with aliquots stored in the dark at room temperature. The following day, I reduced the aliquots using hydroxylamine hydrochloride (NH₂OH-HCl) to remove free halogens. Finally, prior to analysis, I added stannous chloride (SnCl₂) to convert Hg(II) to Hg(0). Using a Tekran® Series 2600 (Tekran, Inc.) Hg(0) was purged from capped clear glass vials using Ultra High Purity 5.0 nitrogen gas (Praxair Canada, Inc.). The Tekran® Series 2600 uses cold vapour atomic fluorescence (CVAf) spectroscopy to quantify total Hg. I analysed duplicate analytical and field samples, matrix spikes, method blanks and check standard (OPRs)

samples according to prescribed U.S. EPA 1631 methods and I analysed samples again if quality assurance and quality controls (QA/QC) failed to meet EPA 1631 recovery protocols. My recoveries for field duplicates (mean \pm standard error, sample size) were ($101 \pm 13\%$, $n= 33$), while my recoveries for analytical duplicates, matrix spikes and OPRs were ($99 \pm 6\%$, $n= 55$), ($101 \pm 10\%$, $n= 107$), ($101 \pm 13\%$, $n= 82$), respectively. The Biotron Analytical Services Laboratory reports a THg method detection limit (MDL) of $0.05 \text{ ng-Hg L}^{-1}$ and a minimum reporting level (MRL) of $0.14 \text{ ng-Hg L}^{-1}$. I analysed all THg samples within 90 days after preservation.

2.2.3.2 Methylmercury in water

I used the U.S. EPA Method 1630 for the analysis of methylmercury in porewater and stream water samples. I analysed all MeHg samples on a Tekran® Model 2700 Automated Methyl Mercury Analysis System. I distilled 40 mL aliquots using Ultra High Purity 5.0 nitrogen gas (Praxair Canada, Inc.) at $125 \text{ }^\circ\text{C}$ using 60 mL Teflon® distillation vessels and polyfluorinated plastic tubing into clear 50 mL borosilicate glass vials. Prior to distillation I added APDC (ammonium pyrrolidine dithiocarbamate) to each 40 mL aliquot to chelate MeHg. After the distillation, I stored samples at room temperature in the dark before final analysis preparation the following day. The following day, I poured out 30 mL of distillate into sterile clear 40 mL borosilicate glass vials fitted with Teflon™ septum and polyethylene caps in preparation for analysis. I then added ascorbic acid ($\text{C}_6\text{H}_8\text{O}_6$) and 2M-acetate buffer (CH_3CO_2) to each sample to remove free halogens and adjust pH to 4.5, respectively. Lastly, I added NaBEt_4 (sodium tetraethyl borate) to ethylate MeHg compounds which was then purged from borosilicate glass vials using pure argon gas (Praxair Canada, Inc.). Tekran® Model 2700 uses a gas chromatography separation of inorganic and organic Hg species followed by CVAf spectroscopy to quantify MeHg. In accordance to U.S. EPA Method 1630, I distilled and analysed matrix spikes, method blanks, OPRs, and field and analytical duplicates for QA/QC. If QA/QC failed, I distilled and analysed subjected samples again. My MeHg QA/QC recoveries for field duplicates, analytical duplicates, matrix spikes and OPRs (mean \pm standard error, sample size) were, ($99 \pm 7\%$, $n= 27$), ($101 \pm 9\%$, $n= 62$), ($90 \pm 8\%$, $n= 124$), ($94 \pm 7\%$,

n= 66), respectively. The MDL for MeHg analysis was 0.006 ng-Hg L⁻¹ and MRL of 0.02 ng-Hg L⁻¹. All MeHg water samples were analysed within 180 days after preservation.

2.2.3.3 Major ions, total nitrogen, and dissolved organic and inorganic carbon in water

Prior to analysis for major ions and dissolved inorganic (DIC) and organic carbon (DOC), samples MNR staff filtered samples through Gelman 0.45 µm filters. Ministry staff analysed anions (HCO₃⁻, Cl⁻, NO₂⁻, NO₃⁻, HPO₄²⁻, SO₄²⁻) on a Dionex Ion Chromatography ICS 2000. Cations (Ca²⁺, Mg²⁺, K⁺, Na⁺) were analysed on a Varian Liberty Series II ICP-OES. Ministry staff measured Total (Kjeldahl) nitrogen (TN) as liberated NH₄⁺ ions using a flow injection system TRAACS 800 (Bran+Luebbe Nordestadt, Germany) auto-analyser. To analyse DOC and DIC MNR staff used a Shimadzu TOC 500. For all analytes, the MNR requires recoveries for duplicates and matrix spikes to be ±10%.

2.2.4 Statistical methods

I used the open statistical platform R.64 version 3.4.0 and Microsoft Excel for all descriptive statistical analysis and data visualisation. For censored major ion data (i.e. non-detects) below the detection limit of 0.01 mg/L, a substitution method (i.e. assigning a value for non-detects) described by Antweiler & Taylor (2008) was employed; where non-detects were assigned a value of 50% the detection limit. There were 26 SO₄²⁻ samples from the intermediate fen and 3 from the poor fen that required substitution. Rather than utilize test statistics (e.g., ANOVAs, *t*-tests) to calculate significant *P*-values, we assumed non-independence with our data set and instead simple compared differences in porewater concentrations.

2.3 Results

2.3.1 Climate and hydrology

Mean monthly temperatures (June–October 2016) were highest in July (16.8 °C) and lowest in October (6.33 °C). July and August were the wettest and driest months with

156.8 mm and 79.9 mm total precipitation, respectively. At the moss-dominated PF the maximum (mean of two reference wells) water table occurred on June 8, 2016, resting 9.2 cm below the peat surface (Figure 2.2). On August 19, 2016, the water table dropped to a minimum of 38 cm below the peat surface whereupon it rose steadily in response to increasing precipitation throughout the duration of late summer and fall. Mean (and standard deviation) poor fen water table level was -21.1 (6.1) cm. In the sedge-dominated IF the water table (mean of two reference wells) had a seasonal minimum of 13 cm below the peat surface on August 19, 2016 and maximum of 9.9 cm above the peat surface on June 6, 2016. Mean (and standard deviation) water table depth was -5.4 (5.1) cm below the peat surface. Fluctuations in water table corresponded to diurnal evapotranspiration (observed in daily sinuosity) and seasonal precipitation inputs. The PF water table increased more compared to the IF in response to the same precipitation inputs. The 24-hour mean water table for each sampling date is shown in Table 2.1.

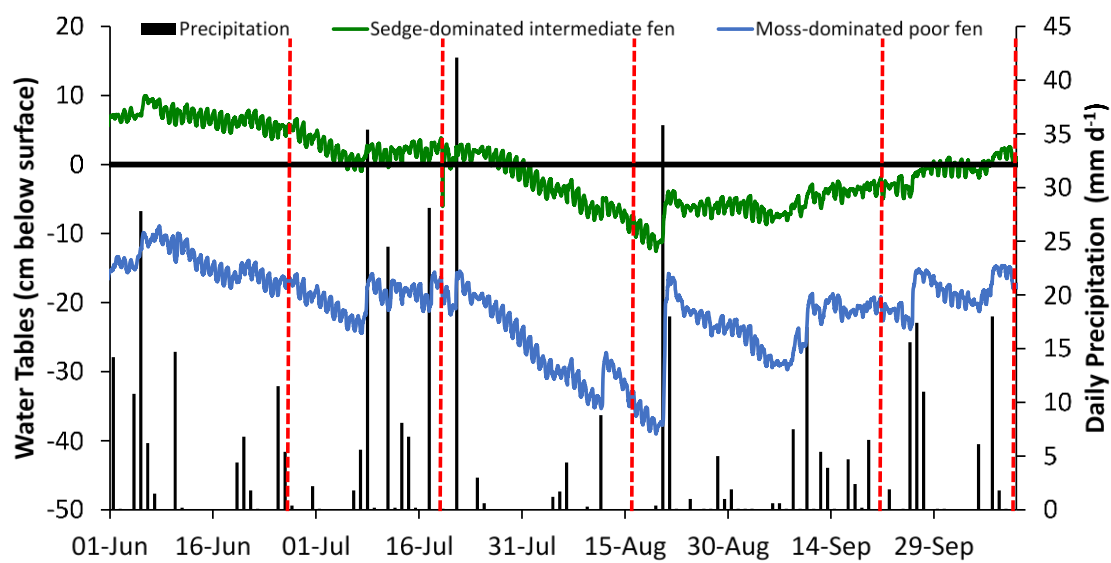


Figure 2.2: Intermediate Fen and Poor Fen water table levels.

Mean water table levels (cm) (mean of two reference wells per site) relative to the surface (left y-axis) for the sedge-dominated IF (green line) and moss-dominated PF (blue line). Peat surface plotted as horizontal solid black line. Daily precipitation (right y-axis) summarized by 24-hour period (black bars). Dates shown are from June 1 to October 11, 2016 as pressure transducers were removed from reference wells on October 11, 2016. Dotted red lines indicate the 24 hour period for which porewater sampling occurred.

Table 2.1: Sampling date water table level.

24-hour mean water table (cm) relative to the peat surface for each porewater sampling date.

Site/Month	June	July	August	September	October*
Poor Fen	-16.8	-18.3	-34.7	-20.3	-17.7
Intermediate Fen	4.9	2.0	-10.5	-3.2	0.7

*Pressure transducers were removed on October 11, 2016 and porewater sampling occurred on October 12, 2016. Therefore, the mean water table from October 11 (prior to pressure transducer removal) were used for October water table levels.

2.3.2 Temporal porewater chemistry comparison

Total Hg concentrations in porewaters in the moss-dominated PF and sedge-dominated IF ranged from 0.30–9.77 ng-Hg L⁻¹ (Figure 2.3A). Median THg concentrations were 18.7% less in the IF compared to the PF. Total Hg varied less seasonally within the PF and IF porewaters than between the PF and IF (Table 2.2). August samples had the lowest and highest median concentrations in the IF and PF, respectively, resulting in the greatest difference.

Across both the IF and PF porewater, MeHg concentrations ranged 0.02–1.34 ng-Hg L⁻¹. Methylmercury at the PF ranged 0.08–1.34 ng-Hg L⁻¹ and at the IF 0.02–1.04 ng-Hg L⁻¹ (Figure 2.3B). Median MeHg concentrations were 3.1 times greater in the PF compared to the IF, with greater variability observed in the PF. Monthly median MeHg concentrations in PF were consistently higher compared to the IF. Poor fen median MeHg concentrations were 4.1–3.2 times greater than IF concentrations in August and September, respectively (Table 2.2). Most notable was August, where the maximum MeHg concentrations in the PF was 1.34 ng-Hg L⁻¹ and 0.19 ng-Hg L⁻¹ in the IF.

The fraction of THg as MeHg (%MeHg) is often calculated as an indirect indicator of ‘methylating potential’ in soils and sediments, and ranged 1.30–29.1% across the IF and PF. In the PF, %MeHg ranged 1.50–29.1% compared to 1.30–25.8% in the IF. Median %MeHg was 2.0 times greater in the PF (13.1%) compared to the IF (6.4%). Across the IF, median %MeHg was greatest in July and October, both at 7.0%, strikingly different from the August minimum of 3.6%. In contrast, PF median %MeHg was consistently greater than IF percentages with June (15.8%) and August (10.7%) representing the maximum and minimum, respectively.

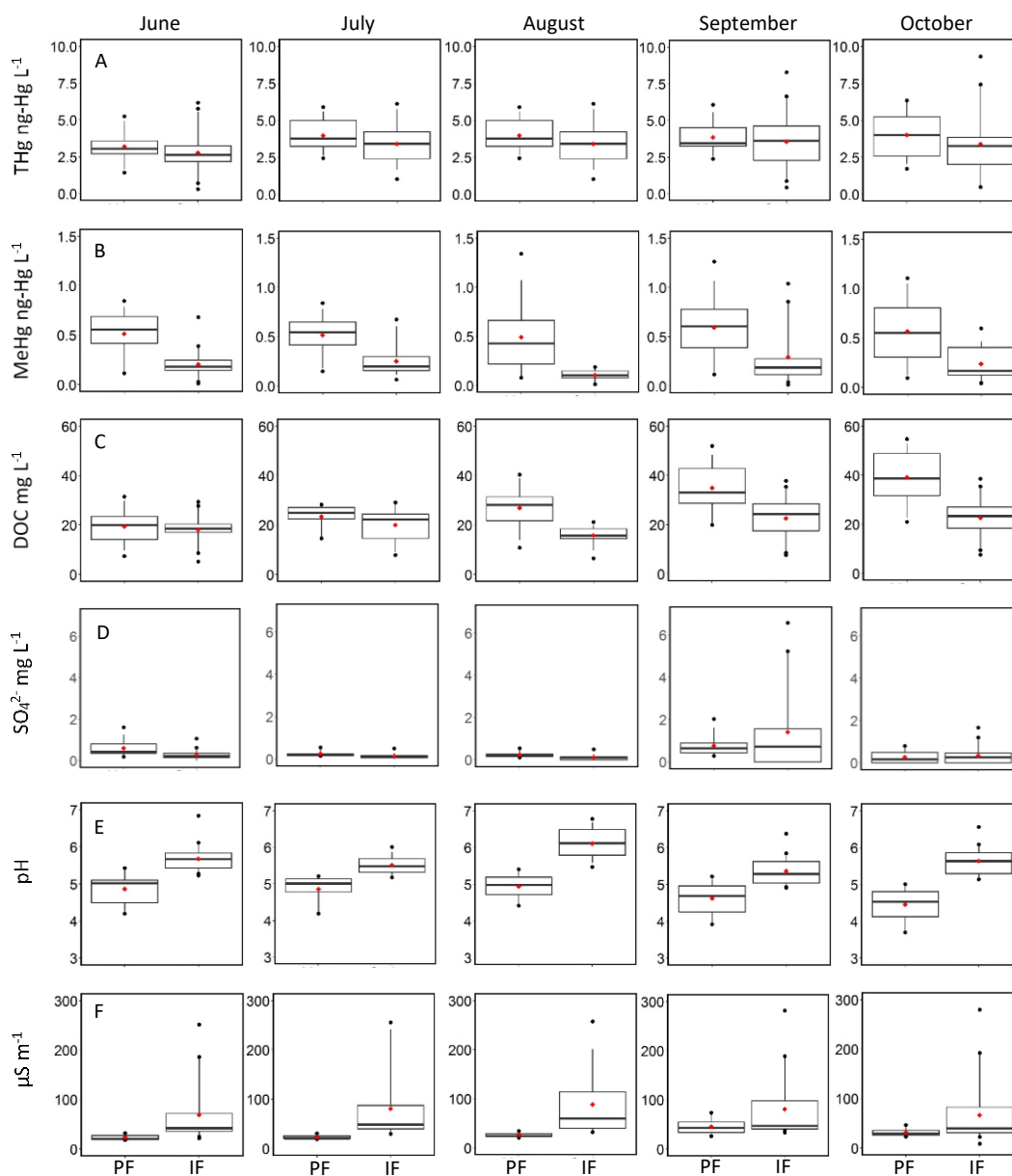


Figure 2.3: Boxplots of PF and IF porewater chemistry.

PF and IF monthly box and whisker plots showing THg (A), MeHg (B), DOC (C), SO_4^{2-} (D), pH (E), and conductivity (F). Box plot displays 25th (lower bound) and 75th (upper bound) percentiles and median. Mean is shown with red dot. Whiskers included all measures between 5th and 25th quantiles (lower bound) and those between the 75th and

95th quantile (upper bound). Values outside the 5th and 95th quantile are plotted as individual points.

Table 2.2: Monthly median and interquartile range of porewater chemistry from the IF and PF near White River, Ontario.

Variable	pH	Conductivity	DOC	DIC	Ca ²⁺	Mg ²⁺	TN	SO ₄ ²⁻
Units		µS m ⁻¹	mg L ⁻¹					
Intermediate Fen								
June	5.66 (0.41)	41.9 (36.5)	18.5 (3.4)	6.49 (6.22)	6.52 (5.72)	1.08 (1.12)	0.42 (0.12)	0.23 (0.22)
July	5.49 (0.37)	48.8 (47.1)	22.3 (9.8)	6.12 (3.43)	7.63 (4.02)	1.21 (0.78)	0.46 (0.16)	0.13 (0.11)
August	6.12 (0.70)	60.2 (73.8)	15.7 (4.0)	8.26 (8.19)	10.28 (14.06)	1.41 (1.46)	0.55 (0.14)	0.11 (0.15)
September	5.29 (0.59)	47.3 (57.6)	24.4 (11.0)	6.80 (6.42)	7.41 (9.63)	1.17 (1.06)	0.70 (0.31)	0.72 (1.56)
October	5.64 (0.57)	39.7 (51.3)	23.4 (8.7)	8.47 (6.00)	6.81 (6.40)	0.94 (1.26)	0.60 (0.32)	0.27 (0.46)
Poor Fen								
June	5.02 (0.62)	21.0 (8.5)	20.0 (9.3)	3.02 (1.71)	2.17 (0.78)	0.31 (0.09)	0.39 (0.21)	0.43 (0.46)
July	5.01 (0.36)	20.9 (5.0)	25.0 (4.7)	1.38 (0.46)	2.55 (0.41)	0.37 (0.10)	0.42 (0.28)	0.22 (0.08)
August	4.99 (0.47)	24.3 (5.4)	28.2 (9.6)	3.86 (2.65)	2.98 (0.92)	0.43 (0.10)	0.76 (0.24)	0.22 (0.11)
September	4.69 (0.71)	43.0 (20.9)	33.1 (14.1)	1.84 (2.43)	3.38 (1.07)	0.54 (0.12)	0.90 (0.25)	0.64 (0.47)
October	4.54 (0.70)	28.9 (9.5)	38.8 (17.1)	5.36 (2.58)	3.47 (1.09)	0.54 (0.14)	0.83 (0.25)	0.17 (0.50)

Dissolved organic carbon ranged 5.21–38.56 mg L⁻¹ at the IF and 7.36–54.81 at the PF (Figure 2.3C). Median DOC concentrations in the PF were 43% greater compared to the IF. Dissolved organic carbon varied more between the IF and PF than seasonally, especially at the PF (Table 2.2). Sulphate ranged 0.005–6.57 mg L⁻¹ at the IF and 0.005–2.03 mg L⁻¹ at the PF (Figure 2.3D). Median SO₄²⁻ concentrations were 46.9% greater in the PF compared to the IF. Sulphate displayed seasonal patterns with minimums in July and August and maximums in September across the PF and IF (Table 2.2). Sulphate was consistently measured at higher concentrations at the PF from June through August, but not in September and October.

Porewater pH ranged 4.91–6.84 at the IF and 3.7–5.43 at the PF (Figure 2.3E). IF porewater pH was acidic with a median of 5.63. While median pH at the PF was more acidic still (4.90). Conductivity ranged 8.6–282.0 $\mu\text{S m}^{-1}$ at the IF and 18.1 to 74.2 $\mu\text{S m}^{-1}$ at the PF (Figure 2.3F). Median conductivity was 43.8 $\mu\text{S m}^{-1}$ at the IF and 26.5 $\mu\text{S m}^{-1}$ at the PF. Seasonal variation in pH and conductivity were less apparent than differences observed between sites (Table 2.2), however, August samples were the least acidic in the IF and most acidic in the PF.

Similar to conductivity, median Ca^{2+} 7.48 mg L^{-1} (N=102) across the IF was 2.6 times greater than across the PF 2.96 mg L^{-1} (N= 53) and varied less seasonally than between peatland types. In contrast, median TN was 44% greater across the PF 0.74 mg L^{-1} (N=53) compared to the IF 0.49 mg L^{-1} (N= 100, 2 non-detects). Potassium ion (K^+), when detected, medians were 0.37 mg L^{-1} (N= 25) and 0.27 mg L^{-1} (N= 35) across the PF and IF, respectively. Median DIC was 6.80 mg L^{-1} (N= 102) at the IF and 2.72 mg L^{-1} (N= 53) at the PF. Following a similar pattern to DIC was Mg^{2+} with median concentrations 1.15 mg L^{-1} (N= 102) across the IF and 0.44 mg L^{-1} (N= 53) across the PF. Similar to seasonal patterns observed in pH and conductivity and Ca^{2+} , DIC and, Mg^{2+} differences were greater between the IF and PF compared to seasonal variation.

2.4 Discussion

2.4.1 Porewater total mercury and methylmercury

Total Hg concentrations in both peatlands were within the range reported from other northern peatland studies (Heyes et al. 2000; Mitchell et al. 2008a; Mitchell et al. 2008c; Regnell & Hammar 2009). Temporal THg patterns were less clear, especially in the PF, compared to differences between sites with the greatest seasonal difference ($\sim 1.9 \text{ ng L}^{-1}$) occurring in August. Methylmercury concentrations in porewaters were also within reported values from several northern peatland studies (Branfireun et al, 1999; Heyes et al. 2000; Mitchell et al. 2008a; Bergman et al. 2012). However, PF and IF median MeHg concentrations and the seasonal maximum concentrations were lower than reported porewater MeHg concentrations in other northern peatlands (Branfireun et al. 1996;

Heyes et al. 2000; Mitchell et al. 2008a; Bergman et al. 2012). Sampling depth was likely behind this difference. The porewater sampling piezometers only integrated porewaters from 30–50 cm below the peat surface at each site, which did not always capture porewaters from the actively methylating layers, which may have been closer to the peat surface. Several studies have shown that the highest MeHg concentrations occur in the zone of water table fluctuation (Branfireun et al. 1996; Heyes et al. 2000; Branfireun & Roulet 2002), closely corresponding to porewaters just below the water table and where SO_4^{2-} concentrations are greatest (Branfireun 2004). Regnell & Hammar (2004) invoked this same explanation when integrating porewaters to 90 cm below the peat surface.

Temporally, porewater MeHg concentrations followed a similar pattern between the IF and PF, with greater concentrations observed in the IF following a water table drawdown. Across both peatlands, fall (September and October) median MeHg concentrations were the greatest, whereas August were the lowest. Late August and September (Fall) porewater MeHg maximum have been observed in boreal wetland impoundments in the Experimental Lakes Area, Ontario (Heyes et al. 2000) and across upland-peatland interfaces in northern Minnesota, USA (Mitchell et al. 2008a; Mitchell et al. 2009). The fall maxima in porewater MeHg concentrations in both the IF and PF follow the same trend. The mid-summer water table 30-day drawdown period from July 21–August 19 and concurrent increase in SO_4^{2-} availability in dewatered peat followed by a steady water table rise from August 19 through September and October explain the elevated MeHg concentrations in September (both sites) and October (PF only). Coleman-Wasik et al. (2015) invoked the regeneration of SO_4^{2-} during periods of water table drawdown (droughts) when formally anoxic peat became exposed to oxic conditions to explain elevated porewater MeHg concentrations in a moss-dominated ombrotrophic bog in northern Minnesota, USA following water table rise. This confirms my first hypothesis, for which temporal patterns of MeHg concentrations corresponded to the hydrologic fluctuations in a both a sedge- and moss-dominated peatland.

The effect of a seasonal water table fluctuation (30-day water table drawdown period) were seen across both the IF and PF when comparing August to September and October porewater MeHg concentrations. However, the effect was seen to a greater degree in the IF and was more of an artifact of limited sampling volumes in August IF piezometers than an underlying hydrologic mechanism. Only 13 of 25 sampling locations in the IF provided sufficient sample volumes for all porewater chemistry variables and ancillary chemistry; of these piezometers pH and conductivity chemistry indicated contributions from groundwater (highest monthly medians), which likely had a diluting effect on porewater chemistry. Despite this limitation, comparing June/July and September/October MeHg and SO_4^{2-} concentrations still support the contention that water table drawdown increased SO_4^{2-} availability and subsequently resulted in increased MeHg concentrations, similar to the results and findings of Coleman-Wasik et al. (2015) in a moss-dominated northern peatland in northern Minnesota, USA.

2.4.2 Conditions effecting porewater methylmercury concentrations between a sedge-dominated and moss-dominated peatland

The inherent porewater chemical conditions at the IF, being higher pH, lower DOC concentrations and stronger groundwater contributions (higher Ca^{2+} , Mg^{2+} , and DIC), all suggest that the greater nutrient status, pH, and groundwater connectivity at the sedge-dominated IF provided conditions less suitable for MeHg production. These porewater variables suggest that more alkaline pH conditions and lower DOC concentrations at the IF limited both MeHg and THg porewater concentrations, likely with greater amounts of Hg(II) and MeHg bound to the peat soil compared to the moss-dominated PF (Drexel et al. 2002). Porewater MeHg concentrations reflect both methylation and demethylation processes and much of the THg pool remains unavailable to SRB as it remains bound up to ligands in DOC molecules (Benoit et al. 2001; Drexel et al. 2002). Both inorganic Hg(II) and organic MeHg are known to have a high affinity to bind with DOC (Driscoll et al. 1995; Barkay et al. 1997; Kelly et al. 2003), in particular, with soft ligands like thiols (-SH) (Benoit et al. 2001). Consequently, pH acts as a major control on

bioavailable Hg(II) (Haitzer et al. 2003) and DOC concentrations (Clark et al. 2005; Evans et al. 2012). In the moss-dominated PF, more acidic porewaters likely increased the bioavailability of Hg(II), and hence, resulted in greater MeHg concentrations. The effects of lower pH in the PF were multi-faceted; more acidic pH increased DOC concentrations and bioavailable Hg(II), while increased DOC concentrations carried with it greater amounts of bound THg and MeHg.

Previous studies comparing MeHg concentrations across peatland nutrient gradients (ombrotrophic bogs to mesotrophic poor fens) have found that poor fens were greater MeHg producing and exporting peatlands (Branfireun & Roulet 2002; Mitchell et al. 2008a; Mitchell et al. 2008c) resulting from greater SO_4^{2-} availability and groundwater upwelling during water table drawdown periods (Heyes et al. 2000; Branfireun & Roulet 2002). A similar result was seen in a bog-fen complex in the discontinuous permafrost region in the southern Northwest Territories (Gordon et al. 2016). Tjerngren et al. (2012b) in comparing methylation and demethylation rates suggested that boreal peatlands reach a threshold of increasing nutrient status in which Hg demethylation processes favour methylation, resulting in nutrient rich boreal peatlands having less net methylmercury production. This may explain why conditions in the IF resulted in less THg and MeHg.

2.5 Conclusions

The results of this study suggest that northern peatland type (i.e., poor fen and intermediate fen) does have a major control on MeHg concentrations in porewaters. Temporal water table fluctuations resulting in greater SO_4^{2-} availability, and northern peatland type characteristics including DOC and pH, act as major controls on MeHg production. Methylmercury concentrations were greatest in the moss-dominated poor fen compared to the sedge-dominated intermediate fen. It was clear that the hydrologic regime (lower water table conditions) and porewater chemistry (lower pH, higher DOC, lower base cations) defining a moss-dominated poor fen (Zoltai & Vitt 1995) resulted in greater amounts of MeHg. Therefore, a climate-driven shift in dominant plant community

from moss to sedge observed by Dieleman et al. (2015) could result in decreasing MeHg concentrations, assuming the shift was accompanied ultimately by higher pH, lower DOC and a higher overall water table in a previously moss-dominated northern peatland. Future work should include *in situ* controlled field experiments to further elucidate the effects of climate change on dominant plant community alongside changes in Hg biogeochemistry. Ultimately, the long-term stability of northern peatland plant communities will determine their potential to methylate Hg.

2.6 References

- Antweiler RC, Taylor HE (2008) Evaluation of statistical treatments of left-censored environmental data using coincident uncensored data sets: Summary statistics. *Environmental Science and Technology* 42: 3732–3738
- Barkay T, Gillman M, Turner RR (1997) Effect of dissolved organic carbon and salinity on bioavailability of mercury. *Applied and Environmental Microbiology* 63: 4267–4271
- Bergman I, Bishop K, Tu Q, Frech W, Åkerblom S, Nilson M (2012) The influence of sulphate deposition on the seasonal variation of peat pore water methyl Hg in a boreal mire. *PLoS ONE* 7: e45547. Doi:10.1371/journal.pone.0045547
- Bloom NS (1992) On the chemical form of mercury in edible fish and marine invertebrate tissue. *Canadian Journal of Fisheries and Aquatic Sciences* 49: 1010–1017
- Boelter DH, Verry ES (1977) Peatland and water in the northern lake states. USDA Forest Service Technical Report NC-31
- Branfireun BA, Roulet NT (2002) Controls on the fate and transport of methylmercury in a boreal headwater catchment, northwestern Ontario, Canada. *Hydrology and Earth Systems Sci* 6: 785–794
- Branfireun BA, Heyes A, Roulet NT (1996) The hydrology and methylmercury dynamics of a Precambrian Shield headwater peatland. *Water Resource Research* 32: 1785–1794
- Branfireun BA, Roulet NT, Kelly CA, Rudd WM (1999) In situ sulphate stimulation of mercury methylation in a boreal peatland: Toward a link between acid rain and methylmercury contamination in remote environments. *Global Biogeochemical cycles* 13: 743–750
- Buttler A, Robroek BJM, Laggouin-Défarage F, Jassey VE, Pochelon C, Bernard G, Delarue F, Gogo S, Mariotte P, Mitchell EAD, Bragazza L (2015) Experimental warming interacts with soil moisture to discriminate plant responses in an ombrotrophic peatland. *Journal of Vegetation Science* 26: 964–974
- Charman, D (2002) Peatlands and Environmental Change. John Wiley & Sons Ltd. West Sussex, UK
- Choi SC, Chase Jr T, Bartha R (1994) Metabolic pathways leading to mercury methylation in *Desulfovibrio desulfuricans*. *Applied Environmental Microbiology* 60: 4072–4077

- Clark JM, Chapman PJ, Adamson JK, Lane SN (2005) Influence of drought-induced acidification on the mobility of dissolved organic carbon in peat soils. *Global Change Biology*: 11: 791–809
- Coleman-Wasik JK, Engstrom DR, Mitchell CPJ, Swain EB, Monson BA, Balogh SJ, Jeremiasson JD, Branfireun BA, Kolka RK, Almendinger JE (2015) The effects of hydrologic fluctuation and sulfate regeneration on mercury cycling in an experimental peatland. *Journal of Geophysical Research: Biogeosciences* 120: 1697–1715
- Coleman-Wasik JK, Mitchell CPJ, Engstrom DR, Swain EB, Monson BA, Balogh SJ, Jeremiasson JD, Branfireun BA, Eggert SL, Kolka RK, Almendinger JE (2012) Methylmercury declines in a boreal peatland when experimental sulfate depositions decrease. *Environmental Science and Technology* 46: 6663–6671
- Collins M, Knutti R, Arblaster J, Dufresne JL, Fichefet P, Friedlingstein P, Gao X, Gutowski WJ, Johns T, Krinner M, Shongwe M, Tebaldi C, Weaver AJ, Wehner M. (2013) Long-term climate change: Projections, commitments and irreversibility. In: *Climate change 2013: The physical science basis. Contributions of Working Group I to the fifth assessment report of the Intergovernmental Panel on Climate Change* (Stocker TF, Qin D, Plattner GK, Tignor M, Allen SK, Boschung J, Nauel A, Xia Y, Bex V, Midgley PM [eds.]). Cambridge University Press, Cambridge, United Kingdom and New York, NY, USA.
- Compeau GC, Bartha R (1985) Sulphate-Reducing Bacteria: Principal methylators of mercury in anoxic estuarine sediment. *Applied Environment Microbiology* 50: 498–402
- Devito KJ, Hill AR, Roulet N (1996) Groundwater—surface water interaction in headwater forested wetlands of the Canadian Shield. *Journal of Hydrology* 181: 127–147
- Dieleman CM, Branfireun BA, McLaughlin JW, Lindo Z (2015) Climate change drives a shift in peatland ecosystem plant community: Implications for ecosystem function and stability. *Global Change Biology*: gcb12643
- Drexel RT, Haitzer M, Ryan JN, Aiken GR, Nagy KL (2002) Mercury(II) sorption to two Florida everglades peats: Evidence for strong and weak binding and competition by dissolved organic matter released from the peat. *Environmental Science and Technology* 36: 4058–4064
- Driscoll CT, Yen C, Schofield L, Munson R, Holsapple J (1994) The chemistry and bioavailability of mercury in remote Adirondack lakes. *Environmental Science & Technology* 28: 136–143

- Driscoll CT, Blette V, Yan C, Schofield CL, Munson R, Holsapple J (1995) The role of dissolved organic carbon in the chemistry and bioavailability of mercury in remote Adirondack Lakes. *Water, Air and Soil Pollution* 80: 499–508
- Environment Canada (2010) Climate normal 1981-2010: Wawa Airport, Ontario. Retrieved from <http://climate.weather.gc.ca/climate_normals/results_1981_2010_e.html?searchType=stnName&txtStationName=wawa&searchMethod=contains&txtCentralLatMin=0&txtCentralLatSec=0&txtCentralLongMin=0&txtCentralLongSec=0&stnID=4099&dispBack=1> on 12.07.2016
- Evans CD, Jones TG, Burden A, Ostle N, Zeiliński, Cooper MD, Peacock M, Clark JM, Oulehle F, Cooper D, Freeman C (2012) Acidity controls on dissolved organic carbon mobility in organic soils. *Global Change Biology* 18: 3317–3331
- Field CB, Mortsch LD, Brklacich M, Forbes DL, Kovacs R, Patz JA, Running SW, Scott MJ (2007) North America. *Climate Change 2007: Impacts, adaptation and vulnerability. Contribution of Working Group II to the Fourth Assessment Report of the Intergovernmental Panel on Climate Change*. 617-652
- Gordon J, Quinton W, Branfireun BA, Olefeldt D (2016) Mercury and methylmercury biogeochemistry in a thawing permafrost wetland complex, Northwest Territories, Canada. *Hydrological Processes*: 30: 3627–3638
- Gorham E (1991) Northern peatland: Role in the carbon cycle and probable responses to climatic warming. *Ecological Applications* 1: 182–195
- Haitzer M, Aiken GR, Ryan JN (2002) Binding mercury(II) to dissolved organic matter: The role of mercury-to-DOM concentration ratio. *Environmental Science & Technology* 36: 3564–3570
- Haitzer M, Aiken GR, Ryan JN (2003) Binding mercury(II) to aquatic humic substances: Influence of pH and source of humic substances. *Environmental Science & Technology* 37: 2436–2441
- Heyes A, Moore TR, Rudd JWM, Dugoua JJ (2000) Methyl mercury in pristine and impounded boreal peatland, Experimental Lakes Area, Ontario. *Canadian Journal of Fisheries and Aquatic Sciences* 57: 2211–2222
- IPCC, 2013 Annex I: Atlas of global and regional climate projections (van Oldenborgh GM, Collins M, Arblaster JH, Christensen J, Marotzke J, Power SB, Rummukainen, Zhou T [eds.]) In: *Climate Change 2013: The physical science basis. Contributions of the Working Group I to the fifth assessment report of the Intergovernmental Panel on Climate Change* (Stocker TF, Qin D, Plattner M, Tignor SK, Allen J, Boschung A, Nauels, Y, Xia V, Bex V, Midgley PM [eds.]

Cambridge University Press, Cambridge, United Kingdom and New York, NY, USA.

- Jeremiason JD, Engstrom DR, Swain EB, Nater EA, Johnson BM, Almendinger JE, Monson BA, Kolka RK (2006) Sulfate additions increase methylmercury production in an experimental wetland. *Environmental Science & Technology* 40: 3080–3806
- Kelly CA, Rudd JWM, Holoka MH (2003) Effect of pH on mercury uptake by an aquatic bacterium: implications for Hg cycling. *Environmental Science & Technology* 37: 2941–2946
- McLaughlin JW, Webster KL (2010) Alkalinity and acidity cycling and fluxes in an intermediate fen peatland in northern Ontario. *Biogeochemistry* 99: 143–155
- McLaughlin JW (2009) Boreal mixed-wood watershed riparian zone cation cycling during two contrasting climatic years. *Soil Science Society of America* 73: 1408–1418
- Mitchell CPJ, Branfireun BA, Kolka RK (2008a) Spatial characteristics of net methylmercury production hot spots in peatlands. *Environmental Science & Technology* 44: 1010–1016
- Mitchell CPJ, Branfireun BA, Kolka RK (2008b) Assessing sulphate and carbon controls on net methylmercury production in peatland: An in situ mesocosm approach. *Applied Geochemistry* 23: 503–518
- Mitchell CPJ, Branfireun BA, Kolka RK (2008c) Total mercury and methylmercury dynamics in upland-peatland watersheds during snowmelt. *Biogeochemistry* 90: 225–241
- Mitchell CPJ, Branfireun BA, Kolka RK. (2009) Methylmercury dynamics at the upland-peatland interface: Topographic and hydrogeochemical controls. *Water Resources Research* 45: W02406
- Myers B, Webster KL, McLaughlin JW, Basiliko N (2012) Microbial activity across a boreal peatland gradient: the role of fungi and bacteria. *Wetlands Ecology Management* 20: 77–88
- Potvin LR, Kane ES, Chimner RA, Kolka RK, Lilleskov, EA (2015) Effects of water table position and plant functional group on plant community, aboveground production, and peat properties in peatland mesocosm experiment (PEATcosm). *Plan Soil* 387: 277–713

- Regnell O, Hammar T (2009) Coupling of methyl and total mercury in a minerotrophic peat bog in southeastern Sweden. *Canadian Journal of Fisheries and Aquatic Sciences* 61: 2014–2023
- Rudd JWM (1995) Sources of methyl mercury to freshwater ecosystems: a review. *Water, Air and Soil Pollution* 80: 697–713
- Rydin H, Jeglum JK (2013) *The Biology of Peatlands*, 2nd Edition. Oxford University Press, Oxford, United Kingdom. PP: 127–147
- St. Louis VL, Rudd JWM, Kelly CA, Beaty KG, Bloom NS, Flett RJ (1994) Importance of wetlands as sources of methylmercury to boreal forest ecosystems. *Canadian Journal of Fisheries and Aquatic Sciences* 51: 1065–1076
- St. Louis VL, Rudd JWM, Kelly CA, Beaty KG, Flett RJ, Roulet NT (1996) Production and loss of methylmercury loss of total mercury from boreal forest catchments containing different types of wetlands. *Environmental Science and Technology* 30: 2719–2729
- St. Louis VL, Rudd JWM, Kelly CA, Bodaly RA (Drew), Paterson MJ, Beaty KG, Hesslein RH, Heyes A, Majewski AR (2004) The rise and fall of mercury methylation in an experimental reservoir. *Environmental Science and Technology* 38: 1348–1358
- Tjerngren I, Karlsson T, Björn E, Skjällberg U (2012a) Potential Hg methylation and MeHg demethylation rates related to nutrient status and different boreal wetlands. *Biogeochemistry* 108: 35–350
- Tjerngren I, Meili M, Björn E, Skjällberg U (2012b) Eight boreal wetland as sources and sinks for methyl mercury in relation to soil acidity, C/N ratio, and small-scale flooding. *Environmental Science & Technology* 46: 8052 –8060
- U.S. Environmental Protection Agency (1999) Mercury in water by oxidation, purge and trap, and cold vapour atomic fluorescence spectroscopy (Method 1631, Revision B). National Service Center for Environmental Publication and Information, Cincinnati, OH
- U.S. Environmental Protection Agency (1998) Methyl mercury in water by distillation, aqueous methylation, purge and trap, and cold vapor atomic fluorescence spectrometry (Method 1630). National Service Center for Environmental Publication and Information, Cincinnati, OH
- UNEP (2013) *Global Mercury Assessment 2013: Sources, emissions, releases and environmental transport*. UNEP Chemicals Branch, Geneva, Switzerland

- Vitt DH, Chee WL (1990) The relationship of vegetation to surface water chemistry and peat chemistry in fens of Alberta, Canada. *Vegetation* 89: 87–106
- Waddington JM, Morris PF, Kettridge N, Granath G, Thompson DK, Moore PR (2015) Hydrological feedbacks in northern peatlands. *Ecohydrology* 8: 113–127
- Webster KL, McLaughlin JW (2010) Importance of water table in controlling dissolved carbon along a fen nutrient gradient. *Soil Science Society of America* 74: 2254–2266
- Zoltai SC, Vitt DH (1995) Canadian wetlands: Environmental gradients and classification. *Vegetatio* 118: 131–137

Chapter 3

3 Production and transport of methylmercury in a sedge-dominated peatland

3.1 Introduction

Methylmercury is a bioaccumulating pollutant produced primarily by SRB in anoxic lake water and sediment, and wetland soils (Ratcliffe et al. 1996; Compeau & Bartha 1985; Branfireun et al. 1996). Northern peatlands (north of 45°) are a type of peat accumulating wetlands (peat depth > 40 cm) where saturated anoxic soils provide biogeochemical conditions suitable for the microbial transformation of bioavailable Hg to MeHg.

Methylmercury produced in northern peatlands can be transported to downstream aquatic environments depending on peatland hydrologic connectivity (Branfireun & Roulet 2002), where bioaccumulation and biomagnification of MeHg increases concentrations in higher trophic level fish to levels that can be a risk to fish consumers, including humans (Ratcliffe et al. 1996).

Net MeHg production is known to occur in biogeochemical ‘hot spots’ (McClain et al. 2003). McClain et al. (2003) defined ‘hot spots’ as patches that show disproportionately higher reaction rates relative to the surrounding matrix in referring to biogeochemical cycles (e.g., N, C, S cycles). At the landscape scale, northern peatlands have been found to be important sources of MeHg. Mitchell et al. (2008a) showed that discrete locations within peatlands (mainly with upland-wetland hydrobiogeochemical connectivity) were ‘hot spots’ for MeHg production, driving this net catchment influence. Similarly, Bishop et al. (1995) and Vidon et al. (2013) have demonstrated the importance of riparian zones for MeHg production and transport to adjacent streams. Sulphate is a known limiting reactant to the production of MeHg in northern peatlands (Branfireun et al. 1999) because the supply SO_4^{2-} is limited by external inputs and internal biogeochemical and hydrologic processes (Devito & Hill 1997). Anoxic peat soils maintain reduced inorganic sulphur species (e.g. FeS or H_2S) (Chapman & Davidson 2001), most (>90%) the sulphur pool in northern peatlands is organically bound (Novák & Wieder 1992), and persistent anoxia

reduces available SO_4^{2-} through the formation of HgS (Benoit et al. 2001). Although SO_4^{2-} can be limited, inputs from upland runoff (Mitchell et al. 2008a), atmospheric deposition (Branfireun et al. 1999; Jeremiason et al. 2006; Mitchell et al. 2008b) or shallow groundwater (Branfireun & Roulet 2002) have been shown or invoked as the mechanism for enhanced MeHg production in spatially discrete zones in northern peatlands. Most recently, *in situ* regeneration of SO_4^{2-} driven by drought-induced water table drawdown and subsequent rewetting has been shown to stimulate methylation (Coleman-Wasik et al. 2015).

The majority of MeHg studies in northern peatlands have investigated the hydrologic and porewater chemistry controls on MeHg production in moss-dominated (*Sphagnum* spp. L.) fens and bog peatlands, leaving an important knowledge gap concerning sedge-dominated (*Carex* spp. L.) fen peatlands. Fen peatlands receive water and nutrient inputs from upland, groundwater, and precipitation sources to varying degrees, with greater contributions from groundwater and upland sources resulting in a higher nutrient status and greater vascular plant abundance such as sedges (Rydin & Jeglum 2013). In contrast, bogs only receive water and nutrient inputs from precipitation (Rydin & Jeglum 2013). Sedge-dominated mesotrophic intermediate fens have higher concentrations of nutrients (e.g., Ca^{2+} , Mg^{2+} , K^+ , P, N) because of greater connectivity to groundwater and/or hillslope runoff (Vitt & Chee 1990). For instance, SO_4^{2-} is more variable in sedge-dominated peatlands in comparison to moss-dominated peatlands (Vitt & Chee 1990). Water tables in sedge-dominated peatlands are often persistently higher than other peatland types because of this hydrological connectivity (Rydin & Jeglum 2013), and surface streams are more likely to develop in sedge-dominated peatlands because of greater hydrological inputs, preferential groundwater flow paths, and the prevalence of vascular plant communities which act to stabilize stream banks once they have developed (Watters & Stanley 2007).

The presence of streams within sedge-dominated intermediate fens result in peatland riparian zones. Peatland riparian zones may be potential ‘hot spots’ for net MeHg

production as elevated levels of MeHg have been reported in non-peatland riparian zones in several studies (Bishop et al. 1995; Lee et al. 1995; Vidon et al. 2013; Regnell et al. 2009; Eklöf et al. 2015). Bishop et al. (1995) showed that the riparian zones of first-order streams in a forested boreal catchment in Sweden had concentrations of MeHg that the authors concluded could not be explained by upland runoff or groundwater contributions alone, suggesting *in situ* production. Greater soil organic matter content and riparian soil anoxic conditions were invoked to explain elevated MeHg concentrations in riparian zones (Bishop et al. 1995). Peat is an organic soil and anoxic conditions correspond to water table position in peatlands (Rydin & Jeglum 2013), therefore one would expect the riparian zones in a sedge-dominated peatland to provide suitable conditions for net MeHg production. Across sedge-dominated peatland riparian zones, other factors would then limit net MeHg production such as SO_4^{2-} availability, water table positions, and nutrient supply (e.g., Mg^{2+} , Ca^{2+} , DIC) influences on alkalinity. Nutrient contributions from groundwater and/or fluctuations in water table position are important mechanisms in controlling biogeochemistry in riparian zones (Vidon & Hill 2004) and can also influence Hg biogeochemistry (Bishop et al. 1995; Vidon et al. 2013). Once produced, MeHg may be transported from riparian zones to surface waters. Interactions amongst surface waters, groundwater, and riparian zone porewaters has been shown to enhance MeHg production and promote subsurface MeHg transport to surface waters so long as reduced conditions were maintained (Regnell et al. 2009).

Transport of MeHg from peatlands to surface waters is foremost a function of hydrologic connectivity (Branfireun & Roulet 2002). Subsurface MeHg transport from riparian zones is likely to be relatively restricted to the near-stream zone because of the relatively low hydraulic conductivity and low hydraulic gradients in sedge-dominated peatlands. Hemond & Fifield (1982) suggested two hydrologic regimes in salt marshes which serve as a morphological analog for these channelized freshwater fens: interior portions of the marshes isolated from incised streams were dominated by evapotranspirative vertical water transfers, and; stream bank (riparian zone) environments with lateral subsurface hydrological connectivity to stream waters. Similar hydrologic characteristics likely are

found in morphologically similar sedge-dominated intermediate fens, which would likely limit subsurface and surface MeHg transport to the near stream zone only. To date, no study has examined the potential for sedge-dominated peatland riparian zones as net MeHg production ‘hot spots’. In addition, subsurface MeHg transport has not been described in sedge-dominated peatlands.

In a sedge-dominated peatland near White River, Ontario, riparian porewater SO_4^{2-} concentrations from exploratory sampling completed in October 2015 suggested differing vertical concentration profiles near two incised stream channels (Figure 3.1A, B). In one stream, Stream A, hence referred to as Discontinuous Stream (DS), porewater SO_4^{2-} concentrations in riparian zones increased with depth $25 < 50 < 100$ cm depth, whereas in the riparian zones of another stream, Stream B, hence referred to as Continuous Stream (CS) the opposite trend was seen with 25 and 50 cm piezometers having the greatest SO_4^{2-} concentrations (i.e., $25 \geq 50 > 100$ cm) (data not shown) (see Appendix A: Figure A4 for a site photo). These preliminary results along with a previous site study suggesting significant groundwater contributions to Continuous Stream (Packalen et al. 2011) motivated further investigations into the influence of groundwater nutrient supply and relevant chemistry affecting MeHg production in riparian zones of a sedge-dominated intermediate fen. Reflecting these research motivations, this study’s objective was to determine if within-peatland patterns of MeHg concentrations in a sedge-dominated intermediate fen peatland are related to internal surface drainage patterns and groundwater nutrient supply. From this objective, two hypotheses were formed:

Hypothesis 1: Higher MeHg concentrations in porewater will be associated with sites of groundwater discharge and higher sulphate concentrations in the riparian zones adjacent to within-peatland stream networks at an intermediate fen.

Hypothesis 2: Transport of MeHg to receiving waters will be dominated by within-peatland stream networks and their associated riparian zones because of both higher porewater MeHg concentrations and complex internal surface drainage patterns, which limit subsurface and surface hydrologic connectivity across interior of fen.

3.2 Methods

3.2.1 Study site description

The study site is a 5.3 ha intermediate fen northern peatland with sedge (*Carex* spp. L.) and ericaceous shrubs primarily consisting of sweet gale (*Myrica gale* L.) as dominant vegetation types (Figure 3.1B) (McLaughlin & Webster 2010). Porewaters are slightly acidic pH (5.5-7) (McLaughlin & Webster 2010) with some sites having local groundwater connectivity, which characterise the fen as a minerotrophic peatland (Zoltai & Vitt 1995; Rydin & Jeglum 2013). Though mostly an open low gradient peatland, limited micro-topography development can be observed in hummocks that had sparse moss cover (*Sphagnum* spp. L.) and ericaceous shrubs (*Myrica gale* L.). Peat soil is between 0.5 and 3 m thick (Myers et al. 2012). A mixture of coarse sand and compacted fine sandy unconsolidated material underlies the peat (McLaughlin & Webster 2010). The water table is typically near the surface of the peat with fluctuations depending on precipitation and evapotranspiration. For a more detailed description of the intermediate fen please see Section 2.2.1 of this thesis.

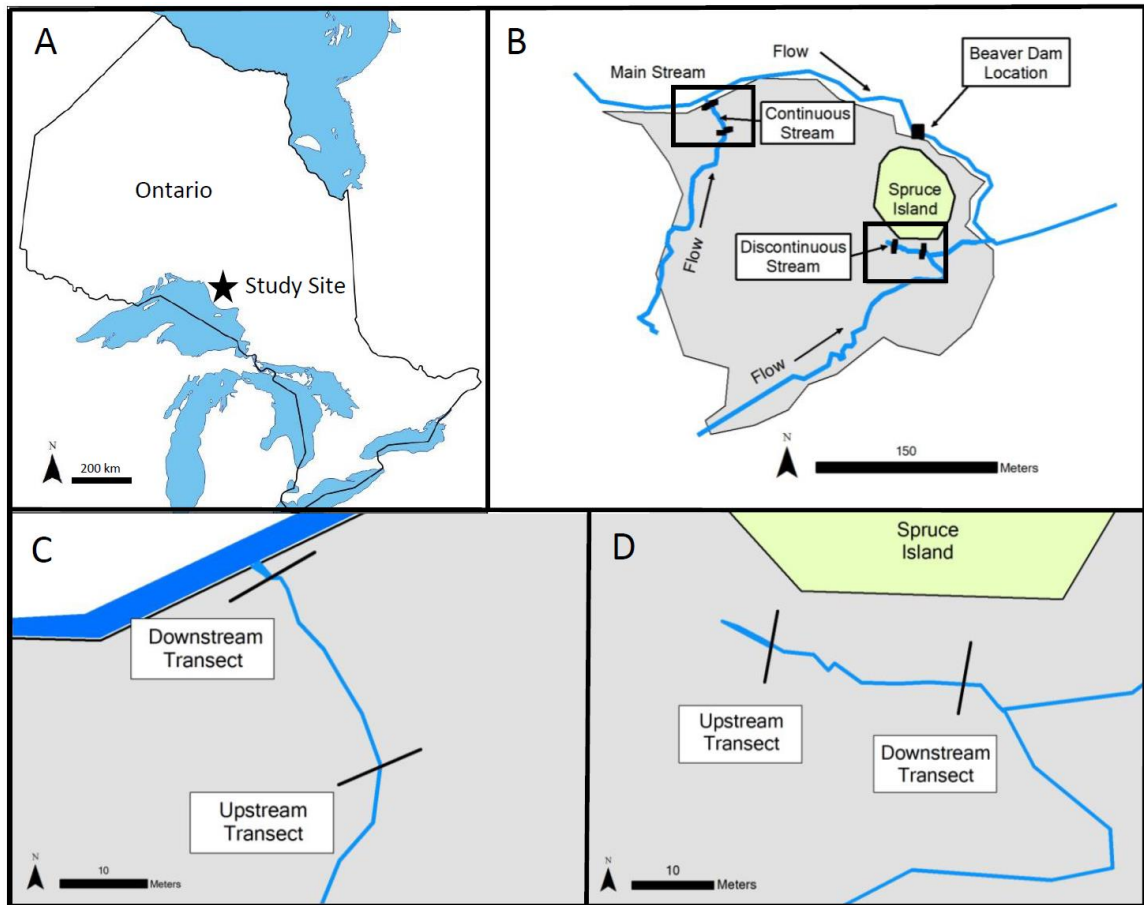


Figure 3.1: Intermediate Fen riparian zone site map.

Panel A shows the location of intermediate fen in northern Ontario. Panel B depicts the sedge-dominated intermediate fen, black boxes highlight the location of the Discontinuous Stream and the Continuous Stream upstream and downstream riparian transects. The solid black box indicates the location of a beaver dam, developed in June 25 and removed in July, panel B. 25 metres separate the riparian zone transects at the Continuous Stream, panel C. 24 metres separate the riparian zone transects at the Discontinuous Stream, panel D.

3.2.1.1 Riparian zone piezometer nests and channel descriptions

Pre-existing piezometer nests installed by the Ontario Ministry of Natural Resources and Forestry (MNR) adjacent to the channels of Continuous Stream (CS) and Discontinuous

Stream (DS) were incorporated into this study design. The piezometers had 20 cm slotted and are installed at 15, 40, 90 cm depths, but are referred to as 25, 50 and 100 cm piezometers referencing their maximum slotted depth. Piezometer depths reflect the absolute installation depth position. All piezometers were constructed from 4.97 cm I.D Schedule 40 PVC pipe. On each stream, we selected two symmetrical drainage piezometer nests at positions upstream and downstream on DS and CS as site locations for the installation of well transects (Figure 3.1C, D). The distances between the upstream and downstream transects were 25 m for CS and 24 m for DS.

Stream channel geomorphology varied substantially across both the CS and DS and the upstream and downstream transect locations. The channel width of the CS increased from 95 cm wide across the upstream riparian zone to 260 cm near its confluence with the Main Stream 26 metres downstream. Maximum channel depths were 25 and 39 cm across the upstream and downstream transects, respectively. The upstream channel incised peat soil 80-95 cm deep, whereas the downstream channel incised peat 200-300 cm deep. Across the DS channel, width increased from 10 cm across the upstream transect to 162 cm, 24 m downstream. The maximum channel depth in upstream DS channel was 8.2 cm, whereas the downstream channel depth was 29 cm. Peat soil surrounding the DS was 30-50 cm deep.

3.2.2 Field Methods

3.2.2.1 Well and stream piezometer construction

For this study I constructed and installed 32 (3.8 cm I.D.) water level monitoring wells and 32 (4.97 cm I.D.) porewater sampling from 10' (3.05 m) Schedule 40 PVC piping. I cut each well to a length of 76.2 cm and fitted with a PVC slip cap. I then slotted wells every 2 cm using a band saw with a 0.635 mm blade thickness. We designed each well to integrated porewaters and reflected water table position in the top 50 cm of peat, leaving approximately 20 cm of slot-free pipe to stick up above the peat surface once installed. I also constructed four stream piezometers from two 10' (3.05 m) Schedule 40 PVC pipes (4.97 cm I.D.). Before going in the field, I only fitted slip caps to the ends of each pipe.

Once in the field, I customised each stream piezometers to the depth of each stream and slotted 5 cm inlets using a metal hacksaw.

3.2.2.2 Determination of transect locations and installation of wells and stream piezometers

I installed wells and stream piezometers parallel to MNRF riparian zone piezometer nests. All transects were 8 m in total length, excluding the width of the stream or 4 m on either side of the stream (see Appendix A: Figure A5, Figure A6 for transect photos). I built and installed wooden raised boardwalks across each transect and stream channel to prevent disturbance of vegetation and peat compaction from trampling. Using a 2" (5.1 cm O.D.) steel Dutch auger (Eijkelkamp Soil and Water Water) I installed all the wells and stream piezometers for each riparian zone transect. We designed stream piezometers to have a 30 cm base installed 40 cm below the streambed for stability followed by a 5 cm slotted length. I then developed all wells and piezometers by purging their total volume at least four times after installation.

3.2.2.3 Hydrology measurement

We measured water levels in wells and piezometers using a custom metred tube. To measure water level, the tube was lowered gradually into the piezometer or well and air blown into the open vinyl end until contact with the water surface was made indicated by bubbling. We then recorded the depth of water. We made measures of water levels made twice monthly, typically a day prior to sampling before purging of piezometers and wells. To convert these measurements into a water table height and hydraulic head, I surveyed the elevation of each well using differential GPS (0.01 m), and depth to water was recalculated as metres above sea level (masl). Precipitation was recorded using a tipping bucket rain gauge (0.1 mm/tip) connected to a Ministry of Natural Resources and Forestry automatic weather station (AWS), which also recorded air and soil temperature, water table depth and wind speed and direction. The AWS recorded every 30 minutes and precipitation was expressed as daily total rainfall.

I measured saturated hydraulic conductivity (K) in several drainage and stream piezometers using the Hvorslev method (Freeze & Cherry 1979). Depending on the recharge time of each piezometer, I recorded the water level response using two types of instruments. For slower recharging piezometers (>2.5 hours), I used pressure transducers (Shlumberger Mini-Diver®) that recording water level every 15 minutes. For faster recharging piezometers (<2.5 hours), I used a stopwatch and made manual recordings of water level.

3.2.2.4 Porewater, stream water, precipitation chemistry

We sampled porewater and stream for THg and MeHg once monthly from mid-June through mid-October 2016. We sampled all Hg porewater samples from the 50 cm (4.97 I.D.) wells following the same protocol as described in section 2.2.2.1 in Chapter 2 of this thesis. We collected a field duplicate sample every ten samples and a pump blank for QA/QC at the end of each sampling campaign. For the collection of stream samples, we used two methods depending on the size of the bottle in use and the accessibility ‘clean hands’ had to the stream channel from which the sample came. For the first method, we used 500 mL ultraclean PETG bottles in concert with an aluminum extendable stream dipper. ‘Dirty hands’ submerged the sample bottle in to the channel using the stream dipper, while ‘clean hands’ manipulated the sample bottle. I then wrapped the PETG bottle in a Nitrile glove prior to being fitted in the stream dipper. For the second method, we did not employ the use of the stream dipper, and instead, we used 250 mL PETG bottles. ‘Clean hands’ then submerging the sample bottle by hand into the stream channel while ‘dirty hands’ assisted with opening and closing sample ziplock bags. We stored all samples in insulated coolers with icepacks until arriving at the field laboratory for filtration and preservation. I did not filter stream samples, they were only acidified. One stream sample had to be rejected for THg and MeHg analysis because of significant particulate matter observed in the sample.

We collected ions (Na^+ , K^+ , Mg^{2+} , Ca^{2+} , Cl^- , NO_3^- , SO_4^{2-}), DOC and DIC samples from stream piezometers and drainage piezometers at the same time as Hg samples in 60 mL

high density polyethylene (HDPE) bottles. We also collected samples for stable isotope analyses (deuterium [^2H] and oxygen-18 [^{18}O]) in 20 mL glass scintillation vials fitted with conical displacement caps. We collected porewaters using a peristaltic pump fitted with C-FlexUltra tubing. We collected field duplicates every ten samples.

After collection, we brought back well and piezometer samples for chemical analyses to the nearby field laboratory and vacuum filtered each using 0.5 μm glass fibre filters (Macherey-Nagel™). We used clean techniques to change filters, rinse filtration equipment with 18.2 MOhm reagent grade water, and handle Hg samples. After we filtered and split porewater well samples into 60 mL HDPE bottles for major ions and DOC/DIC analysis, the remaining volume in 250 mL PETG bottles was immediately preserved to 0.5% by volume using OmniTrace® hydrochloric acid. A filter blank was collected before transitioning to stream and drainage piezometer samples. We filtered and or preserved all samples within 12 hours of collection and stored at $\sim 4^\circ\text{C}$. After filtration, I soaked all filtering equipment in 10% hydrochloric acid overnight, then rinsed three each piece of equipment three times with 18.2 MOhm H_2O .

I collected precipitation samples from a custom funnel and collector, within 12–18 hours of previous rainfall. I collected precipitation as a composite event sample from in a 500 mL PETG bottle. I split samples into 60 mL HDPE bottles for ions and DOC/DIC analysis, and 20 mL scintillation vials for isotope analysis. Following sample collection, I rinsed the funnel, connecting tube, and 500 mL PETG bottle three times with 18.2 MOhm H_2O in preparation for the next precipitation event.

3.2.3 Analytical Methods

The analysis of THg and MeHg in porewater and stream samples followed U.S. EPA Methods 1631 and 1630, respectively. A detailed description of laboratory methods and method recoveries can be found in section 2.2.3 of Chapter 2 of this thesis.

I analysed DOC and DIC simultaneously on an O-I Analytical Aurora Model 1030 using a wet oxidation method. I used 7-12 mL aliquots poured into 40 mL glass vials fitted with

plastics caps and septa. With only one exception (July), I analysed all DIC and DOC samples within 72 hours of collection. We required all duplicates, both field and analytical, matrix spikes, and check standards to have recoveries of $\pm 15\%$. If QA/QC failed, I ran partial reruns ($\sim 10\%$ of analytical run) depending on scope of failure. The reporting limit for DOC and DIC was 0.5 ppm (0.5 mg/L) and the limit of linearity for the calibrated instrument was 120 ppm (120 mg/L).

I analysed major ions by ion chromatography. I used a Dionex 3000 ICS to analyse anions (F^- , Cl^- , NO_3^- , Br^- , PO_4^{3-} , and SO_4^{2-}) using AS14A column and a 0.1 mM and 0.8 mM carbonate ($H_2CO_3^{2-}$,) bicarbonate (HCO_3^-) eluent. For cations (Li^+ , Na^+ , NH_4^+ , K^+ , Mg^{2+} , and Ca^{2+}) analyses, I used a Dionex 1600 ICS using 20 mM methanesulphonic acid (CH_3SO_3H) eluent and a CS12A column. I ran all major ion samples using 0.5 mL aliquots unless dilutions were required. I ran analytical and field duplicate samples, matrix spikes, and check standards regularly (approximately every 10 samples) and recoveries were expected to fall $\pm 15\%$ criterion. I reran samples if QA/QC failed to meet criterion. The reporting limit for both the Dionex ICS 1600 and 3000 was 0.05 mg/L (0.05 ppm). Both instruments were calibrated to analyse major ions between 0.5 mg/L (0.5 ppm) and 50 mg/L (50 ppm).

We analysed the conservative isotopic tracers 2H and ^{18}O to characterise precipitation, stream, ground, and porewater using a Picarro L2120-i (Picarro, Inc.) The Picarro L2120-i operates using cavity ring-down spectroscopy. We use purchased standards from the Reston Stable Isotope Laboratory to calibrate 2H and ^{18}O to 0.8 and 0.4 ‰ precision, respectively. Standards for the calibration curve were all compared relative to the international standard VSMOW (Vienna Standard Mean Ocean Water), which we analysed as well. We ran duplicate samples are run every seven samples along with an internal check standard. I kept all 2H and ^{18}O sample vials tightly sealed until analysis. We used aliquots of 1.8 mL in 2 mL glass vials fitted with plastic caps and septa.

3.3 Results

3.3.1 Hydrology

Daily precipitation from June 1 to October 15 showed a seasonal pattern of relatively frequent precipitation events in early summer (June 1 – July 21) followed by a 30-day period with few precipitation events, and followed again by frequent precipitation events in late summer/fall (August 21-October 15) (Figure 3.2). Stream stage responded to precipitation events at both streams, however, at the Continuous Stream, beaver dam construction likely initiated on June 22 or 23 on the Main Stream upstream of its confluence with the Discontinuous Stream, caused stage to rise 24 cm before the dam was removed on July 18 resulting in a 19 cm drop (Figure 3.5). The water table drawdown period began shortly afterwards (July 21) and both stream experience an similar drop in stage of 9 cm.

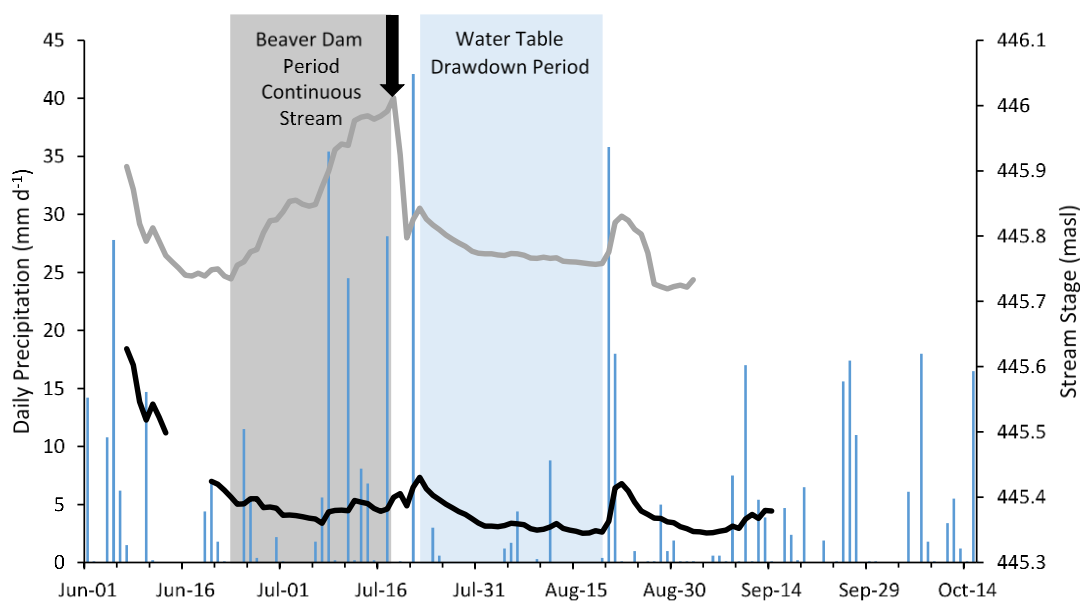


Figure 3.2: Discontinuous Stream and Continuous Stream levels

DS stage (black) shown for the duration of study period, technical error resulted in omission of data from June 13 through June 19. CS stage shown in gray. Two important hydrologic periods are shaded. Beaver dam development and subsequent stage increase (shaded gray) on CS, arrow indicated date of beaver dam removal. A 30-day period (shaded blue) with no significant precipitation ($> 10 \text{ mm d}^{-1}$) resulted in steady decline in stage in both streams. Desiccant saturation in early September and integrator cable failure resulted in stage data omission for the remainder of the study.

Results from Hvorslev bail tests in 100 cm, 50 cm, 25 cm and stream bed piezometers showed that hydraulic conductivity (K) were similar between peat soil and underlying mineral layer, differing by only \sim one order of magnitude (Table 3.1). In the CS, riparian zone peat K decreased with depth amongst 25, 50 and 100 cm piezometers. Peat K did not vary substantially with depth in DS peat, Peat K in the 50 cm piezometer of the CS was one order of magnitude greater than DS peat K at the same depth.

Table 3.1: Hydraulic conductivity (K) from riparian zone peat and underlying sand across the DS and CS

Phase	Transect	Piezometer	K (cm sec⁻¹)
Peat	CS	100 cm	1.3×10^{-4}
Peat	DS	50 cm	3.1×10^{-4}
Peat	CS	50 cm	1.7×10^{-3}
Peat	DS	25 cm	4.5×10^{-4}
Peat	CS	25 cm	2.0×10^{-3}
Underlying Sand	DS	100 cm	4.1×10^{-3}
Underlying Sand	DS	Stream	1.8×10^{-3}
Underlying Sand	CS	Stream	3.6×10^{-3}

3.3.1.1 Discontinuous stream

Riparian water table maxima occurred immediately following significant precipitation events on June 6, June 15, July 22, September 27, raising water tables 5–10 cm above the peat surface for approximately 24 hours. Minimum stream levels and riparian water tables occurred on August 17. Maximum recorded stream depths were 8 cm on June 15 and September 27 across the upstream transect (Figure 3.3A), while the downstream DS channel reached a maximum depth of 38 cm on October 14 (Figure 3.4A). Flow stopped in the upstream channel during much of August in response to the water table drawdown period. Following the dry period in August, the water table rise caused by four significant precipitation events returned the water table to near (± 1 –3 cm) the peat surface across the upstream DS riparian zone. Hydraulic gradients were towards the stream within 2 m of the stream channel. Hydraulic head measurements show quite a consistent pattern of groundwater recharge (Figure 3.3B, C; Figure 3.4B). Where groundwater discharge was measured (Figure 3.4C), differences in hydraulic head were small and only showed discharge at depth from the underlying coarse sand into the peat, with continued surface recharge.

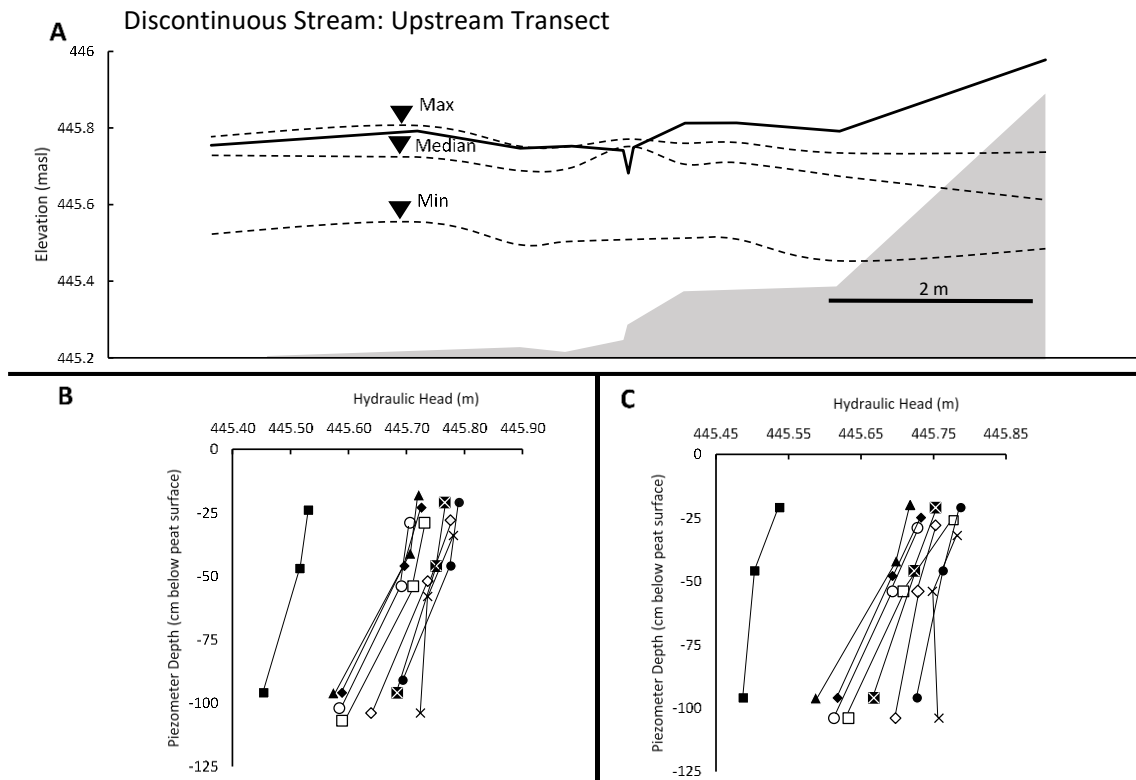


Figure 3.3: Discontinuous Stream: Upstream Transect water table and hydraulic gradients.

Cross-section of DS upstream transect (A). Gray shading represents underlying coarse sand, black solid line represents the peat surface and incised stream channel, peat soil (white), and dotted black line symbolized minimum, maximum, and median water table levels (A). Panels B (left riparian margin) and C (right riparian zone) display hydraulic head measures at 25, 50, 100 cm depths connected using black lines on June 15 (●), June 21 (⊗), July 4 (▲), July 20 (◆), August 17 (■), August 26 (○), September 18 (□), September 28 (◇), and October 14 (×).

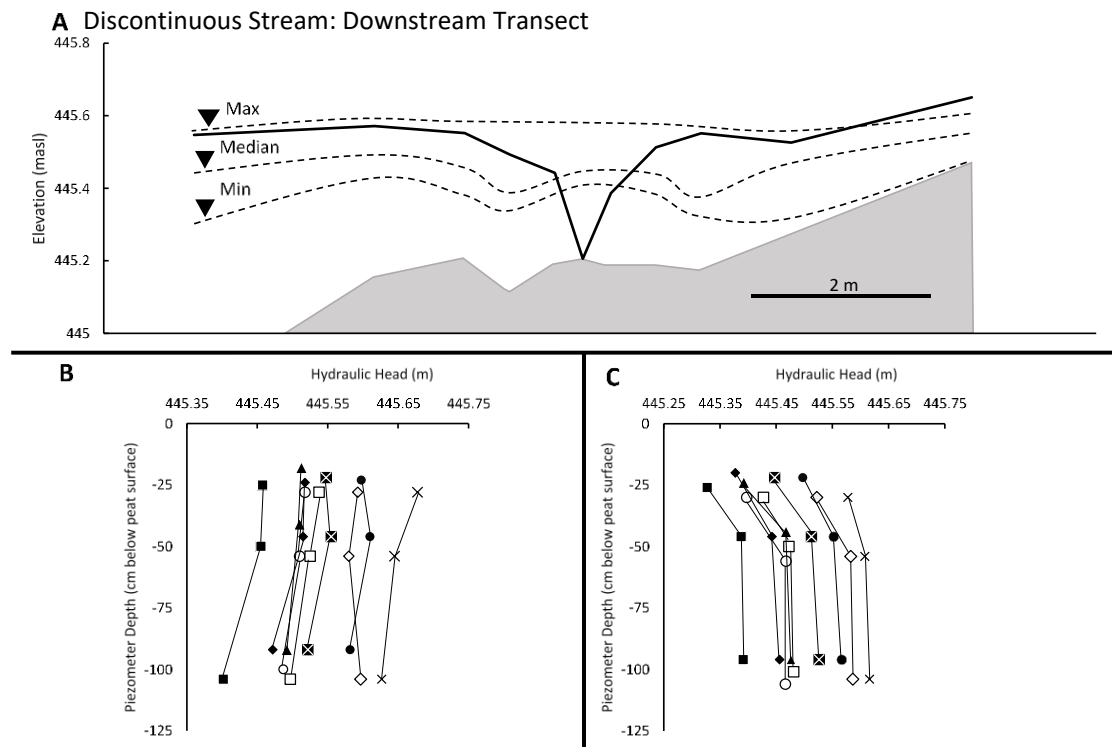


Figure 3.4: Discontinuous Stream: Downstream Transect water table and hydraulic gradients.

Cross-section of DS downstream transect (A). Gray shading represents underlying coarse sand, black solid line represents the peat surface and incised stream channel, peat soil (white), and dotted black line symbolized minimum, maximum, and median water table levels (A). Panels B (left riparian zone) and C (right riparian zone) display hydraulic head measures at 25, 50, 100 cm depths connected using black lines on June 15 (●), June 21 (⊗), July 4 (▲), July 20 (◆), August 17 (■), August 26 (○), September 18 (□), September 28 (◇), and October 14 (×).

3.3.1.2 Continuous Stream

The water table never went above the peat surface across the CS upstream riparian zone. In contrast, the water table was near to above the surface for much of study duration

across the downstream riparian zone. Minimum and maximum water tables occurred on August 17 and September 27, respectively at both CS riparian zone transects. Subsurface hydraulic gradients within 2.0 m of the stream edge were toward the CS channel at both riparian zone transects. CS stream flow persisted throughout the study duration. Across the CS upstream riparian zone, one riparian zone showed consistent downward hydraulic gradients at 100 cm depth and variable groundwater flow directions (both discharge and recharge) at 25 and 50 cm depths (Figure 3.5B). In contrast, the other riparian zone showed a consistent groundwater discharge pattern (Figure 3.5C). For both upstream riparian zones, hydraulic head differences were small. At the downstream riparian zones groundwater discharge was consistent and head differences were the greatest of any other riparian zone.

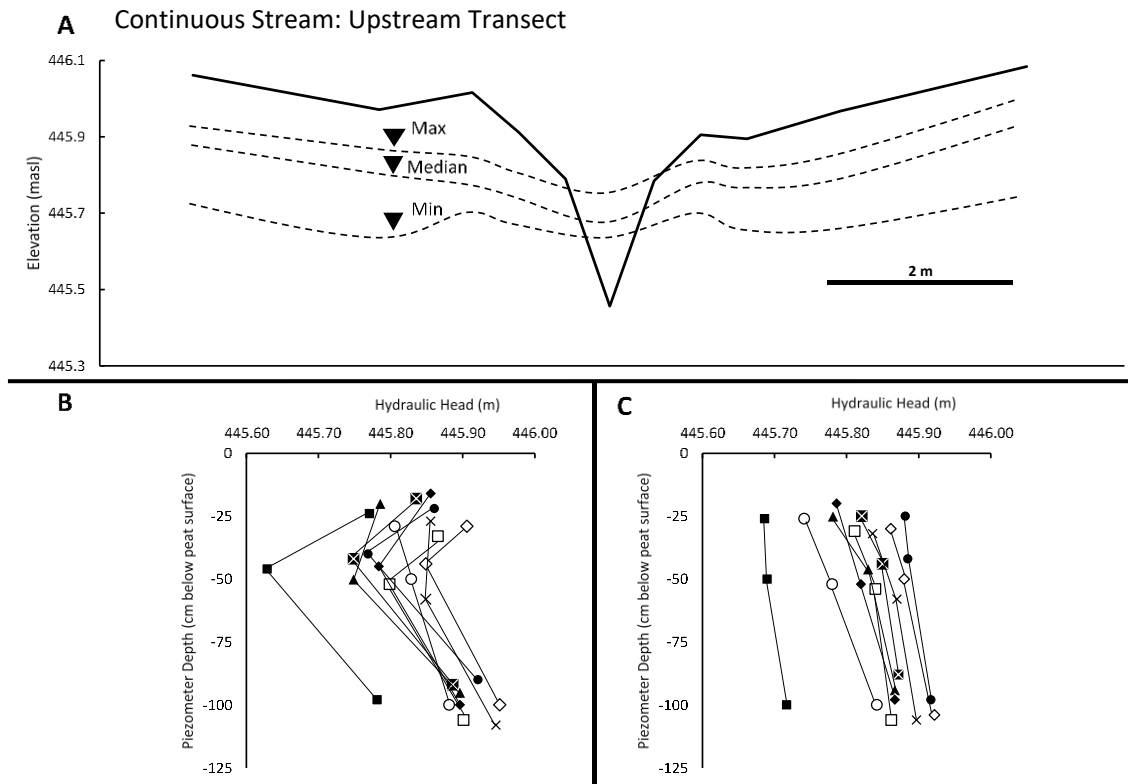


Figure 3.5: Continuous Stream: Upstream Transect water table and hydraulic gradients.

Cross-section of CS upstream transect (A). Black solid line represents the peat surface and incised stream channel, peat soil (white), and dotted black line symbolized minimum, maximum, and median water table levels (A). Panels B (left riparian zone) and C (right riparian zone) display hydraulic head measures at 25, 50, 100 cm depths connected using black lines on June 15 (●), June 21 (⊗), July 4 (▲), July 20 (◆), August 17 (■), August 26 (○), September 18 (□), September 28 (◇), and October 14 (×).

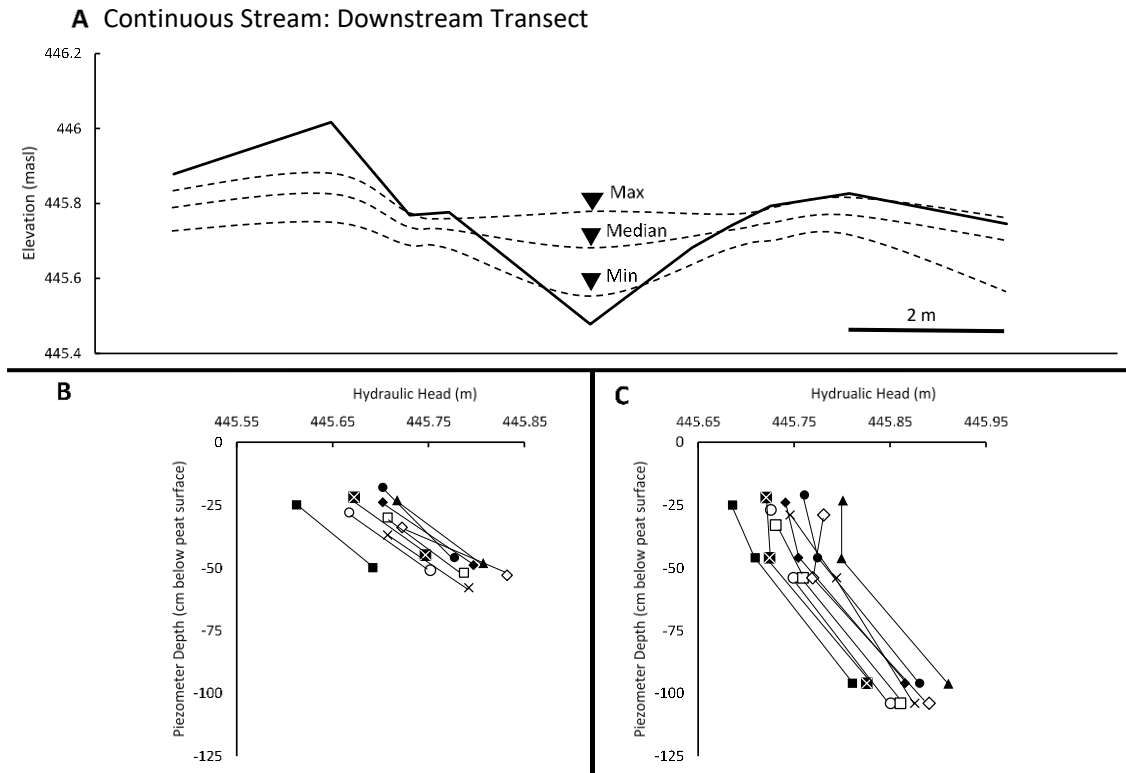


Figure 3.6: Continuous Stream: Downstream Transect water table and hydraulic gradients.

Cross-section of CS downstream transect (A). Black solid line represents the peat surface and incised stream channel, peat soil (white), and dotted black line symbolized minimum, maximum, and median water table levels (A). Panels B (left riparian zone) and C (right riparian zone) display hydraulic head measures at 25, 50, 100 cm depths connected using black lines on June 15 (●), June 21 (⊗), July 4 (▲), July 20 (◆), August 17 (■), August 26 (○), September 18 (□), September 28 (◇), and October 14 (×).

3.3.2 Patterns of pore, stream, and groundwater chemistry

3.3.2.1 Discontinuous Stream

Methylmercury concentrations in the pore and stream waters of the DS ranged from 0.07–1.67 ng-Hg L⁻¹. Temporally, June and August were the months with the highest pore and stream water MeHg concentrations (Figure 3.6A; Figure 3.7A). Porewater MeHg across the upstream DS riparian transect had the greatest temporal variability with the highest concentrations measured in August, which coincided with the lowest overall water table position across the riparian zone. Porewater MeHg concentrations were the greatest ≤ 2.0 m from stream across the downstream riparian transect compared to more distal riparian porewater (4.0 m). Temporally, stream water MeHg was highest in August (0.87 ng-Hg L⁻¹) in the downstream DS, whereas stream MeHg was highest in June in the upstream DS (0.93 ng-Hg L⁻¹). Pore and stream water THg across the DS riparian zones varied by over one order of magnitude (0.88–11.97 ng-Hg L⁻¹). Total Hg was more variable across the downstream riparian zone (0.88–11.44 ng-Hg L⁻¹) than the upstream transect (2.16–11.97 ng-Hg L⁻¹) (Figure 3.6B, Figure 3.7B). Though stream water THg followed the same temporal pattern as MeHg (i.e., greatest in June [upstream] and August [downstream]), concentrations were more consistent (Figure 3.6B; Figure 3.7B). Percent MeHg (%MeHg) ranged from 2.8–33.0% across the upstream DS riparian zone with greatest %MeHg found in wells ≤ 2.0 m from the stream (mean = 10.4%). In the DS downstream riparian zone %MeHg ranged from 2.8–56.4% with wells 1.0 m from the stream having the greatest %MeHg (mean = 23.1%).

Sulphate in pore and stream waters varied over space and time (Figure 3.6C; Figure 3.7C). Across the upstream DS transect, SO₄²⁻ was greatest under the lowest water table conditions in August. At the downstream transect, a horizontal SO₄²⁻ gradient was observed, with greatest concentrations seen furthest from the stream and nearest to the upland. Stream water SO₄²⁻ ranging from detection limit–0.61 mg L⁻¹. In 25, 50, and 100 cm riparian zone piezometers, pore and groundwater SO₄²⁻ were similar at all depths across the upstream riparian transect (Table 3.2). However, porewater in DS upstream 25

and 50 cm piezometers showed greater variability (range = 0.16–1.32 mg L⁻¹) compared groundwater in 100 cm piezometers (range = 0.21–0.80 mg L⁻¹). Conversely, SO₄²⁻ increased with depth (25 < 50 < 100 cm) in pore and groundwater across the DS downstream transect.

Dissolved organic carbon in DS pore and stream waters ranged from 3.72–24.76 mg L⁻¹ (Figure 3.6D; Figure 3.7D). The upstream riparian zone had DOC concentrations which were overall greater and varied less (17.00–24.76 mg L⁻¹) than those across the downstream riparian transect (3.72–22.80 mg L⁻¹). Across both riparian zones, stream water DOC was greater than porewater DOC. Dissolved organic carbon was greatest in porewaters from the 25 and 50 cm piezometers across each the DS riparian transects.

Dissolved inorganic carbon concentrations differed across DS transects (Figure 3.6E; Figure 3.7E). The total range of DIC concentrations was 1.30–57.39 mg L⁻¹, however, DIC concentrations never exceeded 6.50 mg L⁻¹ across the upstream transect. In addition to transect differences, a clear spatial gradient was observed across the DS downstream riparian porewaters. The gradient followed the opposite pattern observed in porewater SO₄²⁻ concentrations. Temporal patterns in porewater DIC were not observed in DS stream waters, while DIC was always greatest in the downstream waters. Temporally, DIC was greatest in August stream water. Dissolved inorganic carbon increased with depth DS upstream riparian pore and groundwater, whereas DIC decreased with depth in downstream riparian pore and groundwater.

Base cations (Ca²⁺ and Mg²⁺) followed a similar pattern to DIC concentrations in both pore and stream waters, whereas K⁺ showed an opposite pattern. Both Ca²⁺ and Mg²⁺ increased with depth across the DS downstream transect, while decreasing with depth across the upstream transect. Chloride concentrations were similar at all piezometer depths (25, 50 and 100 cm) in upstream DS riparian zone pore and groundwater, but increased with depth at the downstream riparian zone.

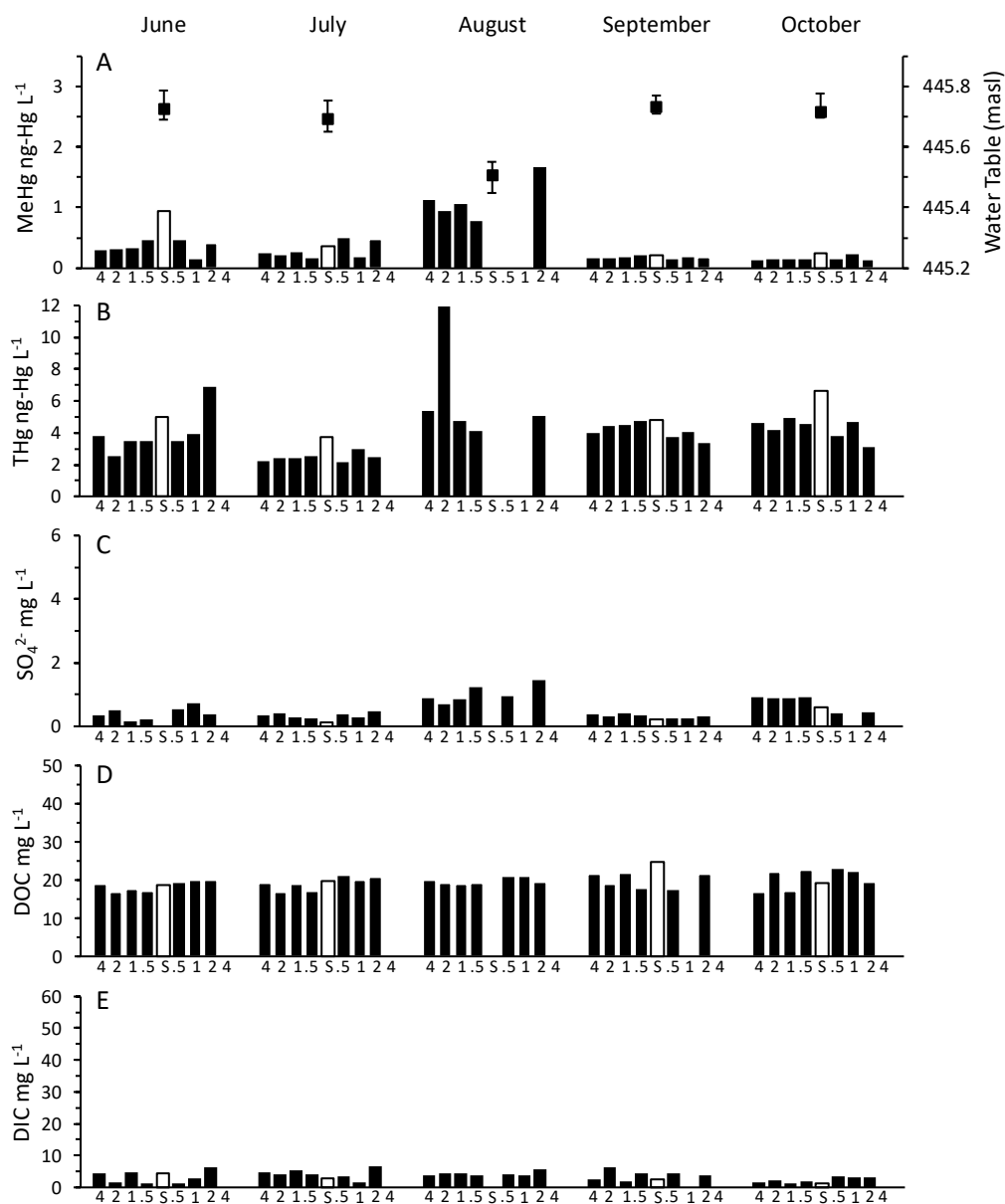


Figure 3.7: Discontinuous Stream: Upstream Transect pore and stream water chemistry.

DS upstream transect monthly pore and stream water MeHg (A), THg (B), SO_4^{2-} (C), DOC (D), and DIC (E) concentrations (left y-axis). Median (●) water table across riparian zones, error bars indicate water table range (right y-axis). Labels on the x-axis refer to the distance from the stream edge (0.5–4.0 m) for pore water samples (black bars) and (S) denotes the stream sample (white bar).

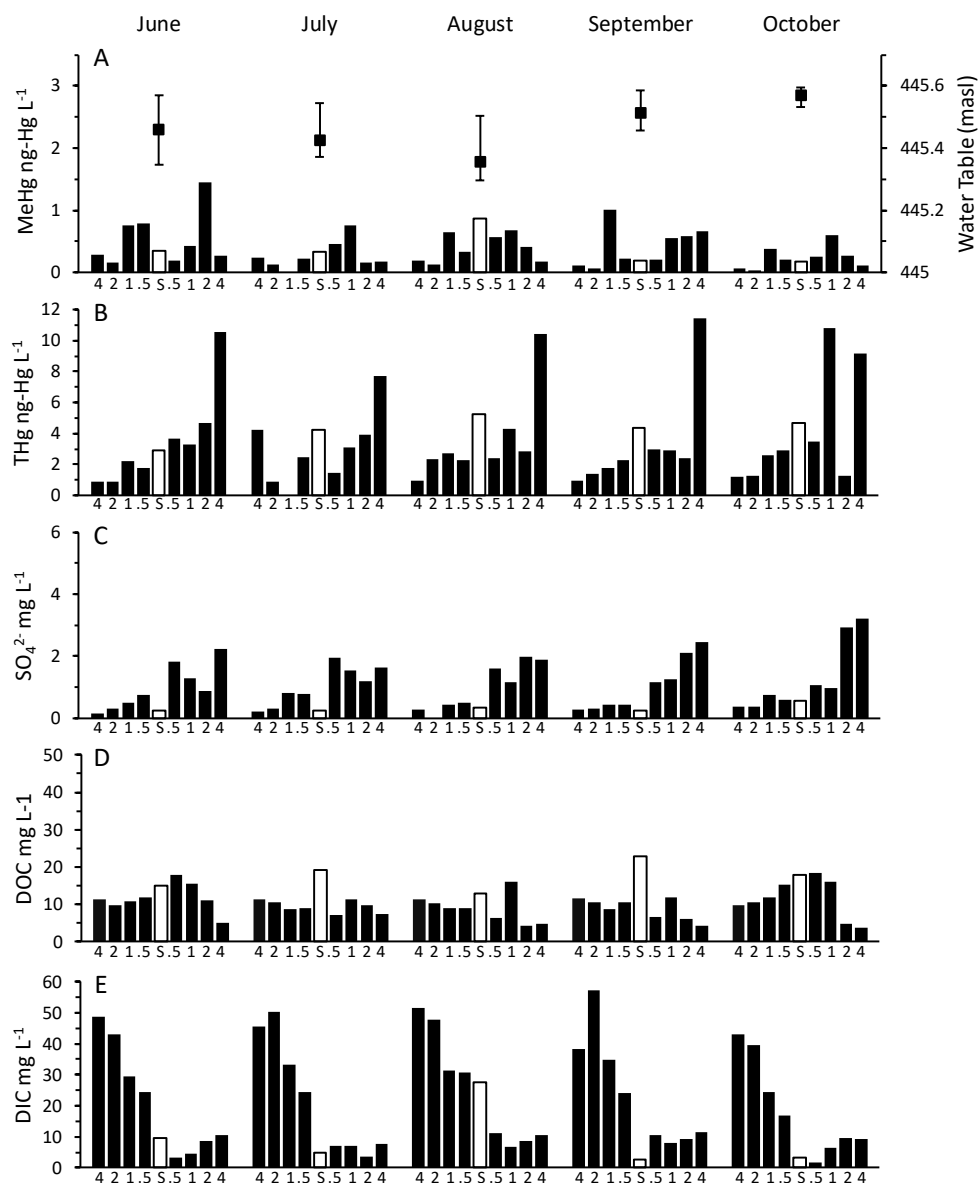


Figure 3.8: Discontinuous Stream: Downstream Transect pore and stream water chemistry.

DS downstream transect monthly pore and stream water MeHg (A), THg (B), SO_4^{2-} (C), DOC (D), and DIC (E) concentrations (left y-axis). Median (●) water table across riparian zones, error bars indicate water table range (right y-axis). Labels on the x-axis refer to the distance from the stream edge (0.5–4.0 m) for pore water samples (black bars) and (S) denotes the stream sample (white bar).

Table 3.2: Monthly piezometer ancillary porewater chemistry.

Mean (and standard deviation) of ancillary porewater chemistry from 25, 50 and 100 cm piezometers collected monthly and averaged over the study duration.

Discontinuous Stream						
Upstream	Piezometer Depth (cm)					
Solute	<u>25</u>	<u>50</u>	<u>100</u>	<u>25</u>	<u>50</u>	<u>100</u>
Cl ⁻ mg L ⁻¹	0.51 (0.20)	0.46 (0.25)	0.36 (25)	0.27 (0.20)	0.34 (0.24)	0.21 (0.08)
Ca ²⁺ mg L ⁻¹	5.64 (0.83)	6.20 (0.85)	28.46 (19.84)	5.22 (0.50)	5.02 (0.29)	50.25 (23.29)
Mg ²⁺ mg L ⁻¹	1.02 (0.25)	1.12 (0.20)	7.06 (6.62)	0.85 (0.09)	0.90 (0.13)	15.13 (7.31)
DIC mg L ⁻¹	4.43 (2.12)	1.53 (1.25)	26.58 (20.10)	4.49 (1.78)	4.03 (1.25)	48.51 (21.38)
DOC mg L ⁻¹	19.09 (2.30)	18.80 (2.40)	15.24 (3.98)	21.25 (1.44)	20.89 (1.52)	11.17 (3.36)
SO ₄ ²⁻ mg L ⁻¹	0.44 (0.26)	0.43 (0.50)	0.46 (0.19)	0.36 (0.06)	0.33 (0.13)	0.32 (0.08)
Downstream						
Cl ⁻ mg L ⁻¹	0.12 (0.07)	0.59 (0.72)	0.29 (0.13)	0.15 (0.07)	0.28 (0.19)	0.23 (0.09)
Ca ²⁺ mg L ⁻¹	52.19 (22.15)	47.50 (29.18)	24.37 (5.25)	14.30 (14.47)	11.84 (0.75)	18.42 (3.54)
Mg ²⁺ mg L ⁻¹	8.60 (1.35)	6.83 (2.53)	4.59 (0.13)	2.72 (2.62)	2.55 (0.09)	4.22 (0.29)
DIC mg L ⁻¹	34.28 (12.54)	48.97 (9.85)	19.40 (2.79)	12.23 (11.29)	10.28 (1.01)	15.13 (2.60)
DOC mg L ⁻¹	10.47 (0.59)	9.90 (1.27)	4.99 (0.57)	12.58 (3.36)	3.30 (0.11)	3.65 (0.47)
SO ₄ ²⁻ mg L ⁻¹	0.35 (0.08)	0.68 (0.57)	1.29 (0.69)	1.42 (0.62)	2.34 (0.50)	2.88 (0.39)
Continuous Stream						
Upstream	Piezometer Depth (cm)					
Solute	<u>25</u>	<u>50</u>	<u>100</u>	<u>25</u>	<u>50</u>	<u>100</u>
Cl ⁻ mg L ⁻¹	0.36 (0.27)	0.15 (0.09)	0.36 (0.12)	0.39 (0.03)	0.57 (0.45)	4.55 (0.66)
Ca ²⁺ mg L ⁻¹	15.71 (5.67)	27.67 (7.76)	47.57 (3.60)	12.90 (3.00)	13.78 (3.00)	88.13 (2.05)
Mg ²⁺ mg L ⁻¹	2.88 (1.26)	5.73 (2.27)	10.32 (0.61)	1.48 (0.23)	1.76 (0.60)	16.44 (0.59)
DIC mg L ⁻¹	14.41 (13.01)	15.26 (5.94)	36.40 (4.91)	11.78 (8.70)	17.22 (12.85)	24.47 (4.91)
DOC mg L ⁻¹	17.07 (9.08)	17.79 (8.04)	4.61 (2.42)	15.32 (6.72)	17.93 (6.35)	5.11 (3.97)
SO ₄ ²⁻ mg L ⁻¹	1.50 (0.68)	0.69 (0.27)	0.41 (0.13)	1.08 (0.43)	1.23 (0.68)	0.45 (0.13)
Downstream						
Cl ⁻ mg L ⁻¹	0.31 (0.20)	0.73 (0.75)	2.21 (0.44)	0.12 (0.08)	3.45 (0.73)	6.41 (0.73)
Ca ²⁺ mg L ⁻¹	11.52 (2.22)	14.06 (2.83)	81.26 (2.25)	15.91 (6.61)	63.63 (6.94)	84.00 (2.17)
Mg ²⁺ mg L ⁻¹	1.63 (0.31)	1.64 (0.11)	6.56 (0.13)	1.54 (0.45)	4.69 (0.37)	7.42 (1.31)
DIC mg L ⁻¹	10.28 (3.84)	21.37 (22.89)	45.85 (19.63)	11.10 (8.03)	48.17 (10.77)	49.81 (17.32)
DOC mg L ⁻¹	21.15 (2.97)	17.80 (8.08)	10.02 (5.09)	14.50 (8.16)	8.57 (3.21)	9.67 (10.71)
SO ₄ ²⁻ mg L ⁻¹	0.67 (0.30)	0.60 (0.41)	0.27 (0.05)	1.16 (1.18)	0.37 (0.19)	0.40 (0.27)

3.3.2.2 Continuous Stream

Pore and stream water MeHg concentrations across the upstream and downstream CS ranged from 0.09–3.36 ng-Hg L⁻¹ (Figure 3.8A; Figure 3.9A). Across the upstream CS transect, September MeHg concentrations in riparian porewater showed a distinct increase following the lowest water table position in August. Spatiotemporal patterns were not readily observed in the CS downstream riparian porewaters and were consistently lower than upstream porewater concentrations. Stream water MeHg was highest in August in upstream and downstream CS transects. Porewaters and stream water THg ranged from 1.07–11.97 ng-Hg L⁻¹ at the CS (Figure 3.8B; Figure 3.9B). Porewater THg was the highest across the CS upstream transect in July, whereas a less distinct pattern was observed in downstream porewaters. Stream water THg was highest in July and August at the CS upstream (6.08 ng-Hg L⁻¹) and downstream (4.96 ng-Hg L⁻¹) transects, respectively. Across the upstream CS riparian zone porewaters %MeHg ranged from 2.8–55.6% with wells 0.5 m from the stream having the highest %MeHg (mean = 20.3%). Percent MeHg ranged between 2.0–16.8% across the downstream CS riparian zone with minimal patterning observed in near stream (0.5 and 1.0 m) and more distal riparian zone wells (2.0 and 4.0 m).

Sulphate concentrations were spatially and temporally variable across the CS transects ranging 0.13–6.02 mg L⁻¹ (Figure 3.8C; Figure 3.9C). Riparian zone porewater SO₄²⁻ concentrations were highest in September, following the period of lowered water table in August. Across the upstream CS transect, a SO₄²⁻ concentration gradient was observed in September, with concentrations increasing with distance from the stream. Stream water SO₄²⁻ followed a similar pattern to porewater with the highest SO₄²⁻ concentrations occurring in September. In 25, 50 and 100 cm piezometers porewater SO₄²⁻ decreased with depth across both CS riparian transects with higher concentrations observed across the upstream CS riparian zones.

Stream and porewater DOC concentrations ranged 2.05–45.00 mg L⁻¹ (Figure 3.8D; Figure 3.9D). Greater porewater and stream water variability was observed at the CS

upstream transect (2.05–45.00 mg L⁻¹) relative to the downstream transect (8.53–40.31 mg L⁻¹). A spatial DOC gradient was observed in porewaters at the CS upstream transect with concentrations increasing with distance from the stream; a similar pattern was not observed across the downstream porewaters. Stream water DOC showed no distinguishable pattern and ranged 8.53–15.74 mg L⁻¹. Similar to the DS, DOC was greatest in the 25 and 50 cm piezometers across each CS riparian zone.

Concentrations of DIC in porewater and stream ranged 2.84–38.10 mg L⁻¹ (Figure 3.8E; Figure 3.9E). Spatial patterns were more evident than temporal patterns in CS stream and porewaters. The CS upstream porewaters had consistently greater DIC concentrations compared to downstream porewaters. Moreover, porewater DIC was greatest in CS upstream well ≤ 2.0 m from the stream channel. Similar to the DS concentrations of DIC and DOC revealed an inverse relationship in CS pore and stream waters. Stream water DIC did not reveal a significant temporal pattern. In 25, 50, and 100 cm piezometers DIC increased with depth in across both CS riparian zones.

Base cations (Ca²⁺ and Mg²⁺) followed a similar pattern to DIC concentrations in both pore and stream waters, while K⁺ showed an opposite pattern. Both Ca²⁺ and Mg²⁺ increased with depth across CS riparian zones. Chloride increased with depth as well and to a greater degree than observed in DS riparian zones. However, one of the CS riparian zone piezometer nests showed that Cl⁻ was invariable with depth.

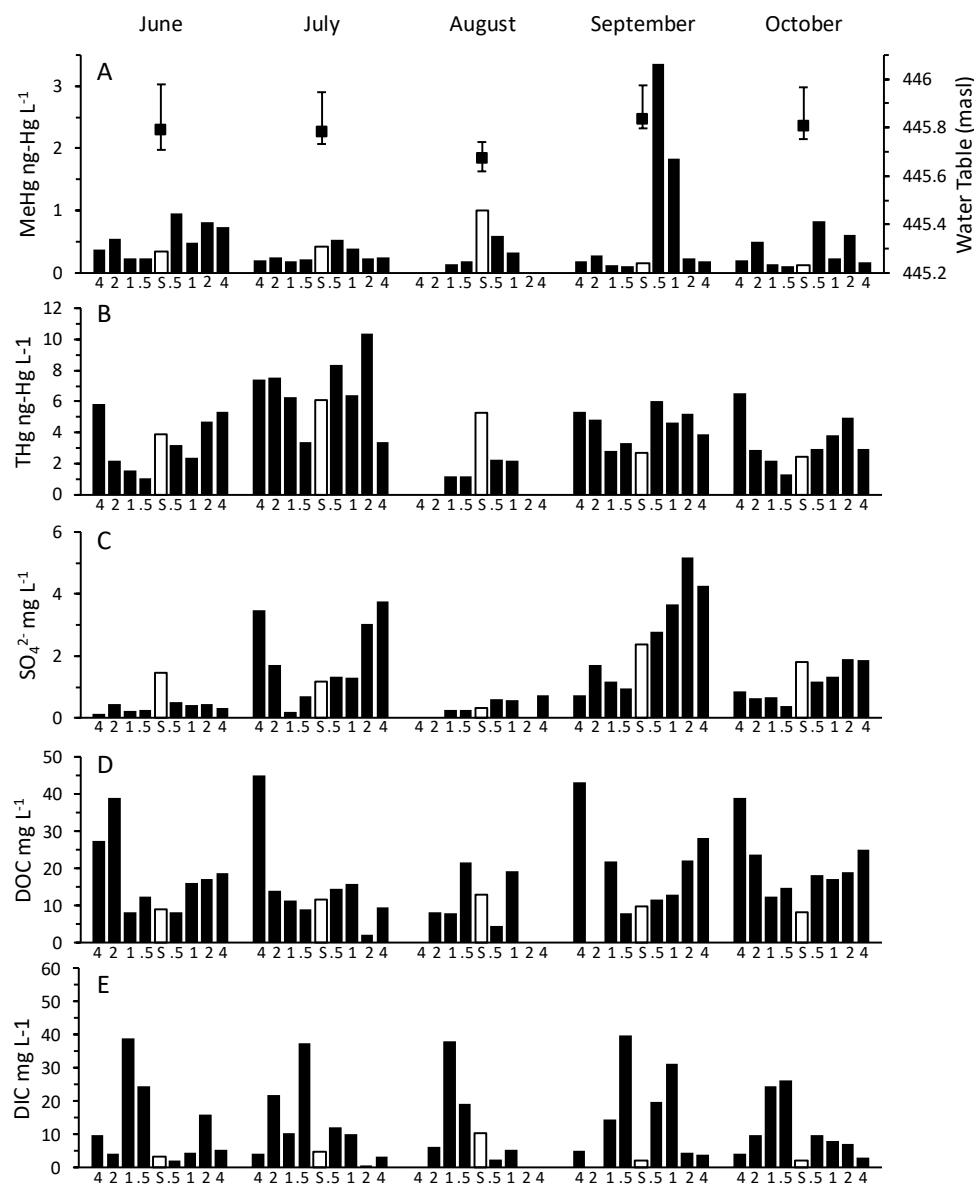


Figure 3.9: Continuous Stream: Upstream Transect pore and stream water chemistry.

CS upstream transect monthly pore and stream water MeHg (A), THg (B), SO_4^{2-} (C), DOC (D), and DIC (E) concentrations (left y-axis). Median (●) water table across riparian zones, error bars indicate water table range (right y-axis). Labels on the x-axis refer to the distance from the stream edge (0.5–4.0 m) for pore water samples (black bars) and (S) denotes the stream sample (white bar).

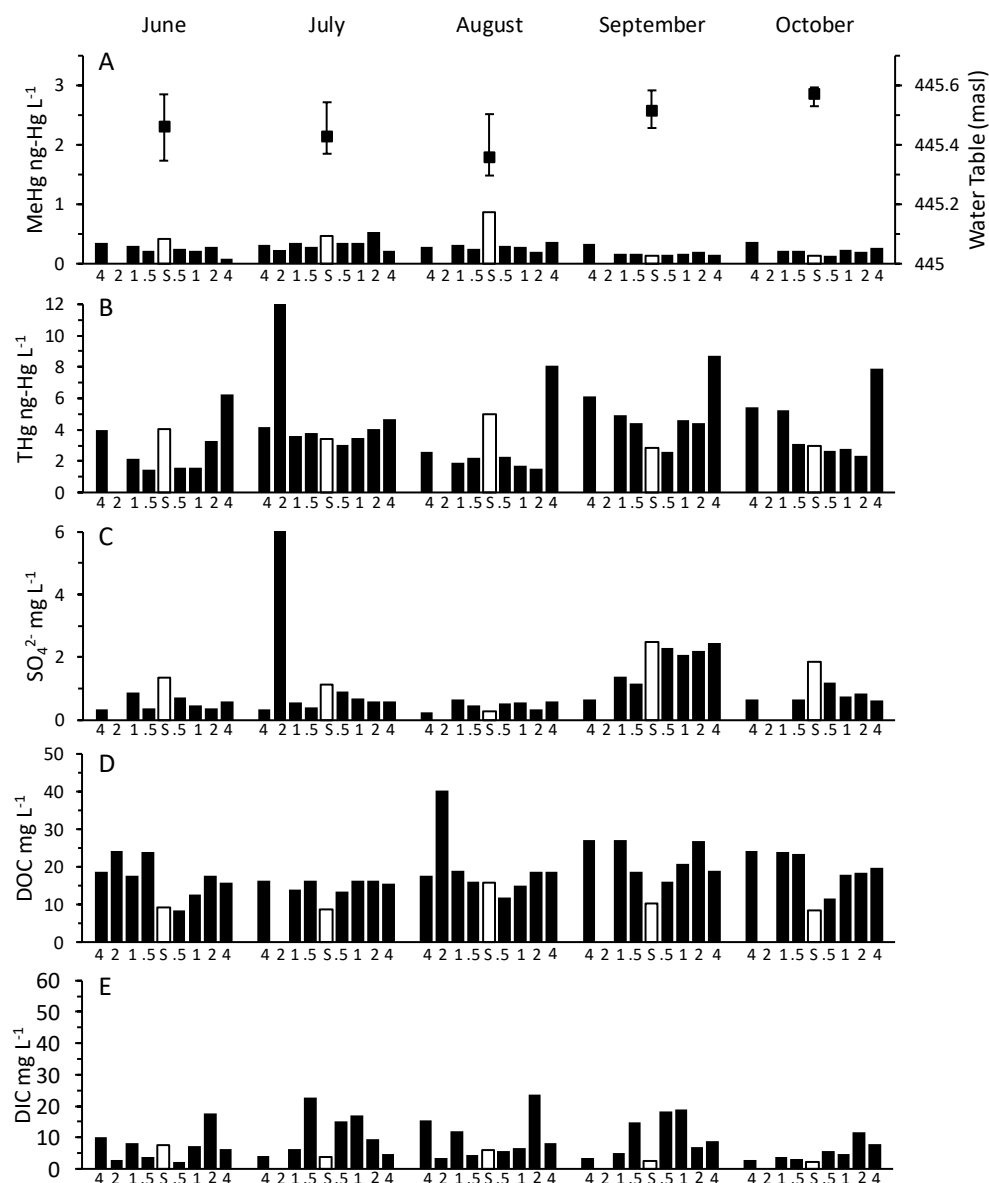


Figure 3.10: Continuous Stream: Downstream Transect pore and stream water chemistry.

CS downstream transect monthly pore and stream water MeHg (A), THg (B), SO_4^{2-} (C), DOC (D), and DIC (E) concentrations (left y-axis). Median (●) water table across riparian zones, error bars indicate water table range (right y-axis). Labels on the x-axis refer to the distance from the stream edge (0.5–4.0 m) for pore water samples (black bars) and (S) denotes the stream sample (white bar).

3.3.3 Stream water and riparian zone porewater interactions

Monthly bivariable diagnostic plots were used to visually evaluate interaction amongst stream water and peat porewaters nearest the DS and CS (e.g., 0.5 and 1.0 m wells) and those more distal (e.g., 2.0 and 4.0 m wells) over time using conservative tracers Cl^- and ^{18}O (Figure 3.11). Deeper porewater/shallow groundwater from 100 cm piezometers and precipitation were plotted as well. The bivariable plots depict precipitation along with stream, pore and groundwater in a space where the relative proximity of different points indicate similarity. Throughout the study duration, stream water from the DS showed strong coherence with riparian zone waters. While stream water from the CS was often isolated from riparian zone waters, aside from July. Stream water ^{18}O from the DS was most similar to riparian zone wells 0.5 and 1.0 m from the stream edge alongside groundwater from the 100 cm piezometers compared riparian wells more distal. Chloride in DS stream water showed less coherence with riparian zone waters. Temporally, ^{18}O was the least enriched in June across DS and CS stream and riparian waters (Figure 3.11A, B). While ^{18}O in August (Figure 3.11E, F) and October (Figure 3.11I, J) stream and riparian waters were the most enriched. Precipitation ^{18}O , although considerable variable shifted from being less enriched in June to more enriched by September (Figure 3.11G, H). In CS and DS stream, pore, and groundwater Cl^- concentrations were the highest August and September, and lowest in July (Figure 3.11C, D). Chloride was most variable in DS stream and porewaters whereas ^{18}O was most variable in CS 100 cm piezometers. Throughout the study duration, low Cl^- concentrations ($< 0.5 \text{ mg L}^{-1}$) occurred in all CS stream waters and precipitation.

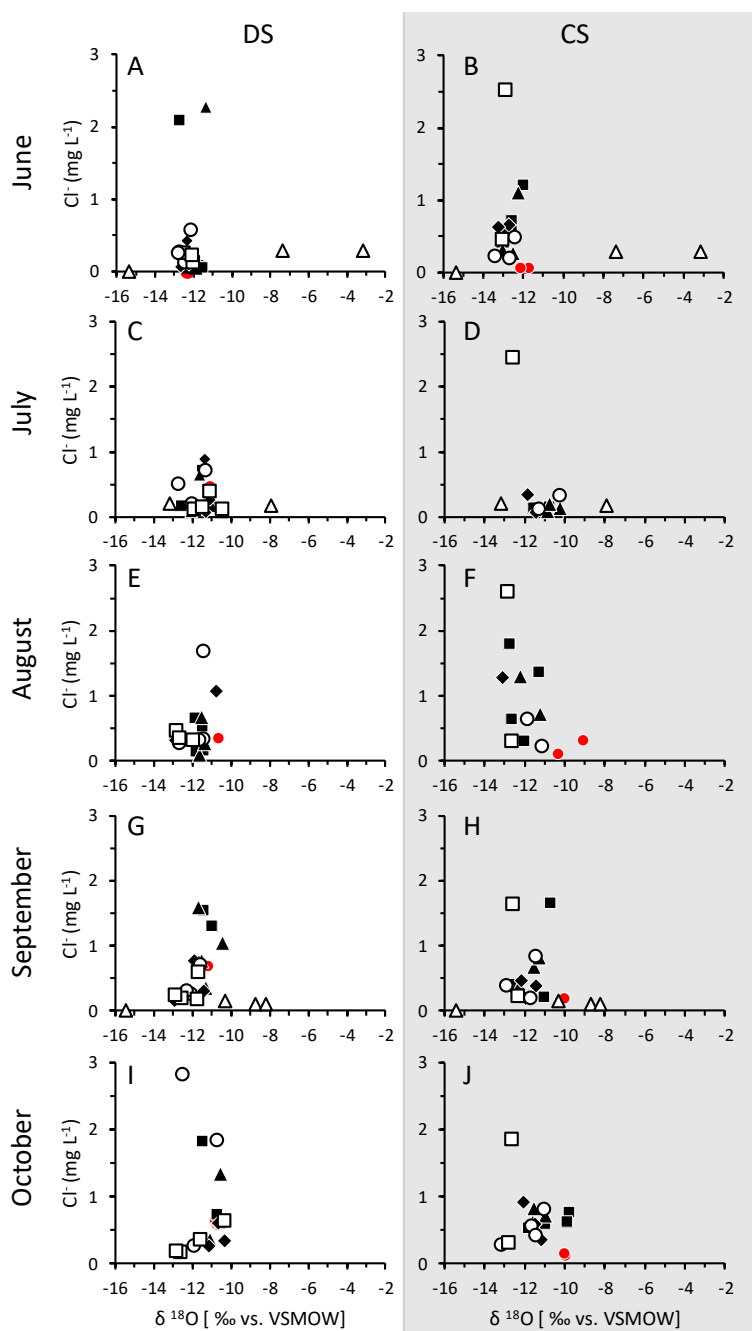


Figure 3.11: Biplots of conservative tracers ^{18}O and Cl^- collected over the study period.

Symbols represent stream water (●), porewater from 0.5 m (■), 1.0 m (▲), 2.0 m (◆), 4.0 m (○) and 100 cm piezometer (□), and precipitation (△). DS waters plotted on the left and CS on the right (gray shading).

3.3.4 Bivariate relationships between total mercury and methylmercury with other chemistry

There was a weak relationship observed between THg and MeHg, and MeHg and DOC, across all stream and porewaters. A strong positive relationship did occur between MeHg and SO_4^{2-} , however, exclusively at the DS upstream transect. The strongest bivariate relationship was found between THg and DOC. Dissolved organic carbon and THg in stream and porewaters were positively related only in the downstream transects of DS and CS (Figure 3.11). Across the DS downstream transect THg was less variable to THg concentrations compared to the CS downstream transect. Both the upstream and downstream DS stream and porewater DOC and THg relationships occurred in distinct clusters. Across the upstream transects of the CS, THg was showed strong variance across all DOC concentrations.

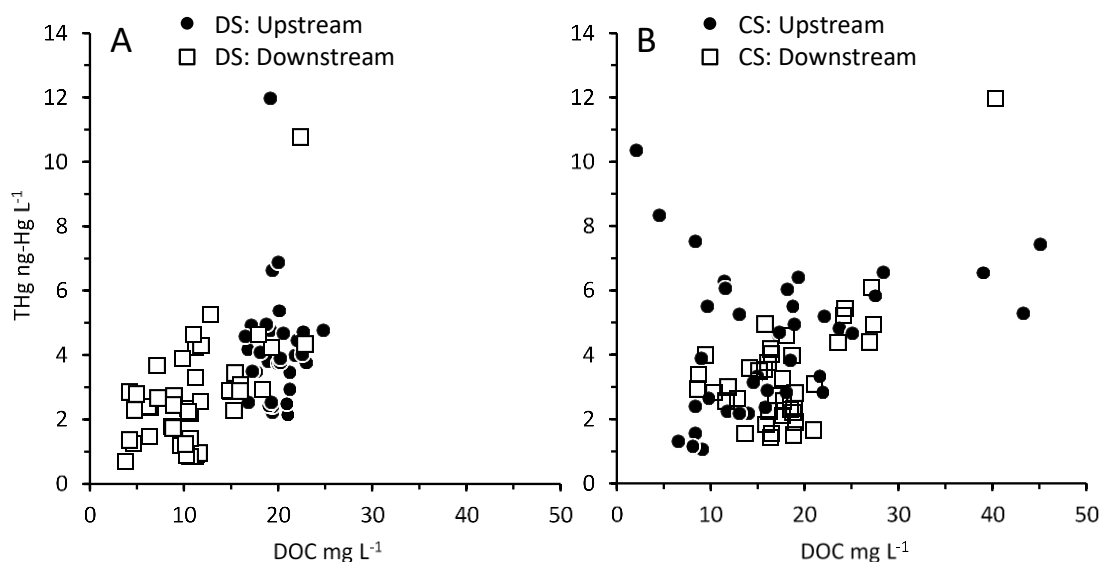


Figure 3.12: Bivariate plots showing THg and DOC in riparian zone pore and stream waters. The DS is shown in panel A and the CS in panel B.

3.4 Discussion

3.4.1 Hydrology and groundwater controls on sulphate delivery

My original hypothesis that MeHg in riparian zones would be controlled by groundwater SO_4^{2-} delivery to peat porewaters was not supported by the observations of this study. Decreasing concentrations of SO_4^{2-} with depth seen in deeper peats and shallow groundwater piezometers were similar to that reported previously across the whole fen (McLaughlin & Webster 2010). In riparian zones where groundwater discharge was observed, gradients were similar to values reported in a poor fen (~10–20 cm between 25 and 100 cm piezometers) by Branfireun & Roulet (2002). Furthermore, Branfireun & Roulet (2002) showed that groundwater discharge corresponded to greater SO_4^{2-} concentrations (sourced from upland and depositional locales) and elevated porewater MeHg concentrations. A similar pattern was not seen in the riparian zones of CS or DS. Earlier work by Devito & Hill (1997) showed that greater till depth in the surrounding uplands of valley bottom wetlands of the southern Canadian Shield resulted greater groundwater storage and residence time allowing for continued groundwater discharge rich in SO_4^{2-} (~10 mg L⁻¹) to interior portions of the wetland. Then as groundwater discharged across the mineral to peat soil interface, a sharp transition to reduced conditions (i.e. SO_4^{2-} reduction) occurred (Devito & Hill 1997). Although groundwater inputs maintain water tables near the peat surface in the intermediate fen (see Ch.2 of this thesis), groundwater was not rich in SO_4^{2-} . The minor components of SO_4^{2-} in riparian zone groundwater can be explained by the chemical makeup of underlying unconsolidated materials below the intermediate fen. Calcite (CaCO_3) and dolomite ($\text{CaMg}(\text{CO}_3)_2$) minerals with small contributions from glacially derived greywacke (sandstone mixed with clay) contain no or minor amounts of SO_4^{2-} and were the main unconsolidated material below the peatland (Prest et al. 2000; Packalen et al. 2011). Major ions Ca^{2+} and Mg^{2+} along with DIC (major component being bicarbonate [HCO_3^-]) in deeper porewater was observed in this study as well as by McLaughlin & Webster (2010). Higher SO_4^{2-} concentrations in 25 and 50 cm porewaters suggested minor upland,

but mostly atmospheric sources of SO_4^{2-} as a more reasonable alternative explanation for patterns observed in the DS and CS riparian zones.

3.4.2 Spatiotemporal patterns of stream and porewater chemistry

3.4.2.1 Upstream riparian margins

The highest measured MeHg concentrations were found in the upstream riparian zones of the DS and CS. Greater range of water table fluctuations and higher SO_4^{2-} concentrations following water table rise after drought corresponded to the higher MeHg concentrations across the upstream riparian zones. Elevated MeHg concentrations may have resulted from SO_4^{2-} regeneration as described by Coleman-Wasik et al. (2015) following a drought period. The period of water table drawdown from July 21 to August 19 across the DS and CS riparian zones was central to explaining net MeHg production. Therefore, 30 days was a sufficient time interval to regenerate SO_4^{2-} and provided anoxic conditions persisted, promoted SRB respiration and in turn net MeHg production. Shorter dewatering events (3-9 days) have been shown to not significantly alter SO_4^{2-} regeneration or microbial communities (Nunes et al. 2015). The months of August and September were when the upstream transects of the DS and CS experienced the highest SO_4^{2-} and MeHg concentrations, respectively. Hydrologic regime differences between these two transects explain the spatiotemporal patterns observed.

By maintaining an unsaturated peat soil layer, the upstream CS riparian zone SO_4^{2-} would likely remain available for SRB as the water table rose through September. In contrast, the water table was already above or near the peat surface across the upstream DS riparian zone in September limiting the availability of SO_4^{2-} to SRB. As observed by Jeremiason et al. (2006) and Mitchell et al. (2008c), SO_4^{2-} is rapidly (1–5 days) utilized by SRB, therefore more frequent sampling of riparian porewaters following the seasonal low water table (August 17) would have better captured the temporal rise and fall of DS and CS SO_4^{2-} and MeHg.

Across both the upstream riparian zones of the DS and CS a clear patterned response to water table drawdown controlled SO_4^{2-} and MeHg. In riparian porewaters with the greatest MeHg concentrations, lower SO_4^{2-} concentrations relative to adjacent riparian porewaters with lower MeHg and higher SO_4^{2-} was consistently observed. Regnell et al. (2009) observed a similar pattern in the riparian zones of a boreal stream in southern Sweden, concluding that SRB respiration was responsible for this trend. Despite these observations, an underlying quantifiable mechanism to explain these hydrologic and biogeochemical patterns remains elusive. An exact water table position or ideal ratio between unsaturated and saturated peat soil conditions was explored to explain the MeHg patterns, but provided inconclusive insight. Qualitatively, however, the drier the riparian zone, either observed as an overall lower water table (CS upstream transect) or through seasonal water table fluctuations (DS upstream transect), the greater net MeHg production observed in the riparian zones of a sedge-dominated intermediate fen.

3.4.2.2 Downstream riparian margins

Across the downstream riparian zones of the DS and CS, smaller seasonal water table fluctuations and higher water tables limited net MeHg production in riparian porewaters. Porewater MeHg was greatest when water table elevations were most variable (June) and lowest overall (August) across the DS downstream riparian zone similar to patterns at the upstream riparian zone. Influences from the upland resulted in a SO_4^{2-} gradient, decreasing with distance from the upland. A previous study found a similar trend across the upland-peatland interface (Mitchell et al. 2009). A similar pattern was not seen at the DS upstream riparian zone where preferential flow paths and upland topography may have resulted in these differences (Mitchell et al. 2009). Importantly, MeHg production did not correspond to the upland SO_4^{2-} gradient as observed by Mitchell et al. (2009). Instead, SO_4^{2-} from upland preferentially flowed underneath the low hydraulic conductivity peat ($K \sim 10^{-4} \text{ cm sec}^{-1}$) through the underlying sand ($K = 10^{-3} \text{ cm sec}^{-1}$), which did not occur in the moss-dominated peatland studied by Mitchell et al. (2009). Porewater SO_4^{2-} increased with depth across the same sedge-dominated peatland

(McLaughlin & Webster 2010) and in the riparian zones of this study, substantiating this hydrologic explanation.

The CS downstream riparian zone had the lowest MeHg concentrations of any transect in this study (maximum concentration = 0.54 ng-Hg L⁻¹). Considering the elevated porewater SO₄²⁻ concentrations (mean = 0.97 mg L⁻¹), the high overall water table and persistent groundwater discharge, the Main Stream appeared to greatly influence porewater chemistry. Elevated SO₄²⁻ and low MeHg concentrations, and moving water all suggested reducing conditions were not present in the CS downstream riparian zones. Although dissolved oxygen was not directly measured, the presence of SO₄²⁻ in deep peat (> 2.4 m) porewaters as well as the confluence of surface waters (the Main Stream and CS) all point to oxic surface water moving through the CS downstream peat soil. When surface waters interacted with riparian peat porewaters, Regnell et al. (2009) observed low MeHg concentrations in riparian zones in Sweden as well.

3.4.3 Transport of total mercury, methylmercury, and other solutes

Temporal patterns of stream water chemistry in the DS and CS indicated the importance of upland and groundwater contributions to each stream. Stream water MeHg concentrations appeared to be influenced by riparian zone porewaters rather than upland or groundwater sources. Total Hg in the DS downstream concentrations in September and October remained high despite higher water tables and low MeHg concentrations. Runoff from the upland soils was the likely source, as THg and DOC were high relative to MeHg concentrations (Kolka et al. 2001). Upland soils are not typically major sources of MeHg, but as Bishop et al. (1995) showed, runoff from upland soils contributed THg to riparian zones where then much of it becomes either bound to peat soil or dissolved organic matter (Drexel et al. 2002). During August, the low water table resulted in no flow in the upstream DS channel bed, while flow continued downstream. Groundwater maintained the DS downstream transect flow as seen by the 4-fold increase in DIC concentrations, and lower DOC and SO₄²⁻ concentrations compared to September and October. Subsurface contributions from riparian zones such as DOC were limited to by hydrologic

connectivity and hydraulic gradients. The maximum MeHg and minimum SO_4^{2-} concentrations in the DS August stream water suggested SRB respiration and Hg methylation in riparian peats hydrologically connected using regenerated SO_4^{2-} .

The CS was not influenced by upland contributions nor strongly by groundwater or riparian zone contributions resulting in overall relatively dilute stream water. Regardless, stream water THg, MeHg, SO_4^{2-} , DOC, and DIC all suggested some contributions from riparian zone pore and groundwater to the CS stream. Stream water THg and DOC corresponded proportionately during all months measured. During August, under the lowest water table levels, evidence of increased acidity was seen with increased DOC and THg. Simultaneously, the lower water table resulted in greater DIC in, suggesting more groundwater contributing to CS stream waters. Similar responses to lowered water tables were seen by Packalen et al. (2011) in CS stream waters. Flushing of SO_4^{2-} occurred in September and October corresponding to SO_4^{2-} regeneration in riparian zones as the water table rose. Considering the low SO_4^{2-} in deeper groundwater, the riparian zones were the clear sources of SO_4^{2-} to CS stream waters. Flushing of SO_4^{2-} following water table drawdown has been observed in other wetlands as well (Devito & Hill 1999). The highest MeHg concentrations and lowest SO_4^{2-} were observed in August in the CS; higher MeHg in August riparian zones nearest to the stream channel suggest net methylation of Hg by SRB.

The stream water chemistries of the DS and CS clearly reflected the size and scope of their individual receiving areas (sub-fen catchments). During periods of lowest water table, groundwater maintains both streams, with greater effect observed at the CS (Packalen et al. 2011). Direct stream water chemistry influences were limited to hydrologically connected riparian zones at the DS. The smaller receiving area of the DS and upland influences resulted in more variable stream water chemistry compared to the CS. Most importantly, unlike most moss-dominated northern peatlands, increased water tables and greater hydrologic connectivity did not result in greater MeHg concentrations

in surface waters (Branfireun & Roulet 2002). This effect was due to the low hydraulic conductivity riparian peat soils and shallow hydraulic gradients towards stream channels.

Riparian zone topography in the first-order streams, riparian peat hydraulic conductivity ($\sim 10^{-4}$ cm sec⁻¹) and conservative tracers (Cl⁻ and ¹⁸O) indicated that under most water table conditions observed during this study (i.e., water table below the peat surface), the receiving area connected to each stream was limited to ≤ 2.0 m from the stream channel. In a previous study by McLaughlin & Webster (2010), the sedge-dominated intermediate fen was divided into four sub-catchments based on using larger-scale topography and the methods described by Waddington & Roulet (1997). These zones correspond well to the topography measured in this study, however, at a finer-scale, small changes in topography (1-5 cm) appear to control hydraulic gradients away from the DS and CS channels towards the interior of the peatland, where other drainage pathways may exist or lead to isolated zones of pooled water. Under the highest water table conditions when much of the site is inundated and connected to surface waters, the finer scale topographic differences matters far less. However, those periods are brief (1-2 days) and unlike in other studies, flushing of MeHg was not observed (Branfireun et al. 1996). A simple calculation of the perennial reaches (where flow was maintained throughout the study) of each stream in the sedge-dominated intermediate fen was performed. The DS had a perennial reach of 24 m and 322 m coming from the primary channel for which it confluences with, while the CS had 140 m. In total, there was 486 m of perennial stream channel reach. Assuming a 2.0 m riparian zone on either stream bank, the contributing area of the entire sedge-dominated peatland was 1944 m². Therefore, out of the 53000 m² of the sedge-dominated intermediate fen area 3.7% was primarily responsible for contributing the annual MeHg flux in continuously connected surface waters. This calculation is an oversimplification of the complex biogeochemistry and riparian zone hydrology that controls MeHg production and transport. Nevertheless, as an approximation, the estimate indicated the importance of riparian zones on influencing MeHg transport to downstream aquatic environments.

3.4.4 Relationships among total mercury, methylmercury, and other solutes

Riparian zones with the highest MeHg concentrations did not always directly relate to the highest THg concentrations. In several instances a small THg concentration corresponded to high MeHg concentration suggesting localized net MeHg production as indicated by elevated %MeHg (Mitchell et al. 2008a). In other instances, THg, MeHg, and DOC concentrations increase simultaneously suggesting that THg and MeHg were strongly bound to DOC (Drexel et al. 2002), however, these instances were exceptions to the overall pattern. Only across the downstream transects of the DS and CS was a strong relationship found between THg and DOC. The strong affinity Hg(II) has with DOC is well established (Drexel et al. 2002) and is influenced by pH (Haitzer et al. 2003) among other controls. Several studies have found a similar relationship in peatland porewaters (Bishop et al. 1995; Kolka et al. 2001; Selvendiran et al. 2008) and streams with significant wetland contributions (Krabbenhoft et al. 1995; Balogh et al. 2005; Regnell et al. 2009; Brigham et al. 2009), however this is not always the case (Regnell & Hammer 2004). Though not measured, differences in pH control DOC and THg binding coefficients (Haitzer et al. 2003) and microbial uptake of Hg(II) (Kelly et al. 2003). McLaughlin and Webster (2010) found that higher concentrations of HCO_3^- ($\geq 30 \text{ mg L}^{-1}$) a major component of DIC, Ca^{2+} ($\geq 11 \text{ mg L}^{-1}$) and Mg^{2+} ($\geq 1.9 \text{ mg L}^{-1}$) corresponded to higher pH (≥ 6.7) in porewaters from 50 cm piezometers in the same sedge-dominated intermediate. In DS and CS riparian zone porewaters where these conditions occur, Hg methylation certainly may be limited by high pH.

3.4.5 Application of riparian zone MeHg dynamics to parsimonious modeling

To better understand the spatial and temporal patterns observed in the riparian zones of an intermediate fen, the pore and stream water data presented lend themselves to the use of parsimonious model. Eklöf et al. (2015) generated a parsimonious model to describe spatial and temporal fluxes of THg and MeHg into several boreal streams from their adjacent riparian zones in northern Sweden. Eklöf et al. (2015) suggested using a

parsimonious model because landscape heterogeneity, the complexity of the Hg biogeochemistry, and the computational complexity of modeling all components of Hg biogeochemistry make understanding riparian zone/stream Hg difficult, therefore a simple model was ideal. Moreover, non-independence amongst pH, DOC, SO_4^{2-} , THg, and MeHg variables violate the assumptions of many statistical tests and models (e.g., linear regression analysis and analysis of variance [ANOVA]). The model presented by Eklöf et al. (2015) suggested that stream discharge and riparian soil water concentrations profiles explained up to 0.76 and 0.85 (Nash-Sutcliffe Coefficient of Efficiency) for THg and MeHg, respectively, when variables for riparian soil water seasonality were included in the model. Riparian zone flow paths and seasonality in riparian zone soil water were the major controls on THg and MeHg in stream water. A similar model for the riparian zone pore and stream water in an intermediate fen may also reveal similar model efficiencies given the effect water table fluctuations had on stream and porewater chemistry.

3.5 Conclusions

Future work needs to elucidate a water table drawdown duration and magnitude where SO_4^{2-} regeneration begins to facilitate net MeHg production. Based on the results Nunes et al. (2015) in a moss-dominated peatland the period is greater than 9 days. This study showed that SO_4^{2-} and MeHg increased in riparian zone peats following a 30-day water table drawdown period, though direct measurement of SO_4^{2-} regeneration did not occur. Measures of SO_4^{2-} and sulphide (e.g., H_2S) along side THg and MeHg on a finer temporal scale (1-2 day) following water table recovery are necessary to substantiate SO_4^{2-} regeneration. Nevertheless, the importance of riparian zones as sites of MeHg production and their proximity to stream channel clearly influenced stream water MeHg. Further understanding of riparian zone biogeochemistry and hydrology, specifically related to SRB electron acceptors (SO_4^{2-}) and donors (labile carbon) and pH, would make underlying mechanisms more clear in explaining MeHg patterns in riparian pore and stream waters.

3.6 References

- Balogh SJ, Swain EB, Nollet YH (2005) Elevated methylmercury concentrations and loadings during flooding in Minnesota rivers. *Science of the Total Environment* 368:138–148
- Benoit JM, Mason RP, Gilmour CC, Aiken GR (2001) Constants for mercury binding by dissolved organic matter isolates from the Florida Everglades. *Geochimica et Cosmochimica Acta* 65: 4445–4451
- Bishop K, Lee YH, Pettersson C, Allard B (1995) Terrestrial sources of methylmercury in surface waters: The importance of the riparian zone on Svartberget catchment. *Water, Air and Soil Pollution* 80: 435–444
- Branfireun BA, Roulet NT (2002) Controls on the fate and transport of methylmercury in a boreal headwater catchment, northwestern Ontario, Canada. *Hydrologic of Earth Systems Sciences* 6: 785–794
- Branfireun BA (2004) Does microtopography influence subsurface pore-water chemistry? Implications for the study of methylmercury in peatlands. *Wetlands* 24: 207–211
- Branfireun BA, Heyes A, Roulet NT (1996) The hydrology and methylmercury dynamics of a Precambrian Shield headwater peatland. *Water Resource Research* 32: 1785–1794
- Branfireun BA, Roulet NT, Kelly CA, Rudd WM (1999) In situ sulphate stimulation of mercury methylation in a boreal peatland: Toward a link between acid rain and methylmercury contamination in remote environments. *Global Biogeochemical cycles* 13: 743–750
- Brigham ME, Wentz DA, Aiken GR, Krabbenhoft DP (2009) Mercury cycling in stream ecosystems. 1. Water column chemistry and transport. *Environmental Science & Technology* 43: 2720–2725
- Chapman SJ, Davidson MS (2001) ³⁵S-sulphate reduction and transformation in peat. *Soil Biology & Biochemistry* 33: 593–602
- Coleman-Wasik JK, Engstrom DR, Mitchell CPJ, Swain EB, Monson BA, Balogh SJ, Jeremiasson JD, Branfireun BA, Kolka RK, Almendinger JE (2015) The effects of hydrologic fluctuation and sulfate regeneration on mercury cycling in an experimental peatland. *Journal of Geophysical Research: Biogeosciences* 120: 1697–1715

- Compeau GC, Bartha R (1985) Sulphate-Reducing Bacteria: Principal methylators of mercury in anoxic estuarine sediment. *Applied Environment Microbiology* 50: 498–402
- Devito KJ, Hill AR (1997) Sulphate dynamics in relation to groundwater-surface water interactions in headwater wetlands of the southern Canadian Shield. *Hydrological Processes* 11: 485–500
- Devito KJ, Hill AR (1999) Sulphate mobilization and porewater chemistry in relation to groundwater hydrology and summer drought in two conifer swamps on the Canadian shield. *Water, Air, and Soil Pollution* 113: 97–114
- Drexel RT, Haitzer M, Ryan JN, Aiken GR, Nagy KL (2003) Mercury(II) sorption to two Florida everglades peats: Evidence for strong and weak binding and competition by dissolved organic matter released from the peat. *Environmental Science and Technology* 36: 4058–4064
- Eklöf K, Kraus A, Futter M, Schelker J, Meili M, Boyer EW, Bishop K (2015) Parsimonious model for simulating total mercury and methylmercury in boreal streams based on riparian flow paths and seasonality. *Environmental Science & Technology* 49: 7851–7859.
- Freeze RA, Cherry JA (1979) *Groundwater*. Prentice-Hall International, Inc, Englewood Cliffs, New Jersey
- Haitzer M, Aiken GR, Ryan JN (2003) Binding mercury(II) to aquatic humic substances: Influence of pH and source of humic substances. *Environmental Science and Technology* 37: 2436–2441
- Hemond HF, Fifield JL (1982) Subsurface flow in salt march peat: A model and field study. *Limnology and Oceanography* 27: 126–136
- Heyes A, Moore TR, Rudd JWM, Dugoua JJ (2000) Methyl mercury in pristine and impounded boreal peatland, Experimental Lakes Area, Ontario. *Canadian Journal of Fisheries and Aquatic Sciences* 57: 2211–2222
- Jeremiason JD, Engstrom DR, Swain EB, Nater EA, Johnson BR, Almendinger JA, Monson BA, Kolka RJ (2006) Sulfate additions increases methylmercury production in an experimental wetland. *Environmental Science & Technology* 40: 3800–3806

- Kelly CA, Rudd, JWM, Holoka MH (2003) Effect of pH on mercury uptake by an aquatic bacterium: implications for Hg cycling. *Environmental Science & Technology* 37: 2941–2946
- Kolka RK, Grigal DF, Nater EA, Verry ES (2001) Hydrologic cycling of mercury and organic carbon in a forest upland-bog watershed. *Soil Science Society of America* 65: 897–905
- Krabbenhoft DP, Benoit JM, Babiarz CL, Hurley JP, Andren AW (1995) Mercury cycling in the Allequash Creek watershed, northern Wisconsin. *Water, Air and Soil Pollution* 80: 425–433
- Lee YH, Bishop K, Pettersson C, Iverfeldt Å, Allard B (1995) Subcatchment output of mercury and methylmercury at Svartberget in northern Sweden. *Water, Air and Soil Pollution* 80: 455–465
- McClain M. E., Boyer E. W., Dent, C.L., Gergel, S.E., Grimm, N.B., Groffman, P.M., Hart, S.C., Harvey, J.W., Johnson, C.A. Mayorga, E., McDowell, W.H. and Pinay, G. 2003. Biogeochemical hot spots and hot moments in terrestrial and aquatic ecosystems. *Ecosystems*, 6: 301–312
- McLaughlin JW, Webster KL (2010) Alkalinity and acidity cycling and fluxes in an intermediate fen peatland in northern Ontario. *Biogeochemistry* 99: 143–155
- Mitchell CPJ, Branfireun BA, Kolka RK (2008a) Spatial characteristics of net methylmercury production hot spots in peatlands. *Environmental Science and Technology* 44: 1010–1016
- Mitchell CPJ, Branfireun BA, Kolka RK (2008b) Assessing sulphate and carbon controls on net methylmercury production in peatland: An in situ mesocosm approach. *Applied Geochemistry* 23: 503–518
- Mitchell CPJ, Branfireun BA, Kolka RK. (2009) Methylmercury dynamics at the upland-peatland interface: Topographic and hydrogeochemical controls. *Water Resources Research* 45: W02406
- Myers B, Webster KL, McLaughlin JW, Basiliko N (2012) Microbial activity across a boreal peatland nutrient gradient: the role of fungi and bacteria. *Wetlands Ecology Management* 20: 77–88
- Novák M, Wieder RK (1992) Inorganic and organic sulfur profiles in nine *Sphagnum* peat bogs in the United States and Czechoslovakia. *Water, Air and Soil Pollution* 65: 353–369

- Nunes FLD, Aquilina L, Ridder JD, Francez AJ, Quaiser A, Caudel JP, Vandenkoornhuysen P, Dufresne A (2015) Time-scales of hydrological forcing on the geochemistry and bacterial community structure of temperate peat soils. *Nature* 5: 14612
- Packalen MS, Bagley ST, McLaughlin JW (2011) Peatland stream lipid biogeochemistry features in an intermediate fen peatland, Ontario Canada. *Wetlands* 31: 353–365
- Prest VK, Donaldson JA, Mooers HD (2000) The OMAR story: the role of OMARS in assessing the glacial history of west-central North America. *Géographie Physique et Quaternaire* 54: 257–270
- Ratcliffe HE, Swanson GM, Fischer LJ (1996) Human exposure to mercury: A critical assessment of the evidence of adverse health effects. *Journal of Toxicology and Environmental Health* 49: 221–270
- Regnell O, Hammar T (2004) Coupling of methyl and total mercury in a minerotrophic peat bog in southeastern Sweden. *Canadian Journal of Fisheries and Aquatic Sciences* 61: 2014–2023
- Regnell O, Watras CJ, Troedsson BA, Helgée A, Hammar T (2009) Mercury in a boreal forest stream- role of historical mercury pollution, TOC, temperature and water discharge. *Environmental Science & Technology* 43: 3514–3521
- Rydin H, Jeglum JK (2013) *The Biology of Peatlands*, 2nd Edition. Oxford University Press
- Selvendiran P, Driscoll CT, Bushey JT, Montesdeoca MR (2008) Wetland influence on mercury fate and transport in a temperate forested watershed. *Environmental Pollution* 154: 46–55
- U.S. Environmental Protection Agency (1999) Mercury in water by oxidation, purge and trap, and cold vapour atomic fluorescence spectroscopy (Method 1631, Revision B). National Service Center for Environmental Publication and Information, Cincinnati, OH
- U.S. Environmental Protection Agency (1998) Methyl mercury in water by distillation, aqueous methylation, purge and trap, and cold vapor atomic fluorescence spectrometry (Method 1630). National Service Center for Environmental Publication and Information, Cincinnati, OH
- Vidon P, Hill AR (2004) Denitrification and patterns of electron donors and acceptors in eight riparian zones with contrasting hydrogeology. *Biogeochemistry* 71: 259–283

- Vidon PG, Mitchell CPJ, Jacinthe PA, Baker ME, Liu X, Fisher KR (2013) Mercury dynamics in groundwater across three distinct riparian zones in the US Midwest. *Environmental Science Processes & Impacts* 15: 2131–2141
- Vitt DH, Chee WL (1990) The relationship of vegetation to surface water chemistry and peat chemistry in fens of Alberta, Canada. *Vegetatio* 89: 87–106
- Waddington JM, Roulet NT (1997) Groundwater flow and dissolved carbon movement in a boreal peatland. *Journal of Hydrology* 1997: 122–138

Chapter 4

4 Conclusions and implications

The findings presented in this thesis suggest that MeHg production in a sedge-dominated intermediate fen and moss-dominated poor fen in northern Ontario, Canada was governed by the availability of SO_4^{2-} , which is in turn primarily influenced by hydrology. Overall, the lower long-term water table position at the moss-dominated poor fen provided more suitable conditions for Hg methylation. Across both northern fen peatlands, SO_4^{2-} availability was a function of seasonal water table drawdown, which exposed previously anaerobic saturated peat to aerobic conditions providing conditions favourable for SO_4^{2-} regeneration. Following a rise in water table position, porewater MeHg concentrations then increased. The greater MeHg concentrations were spatially variable between and within the poor and intermediate fen peatlands. Variability resulted from differences in pH and DOC and potentially differences in bioavailable Hg(II), labile carbon substrate, and microbial community structure. As an additional control on MeHg production, the hydrologic conditions clearly influenced MeHg production differences between the poor and intermediate fen. The moss-dominated poor fen had a relatively lower water table and an unsaturated peat soil layer throughout the study duration. In contrast, the sedge-dominated intermediate fen had a water table that was at or close to the ground surface for most of the study. The effect of a lower water table at the moss-dominated poor fen created conditions more suitable for Hg methylation as SO_4^{2-} would most certainly be available following any rise in the water table position after precipitation events. The period of water table drawdown at the sedge-dominated intermediate fen affected riparian margins more than interior portions (i.e., because less groundwater supply) or had lower median water tables. These riparian zones were more effective Hg methylating sites because a thick aerobic layer developed on either a seasonal and/or more perennial basis (Chapter 3).

4.1 Results as a baseline for climate change experiments

The work presented in this thesis was undertaken in a baseline year prior to the initiation of a field-based climate change experiment that will directly heat soils (+ 6.75 °C above ambient) and increase atmospheric CO₂ concentrations (900 ppm) in open top chambers. Besides direct experimental effects such as a likely increased biomass Hg corresponding to increased primary production (see Krabbenhoft & Sunderland 2013), my research suggested that Hg biogeochemistry is driven primarily by peatland characteristics (hydrology, pH, DOC). The full-factorial design of the planned experiment will capture temporal effects on sulphate (SO₄²⁻) regeneration caused by seasonal water table fluctuations, however, it remains unknown as to how much directly heating the peat soil may enhance evapotranspiration in addition to ambient evapotranspiration. If water table fluctuations are affected by experimentally enhanced evapotranspiration, open top chambers receiving heating may hydrologically diverge from the CO₂ only treatments and experimental controls meaning that multiple experimental effects would need to be deciphered. Based on my data, the combined effects of heating and enhanced evapotranspiration would have a greater effect on MeHg concentrations in the sedge-dominated intermediate fen compared to the moss-dominated poor fen because the average water table is closer to the surface.

4.2 Limitations

The main devices I used to measure net MeHg production and transport were wells and piezometers. The simplicity and fixed location of these hydrologic devices made them ideal for sampling porewater chemistry over time and space. However, the disadvantage of using wells and piezometers was that porewaters were sampled from a relatively large soil and water volume, while biogeochemical processes occur at much smaller scales (Nunes et al. 2015). Dilution of higher MeHg concentrations, or not directly sampling the methylating environment was clearly possible. Despite these problems, each well and piezometer were treated the same (i.e., installed at the same depth, made of the same material, sampled using the same clean techniques) and integrated the same physical

environment. Therefore, for the most part, differences in MeHg concentration reflected biogeochemical and hydrologic differences.

The literature tells us that biogeochemical reactions sometimes occur discretely in space and time. In the context of MeHg biogeochemistry, the greatest biogeochemical changes occur during periods of greatest hydrologic change (e.g., water table drawdown; groundwater flow reversals; snow melt; water table rebound; overland flow) (see e.g., Mitchell et al. 2008a; Mitchell et al. 2008c; Vidon et al. 2010). Therefore, monthly sampling of porewaters only could reflect significant seasonal trends (e.g., higher water tables in June, lowest water tables in August) and the temporal biogeochemical environment occurring at those instances. Having sampled more frequently during periods of greatest hydrologic change, biogeochemical trends relevant to Hg biogeochemical would have been observed providing greater insights into MeHg fate and transport.

A final limitation of this thesis was missing insights into sulphide and the redox environment. The geochemistry data analysed (THg, MeHg, major ions, DOC, DIC, pH, conductivity) revealed clear biogeochemical differences relating to Hg in peat porewater; however, sulphide and redox potential would have provided direct evidence of SO_4^{2-} regeneration and reduction following water table drawdown. Future studies comparing Hg biogeochemistry in a sedge-dominated intermediate fen and a moss-dominated poor fen with clearly different hydrologic conditions (Chapter 2 and Chapter 3) should include measures of porewater sulphide and redox potential similar to those presented by Mitchell & Branfireun (2005).

4.3 References

- Devito KJ, Hill AR, Roulet N (1996) Groundwater-surface water interaction in headwater forested wetlands of the Canadian Shield. *Journal of Hydrology* 181: 127–147
- Krabbenhoft DP, Sunderland EM (2013) Global change and mercury. *Science* 341: 1457–1458
- McClain M. E., Boyer E. W., Dent, C.L., Gergel, S.E., Grimm, N.B., Groffman, P.M., Hart, S.C., Harvey, J.W., Johnson, C.A. Mayorga, E., McDowell, W.H. and Pinay, G. 2003. Biogeochemical hot spots and hot moments in terrestrial and aquatic ecosystems. *Ecosystems*, 6: 301–312
- Mitchell CPJ, Branfireun BA (2005) Hydrogeomorphic controls on reduction-oxidation conditions across boreal upland-peatland interfaces. *Ecosystems* 8: 731–747
- Mitchell CPJ, Branfireun BA, Kolka RK (2008a) Spatial characteristics of net methylmercury production hot spots in peatlands. *Environmental Science and Technology* 44: 1010–1016
- Mitchell CPJ, Branfireun BA, Kolka RK (2008c) Total mercury and methylmercury dynamics in upland-peatland watershed during snowmelt. *Biogeochemistry* 90: 225–241
- Nunes FLD, Aquilina L, Ridder JD, Francez AJ, Quaiser A, Caudel JP, Vandenkoornhuyse P, Dufresne A (2015) Time-scales of hydrological forcing on the geochemistry and bacterial community structure of temperate peat soils. *Nature* 5: 14612
- Vidon P, Allan C, Burns D, Duval TP, Gurwick N, Inamdar S, Lowrance R, Okay J, Scott D, Sebestyen S (2010) Hot spots and hot moments in riparian zones: potential for improved water quality management. *Journal of the American Water Resources Association* 46: 278–298

Appendix

Appendix A: Site Photographs



Figure A1: Poor fen near White River, Ontario. Depicts open area near the adjacent main stream, which is downstream

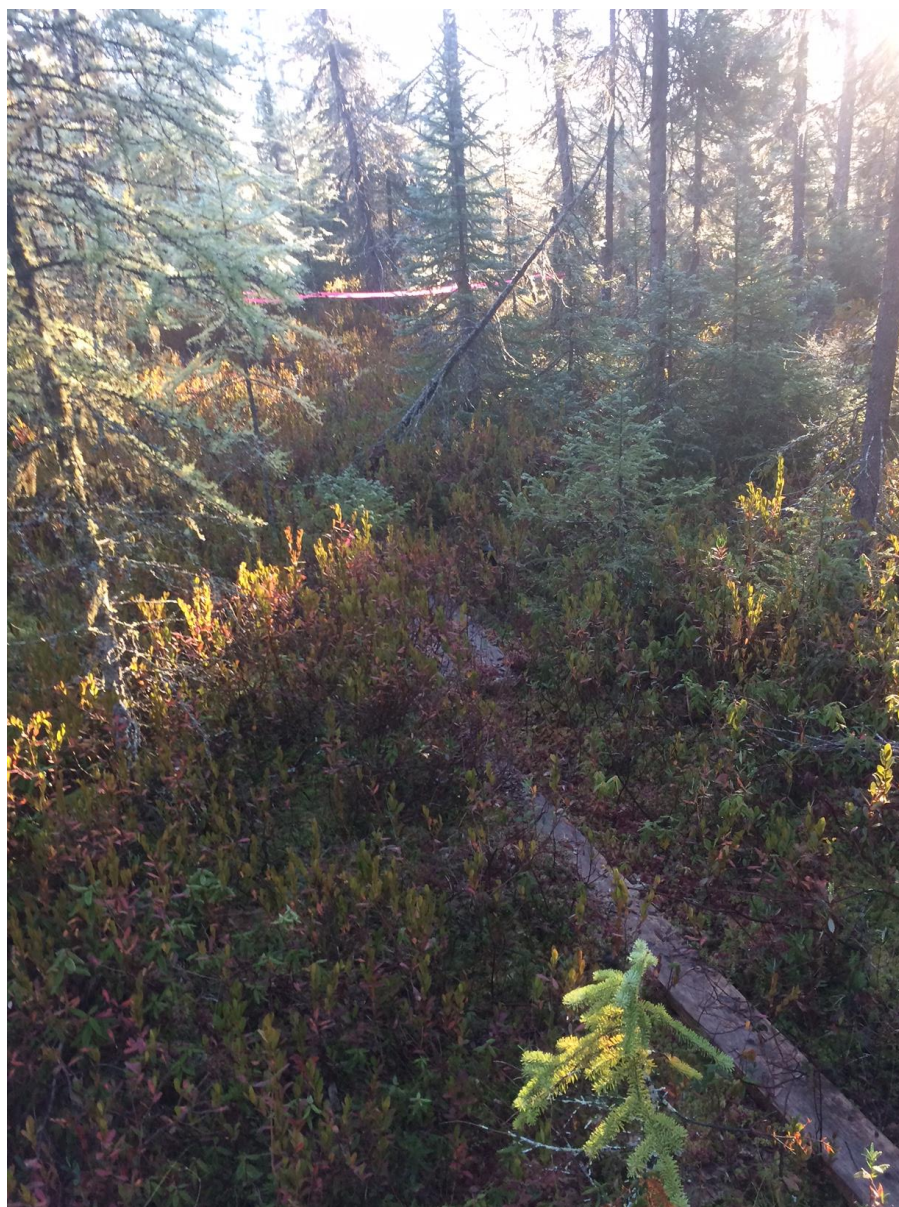


Figure A2: Interior portion of a poor fen near White River, Ontario. Depicts sparse canopy dominated by stunted black spruce (*Picea mariana*) and tamarack (*Larix laricina*).



Figure A3: Intermediate fen near White River, Ontario. Depicted is the confluence of main channel of Stream A (left) and the secondary channel (right) where riparian transects were installed (DS). The main channel of Stream A originates in the upland hillslopes seen past the treeline in the background. The DS originates in the interior portions of the peatland approximately 30 m away.



Figure A4: Intermediate fen near White River, Ontario. Depicts the CS, primarily fed by groundwater. In the background, the automatic weather station and an instrument shed.



Figure A5: Riparian transect across the upstream portion of the DS. The stream channel subsided during much of August 2016.



Figure A6: Riparian transect across the upstream portion of CS. This transect had the greatest methylmercury concentrations of any riparian margin transect.

Curriculum Vitae

Name: Mikhail J. Mack

Post-secondary Education and Degrees: Western University
London, Ontario, Canada
2015-2017 MSc (in progress)
Title: Net methylmercury production in two northern peatlands

University of Minnesota
Minneapolis, Minnesota, United States
2010-2014 B.S.
Title: Stream flow change in Minnesota: Evidence for Minnesota's changing climate

Honours and Awards: Western Graduate Research Scholarship (WGRS)
2015-2017

Member Phi Beta Kappa
Honours Society
2014-present

Related Work Experience Teaching Assistant
The University of Western Ontario
2015- 2017

Hydrologic Technician
USDA Forest Service- Northern Research Station
2014

Junior Scientist
University of Minnesota
2014-2015

Publications:

Bio 9100 Entrance Talk (01-31-2016) London, ON

Title: Climate change impacts on net methylmercury production and transport in northern peatlands

CGU Student Conference Eastern Section Meeting (02-04-2017) Guelph, ON

Title: Methylmercury in an intermediate fen peatland – Spatial and temporal patterns and implications for climate change [Poster]

Bio 9100 Exit Talk (04-07-2017) London, ON

Title: Methylmercury in two northern peatland types